Epigenetic Dysregulation of Tumor Suppressor Genes in CP/CPPS: Assessing the Diagnostic and Prognostic Utilities of Liquid Biopsies

Inaugural Dissertation
submitted to the
Faculty of Medicine
in fulfilment of the requirements
for the PhD-Degree
of the Faculties of Veterinary Medicine and Medicine
of the Justus Liebig University Giessen

Hang Yan

Master of clinical surgery

Gießen, 2023

From the
Research Laboratory Molecular Andrology
and
the Clinic of Urology, Pediatric Urology and Andrology
of the Faculty of Medicine
of the Justus-Liebig-University Giessen

Supervision

First Supervisor: Prof. Dr. med. Florian Wagenlehner, JLU Gießen

Second Supervisor: Prof. Dr. rer. nat. Undraga Schagdarsurengin, JLU Gießen

Examination

First reviewer: Prof. Dr. med. Florian Wagenlehner,
JLU Gießen

Second reviewer: Prof. Dr. Dr. med. univ. Arkadiusz Miernik,
University Hospital Freiburg

Vice-chair: Prof. Dr. rer. nat. Undraga Schagdarsurengin,
JLU Gießen

Chair: Prof. Dr. Christine Wrenzycki,
JLU Gießen

Date of Doctoral Defense:

07 March 2024

Copyright Notice

Declaration of Authorship

Declaration (Justus-Liebig-University)

This thesis is an original work of my research and contains no material which has been accepted for the award of any other degree or diploma at any university or equivalent institution. To the best of my knowledge and belief, this thesis contains no material previously published or written by another person, except where due reference is made in the text of the thesis.

Print Name: Hang Yan

Place, Date: Neu-Ulm, 22.02.2023

Signature:_____

Abstract

Chronic prostatitis/chronic pelvic pain syndrome (CP/CPPS) is a prevalent disorder affecting about 90% of patients with prostatitis syndrome. CP/CPPS can potentially progress to prostate cancer (PCa) in older age. However, the underlying molecular mechanisms of this disease remain unclear. Tumor suppressor genes (TSGs) are essential in preventing the malignant transformation of cells, and their epigenetic dysregulation is commonly observed in cancer. Therefore, we hypothesize that epigenetic aberrations in TSGs may also occur in CP/CPPS and contribute to the development of PCa. This study aims to analyze the epigenetic status of TSGs in CP/CPPS by using liquid biopsies such as ejaculate (EJ) and post-prostatic massage urine (ExU), specifically the promoter methylation and messenger ribonucleic acid (mRNA) expression status of selected PCa-associated TSGs, and to determine which type of liquid biopsy is promising for the establishment of biomarkers.

We utilized pyrosequencing and real-time polymerase chain reaction (RT-PCR) to investigate the promoter methylation and mRNA expression levels of a group of candidate prostatic TSGs. Specially, we analyzed *CDKN2A*, *EDNRB*, *PTGS2*, *BMP4*, *BMP7*, *PITX2*, and *GSTP1* in somatic cells isolated from ejaculate (EJ) and post-prostatic massage urine (ExU) from 30 healthy men and 50 patients diagnosed with CP/CPPS. In addition, to examine the source of hypermethylation and down-regulated mRNA expression of *CDKN2A* in liquid biopsies, we further sorted epithelial cells and leukocytes individually using the magnetic-activated cell sorting system (MACS) from fresh EJ and ExU samples collected from 34 CP/CPPS patients and 26 healthy donors. The efficiency of cell sorting was assessed by immunofluorescent staining (IF) for Prostate-specific antigen (PSA), Epithelial cell adhesion molecule (EpCAM), and Protein tyrosine phosphatase, receptor type, C (CD45). Furthermore, we analyzed the correlations between our experimental data and the clinical parameters. Lastly, we evaluated the influence of exosomes isolated from ExU supernatant on the polarization of the monocyte cell line THP-1 and the expression levels of *CDKN2A*.

Our results showed that the promoter methylation levels of *EDNRB*, *CDKN2A*, *PTGS2*, *BMP7*, and *BMP4* were significantly higher in the somatic cells of the EJ sample from CP/CPPS patients. Additionally, the mRNA expression levels of *CDKN2A* and *PTGS2*

were significantly downregulated in CP/CPPS patients' somatic cells. In the ExU samples, we observed that *EDNRB* and *CDKN2A* were more highly methylated, and *CDKN2A* and *PTGS2* were expressed at lower levels in CP/CPPS patients compared to healthy controls. Given the sensitivity and specificity of *CDKN2A* in demonstrating the differences in methylation and expression levels between CP/CPPS patients and healthy controls, we selected it for further analysis in a MACS-cell sorting experiment. Our results showed that CP/CPPS patients exhibited significantly higher levels of *CDKN2A* methylation in both sorted epithelial cells and leukocytes and lower mRNA expression levels in epithelial cells and leukocytes of EJ. Importantly, we also demonstrated the feasibility of the MACS system in liquid biopsies from CP/CPPS patients and healthy controls containing a low amount of cells. Furthermore, we found significant correlations between our experimental results and clinical parameters such as prostate volume, PSA, NIH Chronic Prostatitis Symptom Index (NIH-CPSI), International Prostate Symptom Score (IPSS), and sperm motility. Finally, we investigated the impact of exosomes derived from ExU supernatant on the polarization of M0 macrophages. Our findings suggest that ExU exosomes may promote the polarization of M0 macrophages towards the M1 phenotype.

This study significantly contributes to identifying potential biomarkers for the prognosis of CP/CPPS from liquid biopsies, suggesting a potential link between CP/CPPS and prostate cancer. Specifically, the study highlights the close correlation between the methylation and downregulation of TSGs in CP/CPPS and various clinical parameters, indicating the potential role of TSGs in the assessment of CP/CPPS severity and prognosis, as well as the fertility of affected individuals. Additionally, the study introduces a practical approach for isolating epithelial cells and leukocytes from liquid biopsies, facilitating more in-depth research into CP/CPPS. Finally, these findings lay the groundwork for future investigations to elucidate the molecular mechanisms underlying CP/CPPS and its potential progression to prostate cancer.

Zusammenfassung

Das chronische Prostatitis/chronische Beckenschmerzsyndrom (CP/CPPS) ist eine häufig auftretende Störung, die etwa 90% der Patienten mit Prostatitis-Syndrom betrifft. CP/CPPS kann sich im Alter potenziell zu Prostatakrebs (PCa) entwickeln. Die zugrunde liegenden molekularen Mechanismen dieser Krankheit sind jedoch unklar. Tumorsuppressor-Gene (TSGs) sind für die Verhinderung von malignen Veränderungen von Zellen unerlässlich, und ihre epigenetische Dysregulationen treten häufig bei Krebs auf. Es wird angenommen, dass epigenetische Aberrationen in TSGs auch bei CP/CPPS auftreten und zur Entwicklung von PCa beitragen können. Ziel dieser Studie ist es, den epigenetischen Status von TSGs bei CP/CPPS, insbesondere der Promotor-Methylierungs- und Messenger-Ribonukleinsäure (mRNA) -Expressionsstatus ausgewählter PCa-assoziierten TSGs zu untersuchen. Hierfür werden flüssige Biopsien wie Ejakulat und Urin verwendet, um die flüssige Biopsie zur Etablierung von vielversprechenden Biomarkern zu nutzen.

Zur Untersuchung der Promotor-Methylierung und mRNA-Expressionsniveaus einer Gruppe von Prostata assoziierten TSGs wurden die Real-Time Polymerase Chain Reaction (RT-PCR) und die Pyrosequenzierung als Methoden verwendet. Es wurden die TSGs *CDKN2A*, *EDNRB*, *PTGS2*, *BMP4*, *BMP7*, *PITX2* und *GSTP1*, in somatischen Zellen, die aus Ejakulat (EJ) und post-prostatischer Massage-Urin (ExU) von 30 gesunden Männern und 50 Patienten mit CP/CPPS isoliert wurden analysiert. Darüber hinaus wurden einzelne Epithelzellen und Leukozyten mithilfe des magnetisch aktivierten Zellsortiersystems (MACS) aus frischen EJ- und ExU-Proben, die von 34 CP/CPPS-Patienten und 26 gesunden Spendern gesammelt wurden, sortiert, um die Ursachen der Hypermethylierung und herab regulierten mRNA-Expression von *CDKN2A* zu untersuchen. Die Effizienz der Zellsortierung wurde durch Immunfluoreszenz-Färbung (IF) für prostataspezifisches Antigen (PSA), Epithelzelladhäsionsmolekül (EpCAM) und Rezeptor-Typ Tyrosin-Proteinphosphatase C (CD45) bewertet. Außerdem wurden Korrelationen zwischen den experimentellen Daten und den klinischen Parametern analysiert. Des Weiteren wurde der Einfluss von Exosomen, die aus ExU-Überstand isoliert wurden, auf die Polarisation der Monozytenzelllinie THP-1 und die Expressionsniveaus von *CDKN2A* untersucht.

Unsere Ergebnisse zeigen, dass die Methylierungslevels der Promotoren von *EDNRB*, *CDKN2A*, *PTGS2*, *BMP7* und *BMP4* in somatischen Zellen der EJ-Probe von CP/CPPS-Patienten signifikant höher waren. Darüber hinaus waren die mRNA-Expressionslevels von *CDKN2A* und *PTGS2* in somatischen Zellen von CP/CPPS-Patienten signifikant herunterreguliert. In den ExU-Proben konnten wir feststellen, dass *EDNRB* und *CDKN2A* stärker methyliert waren und dass *CDKN2A* und *PTGS2* bei CP/CPPS-Patienten im Vergleich zu gesunden Kontrollen auf niedrigeren Ebenen exprimiert wurden. Aufgrund der hohen Sensitivität und Spezifität von *CDKN2A* zur Demonstration der Unterschiede in Methylierungs- und Expressionslevels zwischen CP/CPPS-Patienten und gesunden Kontrollen, haben wir es für weitere Analysen in einem MACS-Zellsortierungsexperiment ausgewählt. Unsere Ergebnisse zeigen, dass CP/CPPS-Patienten in beiden sortierten Epithelzellen und Leukozyten signifikant höhere *CDKN2A*-Methylierungslevels und niedrigere mRNA-Expressionslevels in Epithelzellen und Leukozyten von EJ aufweisen. Es ist von Bedeutung, dass wir die Durchführbarkeit des MACS-Systems in Flüssigbiopsien von CP/CPPS-Patienten und gesunden Kontrollen mit einer geringen Anzahl von Zellen nachweisen konnten. Zusätzlich konnten signifikante Korrelationen zwischen unseren experimentellen Ergebnissen und klinischen Parametern wie Prostatavolumen, PSA, NIH Chronischem Prostatitis Symptom Index (NIH-CPSI), Internationalem Prostata Symptomen Score (IPSS) und Spermienmotilität festgestellt werden. Schließlich untersuchten wir den Einfluss von Exosomen aus ExU-Überstand auf die Polarisation von M0-Makrophagen. Unsere Ergebnisse deuten darauf hin, dass Exosomen aus ExU die Polarisation von M0-Makrophagen in Richtung des M1-Phänotyps fördern können.

Diese Studie leistet einen signifikanten Beitrag zur Identifizierung potenzieller Biomarker für die Prognose von CP/CPPS aus flüssigen Biopsien und legt einen möglichen Zusammenhang zwischen CP/CPPS und Prostatakrebs nahe. Insbesondere betont die Studie die enge Korrelation zwischen der Methylierung und Herunterregulierung von TSGs bei CP/CPPS und verschiedenen klinischen Parametern, was auf die potenzielle Rolle von TSGs bei der Beurteilung von Schweregrad und Prognose von CP/CPPS sowie der Fruchtbarkeit betroffener Personen hinweist. Darüber hinaus stellt die Studie einen praktischen Ansatz zur Isolierung von epithelialen Zellen und Leukozyten aus flüssigen Biopsien vor, der

weitere Forschungsmöglichkeiten in Bezug auf CP/CPPS erleichtert. Schließlich legen diese Erkenntnisse die Grundlage für zukünftige Untersuchungen zur Aufklärung der molekularen Mechanismen von CP/CPPS und ihrer potenziellen Progression zu Prostatakrebs.

Table of contents

List of Abbreviations

Abbreviations	Meaning
BMP4	Bone morphogenetic protein 4
BMP7	Bone morphogenetic protein 7
CDKN2A	Cyclin Dependent Kinase Inhibitor 2A
CNAs	Copy number alternations
CP/CPPS	Chronic prostatitis/chronic pelvic pain syndrome
CP/CPPS IIIa	CP/CPPS subcategory with detectable leukocyte infiltration
CP/CPPS IIIb	CP/CPPS subcategory without detectable leukocyte infiltration
CpG site	Nucleotide sequence where cytosine is followed by guanine in 5' to 3' direction
CPSI	NIH-CPSI: NIH-Chronic prostatitis symptom index
Ct value	Cycle threshold value (Real-time PCR)
CXCL 12	C-X-C motif chemokine 12 (SDF-1)
DEPC	Diethyl pyrocarbonate
DMEM	Dulbecco's modified Eagle's medium
DMSO	Dimethyl sulfoxide
DNA	Deoxyribonucleic acid
dNTP	Deoxynucleotide
DU-145	Immortalized prostate cancer cell line from a central nervous system metastasis
ESCs	Ejaculate somatic cells
EMT	Epithelial-mesenchymal transition
EPS	Expressed prostatic secretions
ERα	Estrogen receptor alpha
FACS	Fluorescence-activated cell sorting
FCS	Fetal calf serum
GSTP1	Glutathione S-transferase P
HIF-1	Hypoxia-inducible factors
IFNγ	Interferon gamma, IFNG gene
IPSS	International prostate symptom score
LNCaP	Lymph node carcinoma of the prostate (Immortalized prostate cancer cell line)
M1 macrophages	Macrophages polarized (e.g. with LPS/IFNγ) towards type 1 (Th1) immunity (also called classically activated macrophages)
MACS	Magnetic-activated cell sorting
M2 macrophages	Macrophages polarized (e.g. with IL-4/IL-13) towards type 2 (Th2) immunity (also called alternatively activated macrophages)
N/A	Not available

NF-κB	Nuclear factor kappa-light-chain-enhancer of activated B
NIH	National institutes of health
PBS	Phosphate-buffered saline
PC3	Immortalized prostate cancer cell line, established from a bone metastasis
PCa	Prostate cancer
PCR	Polymerase chain reaction
PITX2	Paired-like homeodomain transcription factor 2
PMA	Phorbol 12-Myristate 13-Acetate
PSA	Prostate-specific antigen
PTGS2	Prostaglandin-endoperoxide synthase 2
RNA	Ribonucleic acid
RPMI	Roswell Park Memorial Institute medium
RT	Room temperature
RT-PCR	Real-time polymerase chain reaction
SATA3	Signal transducer and activator of transcription 3
THP-1	Immortalized human monocytic cell line (derived from acute monocytic leukemia)
TME	Tumor microenvironment
UKGM	Universitätsklinikum Gießen und Marburg
UPOINT	CP/CPPS classification system by symptoms (U: Urinary; P: Psychosocial; O: Organ specific; I: Infection; N: Neurologic/ Systemic; T: Tenderness)
CD	Cluster of differentiation
WHO	World health organization
OR	Odds ratios
DNMTs	DNA methyltransferases
EJ	Ejaculate
ExU	Post-prostatic massage urine
ERβ	Estrogen receptor β
APC	Adenomatous polyposis coli
BRCA1	Breast cancer type 1
MSH2	DNA mismatch repair protein Msh2
RB1	RB Transcriptional Corepressor 1
EDNRB	Endothelin Receptor Type B
CTC	Circulating tumor cell
cfDNA	Circulating free DNA
cfRNA	Circulating free RNA
SFRP2	Secreted frizzled-related protein 2
RARB	Retinoic Acid Receptor Beta
RASSF1	Ras association domain-containing protein 1
OS	Overall survival

CRPC	Castration-resistant prostate cancer
IL	Interleukin
CXCL12	C-X-C Motif Chemokine Ligand 12
CXCR4	C-X-C chemokine receptor type 4
mRNA	Messenger RNA
BSA	Bovine serum albumin
NaAC	Sodium acetate
ssDNA	Single strain DNA
dATP	Deoxyadenosine triphosphate
dCTP	Deoxycytidine triphosphate
dTTP	Deoxythymidine triphosphate
dGTP	Deoxyguanosine triphosphate
LPS	Lipopolysaccharides
EP tubes	Eppendorf tube
IF	Immunofluorescent staining
rpm	Revolutions per minute
EpCAM	Epithelial cell adhesion molecule
FCS	Fetal calf serum
CK	Cytokeratin
FOXA1	Forkhead Box A1
EZH2	Enhancer of zeste homolog 2
PRC2	Polycomb repressive complex 2
ZBP-89	Zinc-finger binding protein-89
PRC1	Polycomb repressive complex
PTPRC	Protein Tyrosine Phosphatase Receptor Type, C
KLK3	Kallikrein Related Peptidase 3
DRE	Digital rectal examination
SGLT2	Sodium-glucose linked transporter-2
USCs	Urine-derived stem cells
PSMA	Prostate-specific membrane antigen
WGBS	Whole-genome bisulfite sequencing
TSGs	Tumor suppressor genes
ED	Erectile dysfunction
BCL2	B-cell lymphoma 2
TGF-β	Transforming growth factor beta
CCL	C-C motif chemokine
-ΔCt	Minus delta Ct value, -Ct (gene of interest)-Ct (reference gene)

1. Introduction

1.1. Chronic Prostatitis/ Chronic Pelvic Pain Syndrome (CP/CPPS)

Prostatitis is a prevalent medical condition that affects a significant portion of the global population. According to findings from the REduction by DUtasteride of PCa Events (REDUCE) trial, a substantial number of individuals who undergo prostate biopsies exhibit inflammation, with a prevalence rate of 77.6%. Notably, chronic inflammation is observed in 89% of the inflammatory tissue[1]. In addition, pathological reports typically describe prostatitis as a complex and multifaceted condition and a disease characterized by inflammatory cells within the prostate tissue, including neutrophils, lymphocytes, eosinophils, plasma cells, and macrophages[2].

In 1995, the National Institute of Health (NIH) introduced a classification system for prostatitis that comprises four types: Type I, Type II, Type III, and Type IV. Type I and Type II are subtypes of bacterial prostatitis that differ in the duration of symptoms, with Type I being acute and Type II being chronic[3]. Type III and Type IV are nonbacterial prostatitis subtypes, with Type IV patients commonly diagnosed incidentally without symptoms[4]. Type III, also known as chronic prostatitis/chronic pelvic pain syndrome (CP/CPPS), accounts for approximately 90% of all prostatitis cases[5]. CP/CPPS is further classified into Type IIIA (inflammatory CP/CPPS) and Type IIIB (noninflammatory CP/CPPS). Type IIIA is characterized by a higher-than-normal amount of leukocytes (10 leukocytes/high power field[6–8]) in expressed prostatic secretion (EPS), ejaculate (EJ), and post-prostatic massage urine (ExU), while Type IIIB does not exhibit this feature. The most common symptoms of CP/CPPS patients include chronic pain lasting at least three months in the lower back, abdomen, pelvis, rectum, and testis associated with ejaculatory pain and urinary tract symptoms[9–11].

However, unlike bacterial prostatitis, the underlying mechanisms and pathogenesis of CP/CPPS remain unclear, and there is an ongoing debate among researchers in this field. Several factors have been proposed to be associated with developing CP/CPPS, including endocrine, psychological, neurological, and immunological factors. Leukocytes in EPS have been used as a biomarker for diagnosing CP/CPPS, but this method has limitations. Leukocytes can also be detected in asymptomatic patients

and patients with pelvic pain[12], and some Type IIIB patients experience symptoms without excess leukocytes in EPS or seminal plasma. Type IV patients may have leukocytes present but without any symptoms. Additionally, CP/CPPS has been linked to changes in serum hormone levels, smoking, autoimmunity, anxiety, and age[13–16]. Unhealthy diet habits are also regarded as a reason for CP/CPPS. Studies have shown that a fatty diet can contribute to inflammation in the prostate, leading to the activation of pathways such as Signal Transducer and Activator of Transcription (STAT)-3 and Nuclear Factor-kappa B (NF-kappaB). These pathways promote the generation of inflammatory factors, such as cytokines, which can contribute to the development and progression of CP/CPPS[17,18].

The lack of reliable biomarkers and standardized diagnosis and severity assessment criteria further compounds these challenges. However, introducing the NIH-Chronic Prostatitis Symptom Index (NIH-CPSI) has been a positive development. The NIH-CPSI is a nine-item questionnaire that focuses on urinary symptoms, pain, and quality of life, enabling effective prediction of morbidity in CP/CPPS patients[19,20]. CP/CPPS patients are classified with a score > 4 and show ejaculatory or perineal pain[21]. While objective evidence is lacking due to the subjective nature of the questionnaire system, the NIH-CPSI remains a valuable tool in managing this condition. In 2009, the UPOINT classification system was introduced to guide CP/CPPS treatment. This system categorizes patients into six groups based on their symptoms: urinary, psychosocial, organ-specific, infection, neurological, and pelvic floor tenderness[21,22]. This classification scheme offers a more nuanced approach to treatment, with tailored therapies based on the specific symptoms and needs of the patient. Despite these developments, the current treatment options for CP/CPPS remain inadequate, with antibiotics, anti-inflammatory medications, neuromodulators, alpha-blockers, and pelvic floor physical therapy (PFPT) being the most commonly used treatments[23]. However, the current treatment efficiency of CP/CPPS remains poor and the development of treatment methods is slow and inefficient.

1.2. The risk of CP/CPPS developing into prostate cancer (PCa)

Inflammation is a complex biological response of the body to harmful stimuli, typically characterized by the cardinal signs of swelling, redness, pain, and loss of function. Chronic inflammation may occur following recurrent or persistent inflammation[24], and the presence of peripheral blood inflammatory markers is often used as an indicator of inflammation, although the most relevant markers remain unknown. In the early stages of inflammation, macrophages and mast cells secrete specific molecules to guide neutrophils to the site of inflammation, followed by the activation and recruitment of other leukocyte subsets such as lymphocytes, mediated by growth factors and cytokines[25,26]. Rudolf Virchow was the first to describe the presence of leukocytes in tumor tissues and published the correlation between cancer and inflammation in 1863[27]. Subsequent epidemiological and clinical studies have confirmed a link between inflammation and cancer, with C-reactive protein (CRP) being the most frequent factor associated with cancer according to a meta-analysis of 103 articles[28]. The tumor microenvironment (TME), consisting of fibroblasts, vascular cells, and inflammatory immune cells, is regulated by chronic inflammation and plays a critical role in tumor progression[29]. Chronic inflammation can lead to uncontrolled replication, metastasis, and the evasion of growth inhibition and programmed cell death[30]. Inflammation and infections also increase the risk of carcinogenesis in organs such as the prostate, colon, lung, and pancreas, with transcription factors such as NF-κB, STAT-3, and HIF-1 playing critical roles in activating cytokines, chemokines, and PGHS-2, which recruit and activate macrophages, mast cells, and neutrophils in the TME[31,32]. Additionally, the release of macrophage migration inhibitory factors (MIF) from T cells can maintain an anti-apoptotic feedback loop in activated inflammatory cells, leading to the escape of p53 regulation and increased proliferation, genetic deficiencies, and oncogene mutations[33].

Prostatitis has been proposed as a potential risk factor for prostate cancer (PCa)[34]. Inflammatory factors are thought to contribute to prostate carcinogenesis during the prostatitis process via various signaling pathways, such as inhibiting apoptosis, increasing cell proliferation, and causing the loss of tumor suppressor genes (TSGs)[34]. CD4+CD25 high T cells have been found to have a significantly increased occurrence in peripheral blood and cancer tissue of PCa patients[35], while the activation of nitrogen

and oxygen radicals from inflammatory tissue can also restrain tumor suppression and promote tumorigenesis[36]. A meta-analysis including 20 case-control studies conducted between 1990 and 2012 examined the association between prostatitis and PCa. This study showed a higher significant difference in a personal interview than clinical studies[34]. A 15 case-control study in 2017 concluded that there is a high-risk for prostatitis patients progressing to prostate carcinoma[37]. A population-based case-control study showed an association between genitourinary infection and PCa. The prevalence of prostatitis history was observed in 10% of the patient group and 7% of the controls, with a higher prevalence among patients with chronic prostatitis[38]. In addition, Stikbakke et al.[39] found that patients who suffered from chronic prostatitis and had >2.04 mg/l of high-sensitive CRP level had a 30% increased risk of prostate carcinogenesis in a cohort of 509 men who developed PCa after an 11.8-year follow-up.

However, some researchers have suggested that inflammation may be a protective factor against PCa progression later in life[40]. The first study investigating the correlation between PCa and prostatitis showed controversial results, with a positive correlation observed but no significant statistical difference found[41]. Another study involving 4526 patients indicated that inflammation might decrease the risk of progressing to PCa through prostate biopsy[42].

1.3. Epigenetics of carcinogenesis and inflammation

Conrad Waddington introduced epigenetics in 1942 [43] as a concept for regulating gene expression through mechanisms that do not involve changes to the underlying DNA sequence. The regulation of gene expression can be accomplished by various means, including DNA methylation, histone modifications, chromatin remodeling, and non-coding RNA[44]. DNA methylation involves adding methyl groups to cytosine residues in CpG-rich regions, commonly referred to as CpG islands. This process is mediated by DNA methyltransferases (DNMTs), which include three types of enzymes, DNMT1, DNMT3A, and DNMT3B. DNMT3A and DNMT3B are primarily responsible for de novo methylation, whereas DNMT1 maintains existing methylation patterns[45]. In normal cells, most CpG sites are hypermethylated, except for CpG islands[46,47].

In recent years, a growing body of research has indicated that the methylation status of CpG regions in cancer cells is highly variable. In particular, low CpG regions are frequently hypomethylated, whereas CpG islands tend to be hypermethylated[48] (Figure 1). These changes in DNA methylation patterns can significantly affect the activity of transcription factors and lead to gene repression by inhibiting their functions[49]. It is worth noting that CpG islands, defined as sequences longer than 200 base pairs with a CpG content greater than 50%, are present in approximately 60-70% of human genes, with over 50% of these islands located in promoter regions. Methylation of these promoter-associated CpG islands can exert control over gene expression without altering the underlying nucleotide sequence[50].

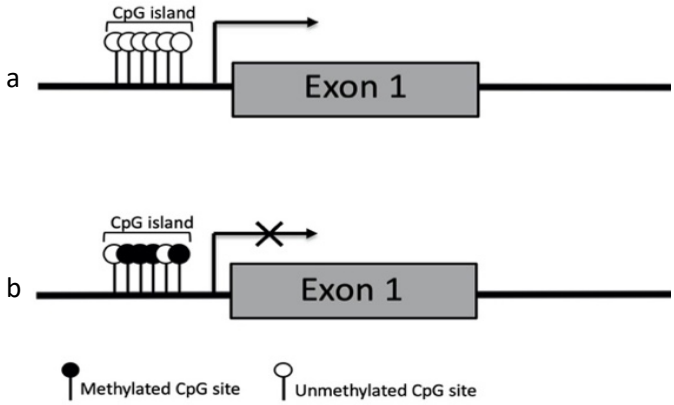

Figure 1: Unmethylated cytosines in CpG promoters associate with gene transcription (a), whereas methylated cytosines associate with transcriptional inactive genes and were often found in TSGs in human cancer (b).

Prostate-specific antigen (PSA) has been a widely admitted biomarker for diagnosing and surveilling the recurrence of PCa. However, it cannot predict the development of the disease. Among epigenetic aberrations, DNA promoter methylation plays a vital role in carcinogenesis because it can restrain the expression of various genes in a similar way to mutations[51]. Epigenetic analyses have been widely established in PCa studies. Recent studies showed that increasing methylation rates of aberrant DNA promoters could be a potential biomarker[52] and hypermethylation which helps to distinguish PCa from benign prostatic tissue, has been found in PCa[53]. The prostate is an organ responsible for sexual hormone changes such as estrogen, androgen, and progesterone. DNA promoter hypermethylation in androgen receptor (AR)-negative PCa cell line was first described in 1998 [54]. In following years, another group used an

inhibitor of cytosine DNA methyltransferase (5,6-dihydro-5'-azacytidine) to treat an androgen-independent PCa cell line and successfully turned the cell line into androgen-sensitive [55]. Glutathione S-transferase Pi (*GSTP1*), a gene that can prevent DNA damage by detoxifying oncogenes, was shown to be hypermethylated in up to 90% of PCa cases[56]. Methylation level of estrogen receptor α (ERα) has been shown to be correlating to the PCa progression[57], and epigenetic analyses in liquid biopsies of CP/CPPS patients showed hypermethylation of ERα and estrogen receptor β (ERβ) in somatic cells of EJ compared to healthy controls.

It has been suggested that chronic inflammation, which is without microbial infections, leads to increased promoter methylation[58]**.** One of the advantages of promoter methylation measurements in liquid biopsies is that tissue biopsies might be avoided, and diseases can be detected in the early stages[59]. Some studies also illustrate that methylation analysis of multiple genes can provide more information about the diagnosis and prognosis of various diseases[60,61]. For example, when the methylation rate of 9 PCa-correlated genes was measured in PCa and benign prostate hyperplasia (BPH) patients, hypermethylation of more than five genes proposed the recurrence of prostate-specific antigen after prostatectomy and associated with Gleason score and pathologic stage[62].

1.4. Inactivation of Tumor Suppressor Genes (TSGs) in prostate cancer

TSGs are a class of genes that play a critical role in regulating cell growth, DNA repair, and apoptosis. These genes act as gatekeepers that prevent uncontrolled cell proliferation and the formation of tumors. TSGs are often involved in complex signaling networks that regulate various aspects of cellular physiology, including cell cycle progression, differentiation, and metabolism. Some TSGs also produce proteins involved in cell adhesion, which prevents cells from becoming detached and metastasizing to other tissues[63]. In general, there are five categories of TSGs: (1) encoding intracellular proteins which allow restraining cells to progress to some cell cycle (e.g., *p16*)[64]; (2) encoding receptor for hormones or signal suppressing cell proliferation (e.g., adenomatous polyposis coli (*APC*)) [65]; (3) encoding proteins

promoting apoptosis (e.g., *p53*)[66]; (4) encoding checkpoint-control proteins contributing to repair DNA damage and chromosomal defect (e.g., breast cancer type 1 susceptibility protein (*BRCA1*))[67]; (5) encoding proteins for repairing DNA mistake (e.g., DNA mismatch repair protein 2 (*MSH2*))[68].

Knudson announced the concept of TSG for the first time in 1969 and proposed that TSG follow the "2-hit" model (Knudson hypothesis). It supposes that only if both alleles are mutated, inactivated, or deleted, the phenotype may change and lead to carcinogenesis and cancer progress[69,70]. If one allele a malfunction, the other one can still be functional and produce the correct protein to maintain the appropriate function of the gene. Hypermethylation of TSGs promoter suggested that epimutation can contribute to oncogenesis[45].

Inactivation of many TSGs has often been observed in PCa. RB Transcription corepressor 1 (RB1) is a well-known TSG protein that controls the cell cycle. The low or decreased expression level of this gene has been detected in leukemia, hepatocellular cancer, PCa, renal cancer, breast cancer and others[70]. Endothelin receptor type B (*EDNRB*) gene encoding an activator of phosphatidylinositol-calcium second messenger system as well as cyclin-dependent kinase inhibitor 2A (*CDKN2A*) gene encoding p16 (INK4A) and p14 (ARF) responsible for cell cycle have been shown to have hypermethylated promoters in prostate cancer[50,71]. Bone morphogenetic proteins (BMPs) which belong to transforming growth factor-beta superfamily play important roles in controlling of differentiation, cell migration and apoptosis[72–75]. In PCa, Bone morphogenetic protein 7 (*BMP7*) has been studied and resulted with downregulation and hypermethylation[76,77]. Another BMPs member Bone morphogenetic protein 4 (*BMP4*) is subordinate in PCa comparing to normal tissue[78] and acts as a suppressor of branching morphogenesis and ductal budding[79]. Besides, *BMP4* reduces apoptosis in tumorigenic prostate cells lines such as LNCaP and PC3[80], Brubaker *et al.* reported *BMP4* inhibits growth effect of LNCaP[81]. Clinically, PCa patients with low *BMP4* expression level show a decreased survival probability than the ones with high expression level[82]. Paired-like homeodomain transcription factor 2 (*PITX2*) gene, which is induced by the Wnt/Beta-catenin pathway and responsible for regulating cell proliferation, and prostaglandin-endoperoxide synthase 2 (*PTGS2*) gene promoting carcinogenesis by an increase of cell growth, have both been shown

to play a role in the recurrence of PCa[83,84]. Bastian *et al.* reported *PTGS2* is epigenetic hypermethylated PCa patients comparing to patients with benign prostatic hyperplasia[61]. *GSTP1* belongs to more and more evidence showing that epigenetic dysregulation of TSGs and microRNAs is crucial in carcinogenesis and that downregulation of TSGs through promoter hypermethylation plays an vital role in PCa development[71,85,86].

1.5. Application of liquid biopsies in biomarker development

Histopathological or tissue biopsy is still the “golden standard” in cancer diagnosis. However, tissue biopsy is invasive and relatively complicated for clinicians and patients. It can only reflect the situation of cancer at a specific time point but is not able to show the whole picture of the disease's procession[87]. Therefore, liquid biopsy such as blood, urine, semen, pleural fluid, breast milk and saliva, has been introduced as a new concept for diagnosis[88] and widely exerted in experimental research and clinical application, especially in cancer research[89]. The most favorable advantage of liquid biopsy is a minimal invasion and real-time informative monitoring and prognosis of diseases. In the age of precise treatment, liquid biopsy also plays an essential role in cancer diagnosis, treatment, and prognosis. Analysis of circulating tumor cell (CTC), cell-free DNA (cfDNA) and RNA (cfRNA), exosomes, and circulating protein and metabolites have been regarded as potential non-invasive sources for the prognosis of PCa[89,90]. Besides, investigating DNA promoter methylation levels of different genes through liquid biopsy has been supposed to be a promising tool for disease observation[91–93]. For example, hypermethylation of TSGs in cfDNA and cancer tissue shows strong correlations to colorectal cancer metastasis[94]. DNA hypermethylation can also be detected in CTCs. A study from Lyberopoulou et al.[95] revealed the first time that hypermethylation of Secreted frizzled-related protein 2 (*SFRP2*) and the first exon (exon 1) of Vimentin (VIM) could be found in CTCs of colorectal cancer patients.

The correlation of methylation levels of TSGs in liquid biopsy with clinical outcomes has been shown in PCa. One study evaluated methylation levels of the genes retinoic acid receptor β (*RARB*), RAS association, domain family member 1 (*RASSF1*), and *GSTP1* in 514 preoperative urine samples from PCa patients. DNA promoter

methylation disorder of at least one gene was detected in over 80% of urine samples[96]. Silva et al.[97] also reported epigenetic dysregulation in urine samples of PCa patients. Combined with PSA, the methylation level of these genes can play a role in upgrading and pathological upstaging in urine samples[96]. Cell-free DNA can also contribute to the detection and surveillance of urothelial carcinoma. The copy number alternations (CNAs) were tested by shallow genome-wide sequencing of cfDNA in urine samples, and the sensitivity and specificity are 86.5% and 94.7%, respectively. Moreover, CNAs changes in cfDNA are also correlated with treatment effects[98]. In another study, promoter methylation levels of *APC* and *GSTP1* in circulating tumor DNA (ctDNA) were measured in castration-resistant prostate cancer (CRPC) and the hypermethylations of *APC* and *GSTP1* in patients before any treatment indicate a worse overall survival (OS)[99].

Prostate tissue biopsies are barely employed in the diagnosis of CP/CPPS. Therefore, developing non-invasive but efficient checking methods and biomarkers is urgent for precise diagnosis and prognosis in CP/CPPS. Liquid biopsies have been gradually recognized as a potential material for evaluating CP/CPPS. A systematic study including 387 Type IIIb patients and 432 healthy controls show that IL6, IL8, TNF-α, and IL1-β in semen samples may play a role in the phenotyping and treatment of CP/CPPS[100]. C-X-C Motif Chemokine 12 (CXCL12) and its receptor C-X-C Chemokine Receptor Type 4 (CXCR4) were found being hypermethylated in liquid biopsies (blood and EJ) of CP/CPPS patients and it could be one of the reasons for the chronic process of inflammation[101]. Therefore, methylation analysis in liquid biopsy could not only be a potential indicator of diagnosis and prognosis in PCa but also could be an alternative to prostate tissue biopsy in CP/CPPS patients and provide information about inflammatory factors in prostate tissue.

1.6. Aims of this study

There is an urgent need to better understand the underlying mechanisms of /CPPS and its potential correlation to PCa in a non-invasive manner. Tissue biopsies are typically recommended for patients with cancer or suspected cancer but are rarely performed in CP/CPPS patients due to the non-urgency and low threat to life posed by the condition. Liquid biopsies represent a promising non-invasive approach for

investigating potential biomarkers in both diseases. This study aimed to evaluate the promoter methylation and gene expression of seven selected PCa-associated TSGs *(EDNRB, CDKN2A, PTGS2, PITX2, GSTP1, BMP7,* and *BMP4*)[62,76,86,102–106] in the EJ and ExU of CP/CPPS patients and healthy controls. These seven TSGs were previously shown to be hypermethylated in PCa or highly correlated with PCa progression. Therefore, analyzing these TSGs in CP/CPPS patients may provide insight into the potential correlation between CP/CPPS and PCa. In addition, TSGs have been proven to be hypermethylated and less expressed in PCa, which makes them ideal candidates for indicating potential correlations between CP/CPPS and PCa. If significant differences in TSG hypermethylation are found in CP/CPPS patients compared to healthy controls, it may play a role in the management and prognosis of CP/CPPS patients and help evaluate potential risks between CP/CPPS and PCa. Furthermore, EJ and ExU have routinely analyzed CP/CPPS clinic materials to distinguish between Type IIIa and Type IIIb CP/CPPS, making them ideal materials for non-invasive biomarker development. By adopting liquid biopsy biomarkers for PCa in CP/CPPS, we would develop promising non-invasive approaches to identify potential biomarkers and gain insight into the potential correlation between CP/CPPS and PCa.

Based on the hypothesis mentioned above, the aims of the current investigation were:

- To investigate the potential epigenetic dysregulation of TSGs associated with PCa in liquid biopsies, specifically EJ and ExU, obtained from patients diagnosed with CP/CPPS.
- To explore the possibilities of sorting epithelial cells and leukocytes from the liquid biopsies and evaluate the methylation and mRNA expression levels of *CDKN2A* in the sorted cell groups.
- To evaluate the correlation of methylation and mRNA expression levels of TSGs and clinical parameters.
- To assess the availabilities of liquid biopsies in the evaluation and prognosis of CP/CPPS

2. Materials and methods

2.1. Materials

2.1.1. Collection of liquid biopsies, selection of clinical parameters, and cryopreservation

45 EJ and 39 ExU samples from CP/CPPS Type III b patients (n=45), 30 EJ samples and 28 ExU samples from healthy donors without existing urological conditions (n=30) were recruited for the study. All samples were collected at the Clinic of Urology, Pediatric Urology and Andrology, JLU Giessen, from January 2011 to February 2016. The collected liquid biopsy samples were examined with clinical routines to confirm CP/CPPS diagnosis and obtain clinical parameters. In addition, ultrasound exams for prostate volume, as well as questionnaire results such as age, CPSI, and International Prostate Symptom Score (IPSS), were employed from the participants. Furthermore, parameters from blood samples, such as PSA and CRP, and semen parameters, such as motility and pH, were recruited for the correlation analysis. The criteria for recruited healthy men were (1) No current urinary system diseases. (2) No treatment history of urinary system diseases. (3) No abnormal parameters of the questionnaire and clinical exams.

Cell pellets of all collected EJ and ExU samples were prepared first and then stored at -80 degrees before use. All patients and healthy controls donated their written consent, and the study was approved by the Ethics Commission of the Medical Faculty of JLU Giessen (ethical vote, AZ 55/13).

2.1.2. Use of fresh liquid biopsies

In order to isolate epithelial cells and leukocytes by using MACS system, fresh EJ and ExU samples were additionally collected from 34 non-treatment CP/CPPS Type III b patients and 26 healthy donors and were directly used for subsequent experiments without cryo-storage. All samples were collected at the Clinic of Urology, Pediatric Urology and Andrology, JLU Giessen, between December 2020 and July 2021. All patients and healthy controls donated their written consent, and the study was

approved by the Ethics Commission of the Medical Faculty of JLU Giessen (ethical vote, AZ 55/13).

2.1.3. Equipment, chemicals and labware

2.1.3.1. Equipment

Device	Company
Benchtop Centrifuge (Universal 320)	Hettich, Germany
Biological safety cabinet (MSC-Advantage)	Thermo Fisher Scientific, Germany
Electrophoresis power supply PowerPac HC	Bio-Rad, Germany
Electrophoresis power supply PowerEase 500	Invitrogen, Karlsruhe
Cell culture CO_2 incubator (HERAcell 150i)	Thermo Fisher Scientific, Germany
CFX96 Touch™ Real-Time PCR Detection System	Bio-Rad, Germany
Eppendorf Thermo Mixer	Eppendorf, Germany
Gel documentation system (BioDocAnalyze)	Biometra, Germany
Heating block (LS 2)	VLM, Germany
HERAfreeze™ HFU T Series -86 °C Freezer	ThermoFisher Scientific, Germany
Heidolph Reax 2000 shaker	Heidolph, Germany
Julabo MP-5 Heating circulator	JULABO GmbH, Germany
Microlitre Centrifuge (MIKRO 220R, Fresco 21)	Hettich, Germany Thermo Fisher Scientific, Germany
Magnetic Stirrer (BLSH0007)	IKAMAG, Germany
Mastercycler	Eppendorf, Germany
Mettler Toledo AE 240 balance	Mettler Toledo, Germany
Microwave oven	LG, South Korea
Milli-Q. Direct Water Purification System	Merck KGaA, Germany
NanoDrop ND-1000	PEQLAB, Germany
Phase-contrast inverted microscope (CK2)	Olympus, Germany
Nikon C1 Inverted Confocal Microscope	Nikon Instruments, Germany
PyroMark Q24 Cartridge	QIAGEN, Germany
Pyromark Q24 instrument	QIAGEN, Germany

SevenEasy S20-K pH meter	Mettler Toledo, Germany
Standard Mini-Centrifuge	Fisherbrand, Germany
T100™ Thermal Cycler	Bio-Rad, Germany

2.1.3.2. Chemicals

Reagent	Company
Acetic acid	Roth, Karlsruhe
Aceton	Roth, Karlsruhe
Agarose	Roth, Karlsruhe
Ammonium chloride (NH4Cl)	Roth, Karlsruhe
Bovine serum albumin (BSA)	Sigma-Aldrich, Steinheim
Chloroform	Roth, Karlsruhe
Diethypyrocarbonate (DEPC)	Sigma-Aldrich, Steinheim
Ethanol	Sigma-Aldrich, Steinheim
Ethylenediamine tetraacetic acid (EDTA)	Roth, Karlsruhe
Glycogen	Invitrogen, Karlsruhe
Histopaque®-1077	Sigma-Aldrich, Steinheim
Hydrogen chloride (HCl), 36%	Roth, Karlsruhe
Isopropanol	Sigma-Aldrich, Steinheim
peqGOLD TriFast™	VWR, Erlangen
Phosphate buffered saline (PBS)	Sigma-Aldrich, Steinheim
Sodium acetate (NaOAc)	Roth, Karlsruhe
Sodium hydroxide (NaOH)	Roth, Karlsruhe
Tetrasodium EDTA	Roth, Karlsruhe
Triton X-100	Sigma-Aldrich, Steinheim
Tween-20	Roth, Karlsruhe

2.1.3.3. Cell culture

Device/ reagent	Company
BD falcon 6-well plates, 10cm plates	BD falcon, Franklin Lake, USA
Cell Tracker green-CMFDA	Invitrogen, Karlsruhe

Dulbecco's Modified Eagle Medium (DMEM)	Life Technologies, Darmstadt
Dulbecco's Modified Eagle Medium (DMEM)-F12	Gibco, Darmstadt
Fetal calf serum	Biochrom AG, Berlin
LPS (Cat. No. L4391)	Sigma-Aldrich, Darmstadt
Penicillin/Streptomycin	Gibco, Darmstadt
PMA (Phorbol-12-Myristate-13-acetate) (Cat. No. ab120297)	Abcam, Cambridge (UK)
Recombinant Human IFNγ (Cat. No. 300-02)	Peprotech, Hamburg
Recombinant Human IL-13 (Cat. No. 200-13)	Peprotech, Hamburg
Recombinant Human IL-4 (Cat. No. 200-04)	Peprotech, Hamburg
Roswell Park Memorial Institute (RPMI)-1640 medium	Life Technologies, Darmstadt
Synth-a-Freeze cryopreservation	Gibco, Darmstadt
Total Exosome Isolation reagent (from urine) (Cat No. 4484452)	ThermoFisher Scientific, Germany
T-25 flasks	Life Technologies, Darmstadt
T-75 flasks	Life Technologies, Darmstadt
T-175 flasks	Life Technologies, Darmstadt

2.1.3.4. Magnetic-activated cell sorting (MACS)

Device/ reagent	Company
MACS Multistand	Miltenyi Biotec, Germany
CD326 (EpCAM) MicroBeads human (Cat. 130-061-101)	Miltenyi Biotec, Germany
CD45 MicroBeads human (Cat. 130-045-801)	Miltenyi Biotec, Germany
LS Column (Cat. 130-042-401)	Miltenyi Biotec, Germany
MS Column (Cat. 130-042-201)	Miltenyi Biotec, Germany
MidiMACS Separator (Cat. 130-042-302)	Miltenyi Biotec, Germany
MiniMACS Separator (Cat. 130-042-102)	Miltenyi Biotec, Germany
MACSprep Forensic Sperm MicroBead Kit, human (Cat. 130-125-280)	Miltenyi Biotec, Germany

2.1.3.5. Polymerase Chain Reaction (PCR) and real-time Polymerase Chain Reaction (RT-PCR)

Reagent	Company
dNTP Mix 10mM (Cat. U1515)	Promega, Mannheim
GelRed Nucleic Acid Gel Stain	Biotium, Fremont
HyperLadder™ 100bp	Meridian Bioscience Inc, USA
Hexamer	Invitrogen, Karlsruhe
M-MLV Reverse Transcriptase (Cat. M1705)	Promega, Mannheim
Oligo dT	Invitrogen, Karlsruhe
Orange G	Merck, Darmstadt
PyroMark PCR Kit (Cat. 978703)	QIAGEN, Hilden
RNasin Ribonuclease Inhibitor (Cat. N2511)	Promega, Mannheim
RNeasy Mini Kit (Cat No. 74104)	QIAGEN, Hilden
QuantiFast SYBR® Green PCR Kit (Cat. 204056)	QIAGEN, Hilden

2.1.3.6. Methylation analysis

Reagent	Company
EZ DNA Methylation kit (CT Conversion Reagent, M-Binding buffer, Zymo-Spin IC Column, Collection tube, M-Wash buffer, M-Desulphonation buffer, M-Elution buffer. Cat. D5002)	ZYMO Research, Germany
EpiTect PCR Control DNA Set (Cat. 59695)	QIAGEN, Hilden
PyroMark Annealing Buffer (Cat. 979009)	QIAGEN, Hilden
PyroMark Binding Buffer (Cat.979006)	QIAGEN, Hilden
PyroMark Denaturation Solution (Cat. 979007)	QIAGEN, Hilden
PyroMark Gold Q24 Reagents (Cat. 970802)	QIAGEN, Hilden
PyroMark Q24 plate (Cat. 979201)	QIAGEN, Hilden
PyroMark Wash Buffer QIAGEN (Cat. 979008)	QIAGEN, Hilden
Streptavidin-coated Sepharose beads (Cat. GE17-5113-01)	GE Healthcare, Freiburg

2.1.3.7. Immunofluorescence staining

Device/ reagent	Company
Goat Anti-Rat IgG (Alexa Fluor 555) preadsorbed (Cat. ab150166)	Abcam, UK
Anti-Cytokeratin 8+18+19 antibody (Cat. ab41825)	Abcam, UK
Anti-Prostate Specific Antigen antibody (Cat. ab140337)	Abcam, UK
CD45 Monoclonal Antibody (YAML501.4) (Cat. MA5-17687)	ThermoFisher Scientific, Germany
Goat anti-Mouse IgG (H+L) Superclonal™ Secondary Antibody, Alexa Fluor 488 (Cat. A28175)	ThermoFisher Scientific, Germany
Hoechst 33342, Trihydrochloride, Trihydrate - 10 mg/mL Solution in Water (Cat. H3570)	ThermoFisher Scientific, Germany
SuperFrost Plus Microscope Slides	R. Langenbrinck, Germany
Faramount Aqueous Mounting Medium	Dako, Denmark
ImmEdge Pen	VECTOR Laboratories, USA

2.2. Methods

2.2.1. Isolation of somatic cells from ejaculate (EJ) and post prostatic massage urine (ExU) samples

Isolation of somatic cells of EJ was processed by density gradient centrifugation. EJ pellet samples were thawed on ice once removed from a -80°C refrigerator and centrifuged at 1000x g for 10 min at 4°C. Cell pellets were then mixed well with 300 µL DMEM medium (without adding fetal bovine serum). The DMEM-cell suspension was added gently to the prepared 500 µL 90 % Histopaque-PBS solution and centrifuged at 400x g for 5 min, at 4°C. Then the supernatants were carefully aspirated and added on top of 1100 µL newly prepared 90 % Histopaque-PBS solution, centrifuged at 400x g for 20 min, at 4°C. Next, the supernatant was added to a new 2 mL Eppendorf tube (EP tube) and centrifuged at 13000 rpm for 2 min, 4°C. Then the cell pellets were used for DNA/RNA extraction.

ExU pellet samples were thawed on ice once taken from the -80°C refrigerator and centrifuged at 13000 rpm for 10 min, 4°C. Then the subsequent supernatant was

carefully discarded, and the remaining cell pellets were directly used for DNA/RNA extraction and immunofluorescence staining (IF).

2.2.2. Cell culture of PC3, DU145, LNCaP and THP-1 cells

Prostate cancer cell lines (PC3, DU145, and LNCaP) and monocyte cell line (THP-1) were used as controls for real-time polymerase chain reaction (RT-PCR) primers and primary and secondary antibodies for IF. All used culture mediums were prepared with 10% fetal bovine serum and 1% penicillin/streptomycin. First, cryovial-containing cells were taken out from liquid nitrogen and incubated in a 37°C water bath immediately until fully thawed. Next, 1 mL corresponding culture medium was added to the cryovial and mixed well. Next, the cell suspension was transferred into a 15 mL falcon and centrifuged at 280x g for 2 min at RT. Then the supernatant was carefully discarded, and the remaining cell pellet was mixed well with 1 mL culture medium. For PCa epithelial cells (PC3, DU145, and LNCaP), the cell suspension was added equably into a 10 cm culture dish. For THP-1 cells, the cell suspension was added to the T75 cell culture flask. Then 9 mL RPMI 1640 (for THP-1 and LNCaP), Dulbecco's Modified Eagle Medium (DMEM) (for DU145), and DMEM-F12 (for PC3) were added to the culture dish or the flask. Next, the cell suspension was gently mixed by swaying the culture dish or flask and kept at 37°C, 5% CO_2, in an incubator.

For prostate cancer cell lines, the cells were split after 2-3 days once the confluency reached approximately 80-90 %. First, the culture medium was aspirated thoroughly, 3 mL PBS solution was added to the dishes for cell washing, and then aspirated. Next, 1 mL trypsin solution was added to the culture dish and then incubated at 37°C, 5% CO_2, in an incubator for 2-5 min until most cells detached from the dish. Then 2 mL culture medium was added and gently pipetted. The cell suspension was on the bottom of the dish to wash down the remaining cells. Then, the cell suspension was transferred to a new 15 mL falcon and centrifuged at 280x g for 2 min. Next, the supernatant was carefully discarded, and the cell pellet was resuspended by 3-4 mL culture medium (depending on the final amount of dishes needed). Then 1 mL cell suspension and 9 mL culture medium were added to each culture dish, and the dish was kept at 37°C, 5% CO_2 in the incubator.

For THP-1 cell line, the whole cell suspension was aspirated and transferred to a new 15 mL falcon. After centrifugation at 280x g for 2min, the supernatant was discarded and resuspended by 3-4 mL culture medium (depending on the final amount of flasks needed). Next, 1 mL cell suspension and 9 mL culture medium were added to each flask and kept at 37°C, 5% CO_2, in the incubator.

For cell cryopreservation (both prostate cell lines and THP-1 cell line), cells were harvested as described above, then the cell pellets were resuspended in a cell-freeze medium (1 mL per $5x10^5$ – $1x10^6$ cells). After that, each cryovial was added 1 mL cell-cell freeze medium mixture and the vials were kept in a cell freezing container at -80°C. On the second day, the vials were transferred into liquid nitrogen.

2.2.2.1. Polarization of THP-1 cells into M0, M1, M2 macrophages and exosome treatment

THP-1 cell line was also used for the exosomes treatment experiment. After the preparation of THP-1 cells as described above, the number of THP-1 cells was counted, and 1.25x 10^6 cells were seeded in each well of a 6-well plate. 2 mL RPMI 1640 medium with phorbol-12-Myristate-13-acetate (PMA) (20 µg/mL) were then added to each well and kept in an incubator at 37°C, 5% CO_2. After 48 h, the cells were polarized and attached to the wells. RPMI 1640 with PMA medium was aspirated, and 1 mL 1x PBS was added to each well for washing. Then 2 mL FCS-PMA-free RPMI 1640 medium was added to each well and incubated in an incubator for 24 h at 37°C, 5% CO_2. The next day, the FCS-PMA-free RPMI 1640 medium was aspirated and washed as described before. Next, the differentiated M0 macrophages were divided into four groups: (1) M0 unpolarized control, with 2 mL FCS-RPMI 1640 medium. (2) M1 macrophages, with IFN-γ (40ng/mL) and LPS (20pg/mL) in 2mL FCS-RPMI 1640 medium. (3) M2 macrophages, with IL-4 (40ng/mL) and IL-13(40 ng/mL) in 2 mL FCS-RPMI 1640 medium. (4) Exosomes treatment group, with 25uL exosome in 1.975 mL FCS-RPMI 1640 medium. Each group was doubled and kept at 37°C, 5% CO_2 for 24h and 48h, respectively.

For each well, cells were then trypsinized (1 mL/ well) at 37°C for 7-8 minutes. Following was an addition of 2 mL FCS-RPMI 1640 medium to the wells and then a thoroughly mix

of the cell suspension. The in total 3 mL cell suspension was averagely divided into two 2 mL EP tubes, followed a centrifugation at 550g for 5 min. One of the two tubes was mixed well with 1 mL Synth-a-Freeze CTS freezing medium and frozen at -80°C. Cells from another tube were directly used for RNA extraction.

2.2.3. Immunofluorescence staining (IF)

A volume of 100-150 µL prepared cell suspension (cell lines or collected somatic cells isolated from EJ and ExU) was added directly on SuperFrost Plus microscope slides and left at RT until fully air-dried. Then the slides were incubated in pure pre-cold acetone for 20 min and washed 3 times with PBS solution for each 5 min. Next, 100-150 µL of 0.1% Triton-X100 was added directly to the cells and incubated in a moisture chamber at RT for 10 min. The slides were then washed with PBS for 5 min, three times, blocked with 1% Bovine serum albumin (BSA) solution (1% in 1x PBS solution) in the moisture chamber for 30 min at RT. Primary antibody (PSA, 1:100, ab140337, Abcam; CK8/18/19, 1:100, ab41825, Abcam; CD45, 1:500, MA5-17687, ThermoFisher Scientific) was diluted in 1% BSA solution during the blocking. After the blocking 1 % BSA solution was discarded, the primary antibody was directly added to the samples (150 µL per sample) and incubated at 4°C overnight. When it was multi-channel staining, primary antibodies were added subsequently. The incubations were at RT for 1 h and then washed for 5 min, 3 times. The last added primary antibody was incubated at 4°C overnight. On the second day, secondary antibodies were prepared beforehand. Secondary antibodies (Alexa Fluor 555, 1:1000, ab150166, Abcam; Alexa Fluor 488, 1:1000, A28175, ThermoFisher Scientific) and Hoechst 33342 (1:500, H3570, ThermoFisher Scientific) were diluted together in 1% BSA solution. The slides were washed for 5 min 3 times, and the prepared secondary antibody solution was dropped onto the samples directly (150 µL per sample) and incubated for 1h at RT. Next, the slides were washed for 5 min, 3 times, and mounted with mounting medium.

2.2.4. DNA/RNA extraction from liquid biopsies

peqGOLD TriFast was used for DNA and RNA extraction from somatic cells of frozen EJ and ExU pellets and the sorted epithelial cells and leukocytes from fresh EJ and ExU samples. First, the cell pellet was lysed well by pipetting up and down with 1 mL peqGOLD TriFast in a 2 mL microcentrifuge tube. Then 200 µL chloroform was added and mixed thoroughly. After incubation at RT for 5 min without agitation, the lysate was centrifuged at 13000 rpm for 10min at 4 °C. The lysate was then separated into upper transparent aqueous phase (RNA), interphase, and lower organic phase (DNA). The aqueous phase was carefully transferred to a new 1.5 mL tube, following the addition of 500 µL 100 % isopropanol, 20 µL sodium acetate (NaOAc), and 5 µL 20% glycogen. The mixture was vortexed shortly. Next, 600 µL 100% ethanol, 5 µL 20% glycogen, and 30 µL NaOAc were added to the left interphase and organic phase, vortexed thoroughly, and shaken by hand vigorously. Both DNA and RNA parts were precipitated at -20 °C overnight. DNA and RNA parts were centrifuged for 20 min at 4°C, 13000 rpm on the second day. Then the supernatant was carefully discarded, and 300 µL 70 % ethanol was added to RNA and DNA pellets without mixing. After centrifugation at 13000 rpm, 4°C for 5 min, the supernatant was discarded, and the DNA and RNA pellets were air-dried until the pellets became nearly transparent. RNA pellet was dissolved in 20 µL DEPC water, and DNA was in 30 µL ddH2O. The concentration of DNA and RNA samples were measured by NanoDrop 1000.

RNeasy Mini Kit (Cat. 74104, QIAGEN) was used for RNA extraction from the THP-1 cell line and the polarized macrophages. All reagents and columns mentioned below were from the kit. After pelleting the cells, 600 µL of Buffer RLT buffer was mixed with the cell pellet, then 600 mL 70% ethanol was added to the lysate and mixed well by pipetting. The RNeasy Mini spin column was placed in a supplied 2 mL collection tube, and 600 µL of the lysate was then transferred, following centrifugation for 1 min at 13000 rpm. The flow-through was then discarded. The other 600 µL lysate was added to the RNeasy Mini spin column and centrifuged at 13000 rpm for 1 min. Next, 350 µL buffer RW1 was added to the column membrane and centrifuged at 13000 rpm for 1 min. Then 80 µL DNase I incubation mix (10 µL DNase I stock solution +70 µL buffer RDD) was added directly onto the column membrane, left at benchtop for 15 min at RT, following the addition of 350 µL buffer RW1 and centrifuged at 13000 rpm for 1

min. Again, the flow-through was discarded, and 500 µL RPE buffer was added to the column, centrifuged at 13000 rpm for 1 min, and the flow-through was discarded again. Then 500 µl RPE buffer was added to the column membrane and centrifuged at 13000 rpm for 2 min. Next, the column was placed in a new 1.5 mL collection tube, and 50 µL RNase-free water was added directly to the bcolumn membrane and centrifuged at 13000 rpm for 1 min to elute the RNA. The extracted RNA concentration was measured by NanoDrop 1000.

2.2.5. DNA promoter methylation analysis

2.2.5.1. Bisulfite treatment of DNA

Bisulfite treatment of all DNA samples was handled by EZ DNA Methylation Kit (Cat. D5002, ZYMO Research). All reagents and columns mentioned below were from this kit. An amount of 200-500ng per DNA sample was used for the bisulfite treatment. Thus, 5 µL M-Dilution buffer was added to the DNA sample in a 200 µL tube, and a total volume of 50 µL was reached by adding Milli-Q water. The solution was mixed well and then incubated at 37 °C for 15 min in a PCR machine. After that, 100 µL prepared CT Conversion Reagent was added to the sample and mixed well by pipetting up and down following incubation at 50 °C for 16 h in a PCR machine and kept at 4 °C for at least 10 min (no more than 20 h). On the second day, 400 µL of M-Binding buffer was added to Zymo-Spin IC Column and placed into a provided Collection tube. Then the sample was added into the Zymo-Spin IC Column containing M-Binding buffer and mixed by inverting the column serval times. Next, the sample was centrifuged at 13000 rpm for 30 s at RT, and the flow-through was discarded. Next, a 100 µL M-Wash buffer volume was added onto the column and centrifuged at 13000 rpm for 30 s at RT. After that, 200 µL M-Desulphonation buffer was added to the column and followed by incubation for 18 min at RT. Then the column was centrifuged at 13000 rpm for the 30 s. For washing purposes, 200 µL M Wash buffer was added to the column and centrifuged at 13000 rpm for 30 s. This step was repeated once. Next, the column was put onto a new 1.5 mL microcentrifuge tube, and 20 µL M-Elution buffer was added to the column matrix, incubated for 2 min and then

centrifuged at 13000 rpm for 30 s. The flow-through containing bisulfite treated single strain DNA (ssDNA) (20 µL) and was ready for PCR of subsequent pyrosequencing.

2.2.5.2. Control PCR and Pyrosequencing

The ssDNA sample was used for pyrosequencing. All primers with desired gene regions were designed and ordered from QIAGEN (Table 1). All the reagents mentioned below were from PyroMark PCR Kit (Cat. 978703, QIAGEN). For each sample, 12.5 µL Pyromark PCR Master Mix 2x, 2.5 µL CoralLoad Concentrate 10x, 2.5 µL primer, 6 µL ddH2O, and 1.5 µL template ssDNA sample were mixed well for PCR.

The PCR protocol is as below:

1. 95°C for 15 minutes,
2. 94°C for 30 seconds
3. 56°C for 30 seconds,
4. 72°C for 30 seconds

   Repeated to step 2 for 45 times

5. Final extension at 72°C for 10min
6. 4°C on hold

A 2 % agarose gel was prepared for electrophoresis to check the PCR amplification quality. 5 µL of 1x ladder and 4 µL of the PCR product (per sample) were loaded on the gel. The electrophoresis was conducted under 120 V for 25 min- 35 min, according to the size of the gel. The gel was checked under UV light, and only samples showing the specific band with the correct size were used for pyrosequencing.

Table 1: Primers for Pyrosequencing from QIAGEN

Gene	Sequence to analyze	Numbers of CpG sites	Amplicon length
CDKN2A_02 PM00039907	TCGCTAAGTGCTCGGAGTTAATAGCACC TCCTCCGAGCACTCGCTCACGGCGT	6	199
BMP4_01 PM00056525	ACGCGAGCCTGAGACGCCGCTGCTGCTC CGGC	5	196

BMP7_01 PM00079345	TGTCGGCGTCGGT	3	235
EDNRB_02 PM00054768	CGTCTTAGTTAAGCGTGCGTGGGAACC GCGGA	5	184
PTGS2_01 PM00000525	CTTTTCTTCTTCGCAGTCTTTGCCCGAG CGCTTCCGA	4	211
PITX2_02 PM00019425	GGCAGCGCCGCCTGGGAGGGCGCCGG TGGGGCGC	5	246
GSTP1_02 PM00151816	CCCTCCCCGGGTTGCTGCGAGGCGGA GTCGGCCCGGT	5	251

The rest of the 21 µL of PCR product was used for the pyrosequencing. A pre-run information sheet was prepared using PyroMark software to define the running program beforehand. Approximately 40 mL ethanol (70%), 40 mL Denaturation buffer (Cat. 979007, QIAGEN), 50 mL 1x Wash Buffer (Cat. 979008, QIAGEN), 50 mL Milli-Q water, and 70 mL Milli-Q water were added into the provided two plastic troughs, respectively, and put on the PyroMark Q24 Vacuum Workstation. The reaction solution was prepared by mixing 1 mL Binding buffer (Cat. 979006, QIAGEN), 100 µL streptavidin-coated Sepharose beads (Cat. GE-17-5113-01, GE Healthcare) with 400 µL Milli-Q water in a 2 mL tube (for 24 samples). A 60 µL of the mixed reaction solution was added to the wells of a 96-well plate, respectively. Then the PCR products were added to corresponding wells according to the pre-run information sheet. The plate was sealed with a dedicated glue film and shaken at 1400 rpm for 10 min. During the shaking, 25 µL of 1 x sequencing primer solution was added in the wells of a PyroMark Q24 plate (Cat. 979201, QIAGEN), and the corresponding volume of enzyme, substrate, dATP, dCTP, dTTP, and dGTP (Cat. 970802. QIAGEN) were subsequently added to the cartridge based on the pre-run information. Next, the cartridge was carefully inserted into the PyroMark Q24 machine. After the shaking, the vacuum pump was turned on and applied vacuum to the vacuum tool by opening the vacuum switch. For flushing the probes, the vacuum pump was washed by lowering the probes into the trough with Milli-Q water. Then the vacuum pump carefully lowered into the 96-well plate to capture the beads containing the immobilized template for 15 s without touching the wall and bottom of each well. Then the tool was transferred to the trough containing 70% ethanol for 5 s, next to the trough containing Denaturation solution for 5 s, and finally to the trough with wash buffer for 15 s. For draining liquid from the filter probes, the tool was raised beyond 90 °C vertically for 5 s. The vacuum was switched

off and waited for 1 min until the pressure in the tube was relieved. Beads were then released in the PyroMark Q24 plate containing the sequencing prime by agitating the tool gently. Incubation took place on the PyroMark Q24 plate holder at 80 °C for 2 min, and then the plate was cooled on a cool plate holder and left at RT for 8 min. During the waiting time, the vacuum pump was washed in the second trough containing Milli-Q water. The cooled plate was carefully put in the PyroMark Q24 machine, and the pyrosequencing program was started. Results were processed by PyroMark Q24 software, and percentages of methylation levels were archived.

2.2.6. mRNA expression analysis

2.2.6.1. Reverse transcription

300-600 ng RNA sample (EJ: 600ng, ExU: 300ng) was used for reverse transcription. A mix of 4 µL M-MLV 5X Reaction buffer (provided with M-MLV RT (H-) Point Mutant), 5 µL 10mM dNTP solution (Cat. U1515, Promega), 1 µL 1x Oligo (dT), 1 µL Hexamer and a corresponding amount of RNA were prepared in a 200 µL centrifuge tube, and the total reaction volume was adjusted to 20 µL by RNase-Free water. The sample was incubated at 62 °C for 10 min and put on ice immediately. Next, 1 µL M-MLV Reverse Transcriptase (Cat. M1705, Promega) and 0.5 µL RNasin Ribonuclease Inhibitor (Cat. N2511, Promega) were added to the reaction mixture (per sample) and mixed well by pipetting up and down. Samples were incubated at 42 °C for 1 h and 90 °C for 5 min. The reverse transcribed cDNA samples were used for RT-PCR.

2.2.6.2. RT-PCR

For each sample, 5 µL 2x QuantiFast SYBR Green PCR Master Mix (Cat. 204056, QIAGEN), 0.5 µL 1x forward primer, 0.5 µL 1x reverse primer, 3 µL DEPC H_2O and 1 µL cDNA template were mixed in the well of reaction plate. The running protocol is as below:

1. 95°C for 5min
2. 95°C for 10s

3. 55.7°C-60°C for 45s

Repeated to step 2 for 45 times

4. 65°C- 95°C, 0.5°C gradient
5. 12°C on hold

The primer sets for RT-PCR (Table 2) are shown below:

Table 2: Primer sets used for mRNA expression level quantification

Gene	Forward primer	Reverse primer	Product length	Annealing temperature
CDKN2A	GACCTGGCTGAGGAGCTG	AATCGGGGATGTCTGAGGGA	124	55.7°C
BMP4	CTTCCACCACGAAGAACATCT	GGAGATCACCTCGTTCTCAGG	106	60°C
BMP7	GGGCTTCTCCTACCCCTACA	TGTTCCACGAGGTTGACGAA	123	55.7
EDNRB	CTTGCCATTGGCCATCACTG	CCACTTCCCGTCTCTGCTTT	116	59°C
PTGS2	GCTGTTCCCACCCATGTCAA	AAATTCCGGTGTTGAGCAGT	116	58°C
PITX2	CGTGTGTGCAATTAGGCGT	GAGAGTCCGTGAACTCGACC	90	60°C
GSTP1	CAGGAGGGCTCACTCAAAGC	AGGTGACGCAGGATGGTATTG	101	60°C
GAPDH	GCAAATTCCATGGCACCGT	TCGCCCCACTTGATTTTGG	106	60°C

2.2.7. MACS cell isolation using EJ samples

Epithelial cells and leukocytes somatic cells of fresh EJ and ExU samples were sorted by MACS for methylation and RNA expression measurement of *CDKN2A*. MACSprep™ Forensic Sperm MicroBead Kit, human (Cat. 130-125-280, Miltenyi Biotec) was used to eliminate the sperms in EJ samples. All reagents and buffers for sperm elimination were from this kit. Overall, 300-500 µL of fresh native EJ sample was used for the isolation. The native EJ sample was transferred into a 1.5 mL tube and centrifuged at 1000x g, 4 °C for 10 min. The seminal plasma (supernatant) was discarded carefully. Based on the size of the pellet, 40-60 µL of prepared Free-DNA removal buffer plus 40-60 µL Anti Spermatozoa Microbeads (Free-DNA removal buffer: Anti Spermatozoa Microbeads=6:4) were added and mixed well with the pellet, followed an incubation for 20 min at RT without agitation. An LS column (Cat. 130-042-401, Miltenyi Biotec) was placed in the magnetic field of a MidiMACS Separator

(Cat. 130-042-302, Miltenyi Biotec). The column was rinsed with 3 mL of MACSprep Forensic Buffer at 1 min before the end of the incubation. Subsequently, the incubated cell suspension was mixed with 1 mL MACSprep Forensic Buffer and applied directly to the MS column. Another 1 mL MACSprep Forensic Buffer was added to the empty 1.5 mL tube and then transferred to the column to recover residual material. The column was washed with 3 mL of MACSprep Forensic Buffer another two times. Then the column was removed from the separator, and 5 mL MACSprep Forensic Buffer was pipetted onto the column after the last washing. The magnetically labeled cells were flushed out by firmly pushing the plunger into the column. The flow-through contained unlabeled somatic cells and sperms were absorbed on the column.

The flow-through was centrifuged at 1000x g for 5 min at RT, and the pellet was resuspended with 70-80 µL sorting buffer (1x PBS solution containing 1% BSA and 2 mM EDTA (PH=7.2)) and 20-30 µL CD326 (EpCAM) MicroBeads, human (Cat. 130-061-101, Miltenyi Biotec). After incubation for 20 min at 4 °C, 1 mL sorting buffer was added to the cell suspension and centrifuged at 1500x g at RT for 5 min. The supernatant was discarded, and the pellet was resuspended with 500 µL sorting buffer. A new MS column (Cat. 130-042-201, Miltenyi Biotec) was then placed onto a MiniMACS Separator (Cat. 130-042-102, Miltenyi Biotec) and rinsed by adding 500 µL sorting buffer. The resuspended cell solution was added directly to the column and followed by three washing steps with 500 µL sorting buffer. The flow-through containing leukocytes was collected in a 15 mL centrifuge tube. Epithelial cells were bound on the column and were put on a new 15 mL centrifuge tube. The magnetically labeled epithelial cells were immediately flushed out by firmly pushing the plunger supplied with the column. This step was repeated once. These two 15 mL centrifuge tubes were centrifuged at 1500x g for 5 min at RT. The epithelial cells were directly processed to peqGOLD TriFast DNA/RNA extraction, and the leukocyte pellet was resuspended with 70-80 µL sorting buffer and mixed well with 20-30 µL CD45 MicroBeads, human (Cat. 130-045-801, Miltenyi Biotec), followed an incubation for 20 min at 4°C. 1 mL of sorting buffer was then mixed with cell suspension and centrifuged at 1500x g for 5 min at RT. Next, the pellet was used for cell sorting, and the procedure was identical to the isolation protocol of epithelial cells. The sorted leukocytes were directly processed into DNA/RNA extracts.

2.2.8. MACS cell isolation using ExU samples

Isolations of epithelial cells and leukocytes from ExU were identical to the procedure of EJ without the sperm isolation step.

2.2.9. Exosomes isolation using ExU supernatant

Exosome isolation was performed with Total Exosome Isolation reagent (from urine) (Cat No. 4484452, ThermoFisher Scientific). First, frozen ExU supernatant samples were fully thawed in a 37°C water bath. Next, 2 mL ExU supernatant was transferred to a new tube and was mixed well with 1 mL of the Total Exosome Isolation (from urine) reagent, followed by incubation at RT for 1h and then centrifuged at 10000x g for 1h at 4°C. After discarding the supernatant, the exosome pellet was resuspended in 150 µL autoclaved ddH2O and stored at -20°C or directly used for cell treatment.

2.2.10. Statistical analysis and used software

Data calculations and statistical analyses were performed with Microsoft Excel (Microsoft Corporation, Redmond, WA, USA), SPSS 26.0 software (IBM, Chicago, USA), and Prism 9.0 (GraphPad) by setting $p<0.05$ as significant. Statistical analysis between values within two groups was analyzed by the Mann-Whitney U test (two-tailed). Mean values, including ranges (lowest to highest), were calculated for characteristics of patients and healthy controls at baseline, and an overview of methylation and mRNA expression results in genes of the target. Relationships between variables were calculated with Spearman`s rank correlation.

3. Results

3.1. Detection of PC3 and THP-1 cells using IF

Somatic cells in EJ and ExU samples were the target of our experiment, so proving the existence and an overview of the cell proportion of epithelial cells and leukocytes in both EJ and ExU samples was crucial. IF was used as a method for the verification experiments. Cytokeratins (CKs) are groups of intermediate filament proteins which can form cytoskeleton, helping the cells to resist mechanical stress. They are affluent in epithelial cells[107–109]. Protein tyrosine phosphatase, receptor type C (PTPRC), known as CD45, is a cell membrane maker highly expressed in all leukocytes[110,111].

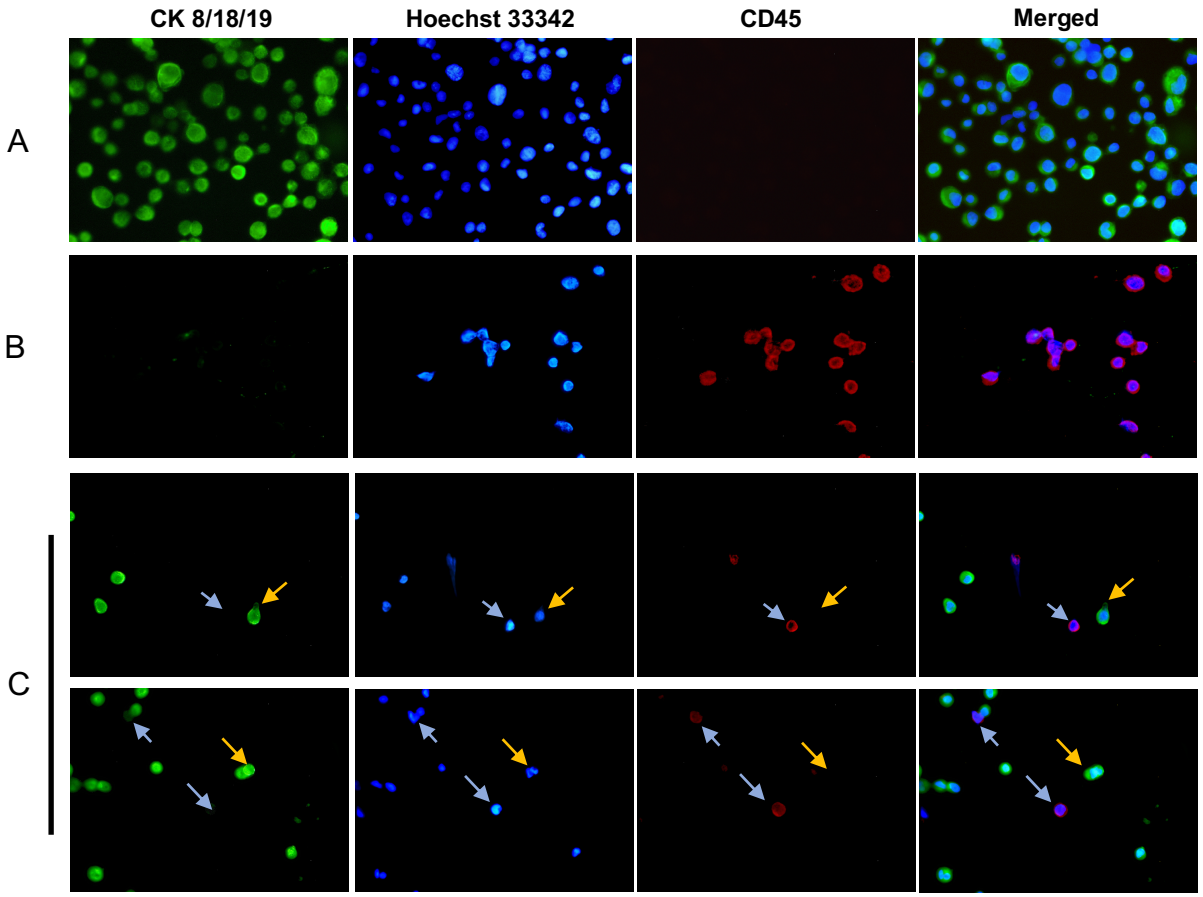

Figure 2: PC3 and THP-1 cells were distinguished using IF. (A) PC3 cells were used as a positive control for CK 8/18/19 primary antibody. PC3 cells were only CK 8/18/19 (+) and CD45 (-). (B) THP-1 cells were used as a positive control for CD45 primary antibody. THP-1 cells were only CD45 (+) and CK 8/18/19 (-). (C) PC3 and THP-1 cells. PC3 cells with green signal (CK 8/18/19 +) and THP-1 cells with red signal (CD45 +) were shown in the same field. PC3 cells and THP-1 cells were specifically distinguished, and no unspecific staining existed. Yellow arrow: PC3 cells. Blue arrow: THP-1 cells.

Because of the homogeneity of cultured cells, PC3 and THP-1 cells were used as controls of prostatic epithelial cells and leukocytes and were represented in the same field (Figure 2). PC3 and THP-1 cells were mixed in a ratio of 1:1. CK 8/18/19 and CD45 were used as primary antibodies detecting PC3 cells and THP-1 cells, respectively, and correspondingly Alexa Fluor 488 (green signal) and Alexa Fluor 555 (red signal) were used as secondary antibodies. PC3 cells were defined as CK 8/18/19+, CD45- and Hoechst 33342+. THP-1 cells were defined as CD45+, CK 8/18/19- and Hoechst 33342+. Dots or particles that are either only CK/8/18/19 and CD45 positive or Hoechst 33342 positive were not defined as cells. The primary and secondary antibodies are effective and specific with homogeneous prostatic epithelial cells and leukocytes.

3.2. Verification of IF primary and secondary antibodies in EJ and ExU samples

The performance of the primary and secondary antibodies in the native samples was furtherly tested using native EJ and fresh urine samples. PC3 cells and THP-1 cells were mixed at portion 1:1 and added to fresh EJ (≈ 3.6 mL) and fresh urine samples (50 mL). The process of collection of ejaculate somatic cells (ESCs) and fresh urine pellet was also done to mimic the actual operation when other samples arrived to us. Sperm cells from EJ were first excluded by using gradient density centrifugation. Then, the ESCs and pellets from the urine sample were used for IF.

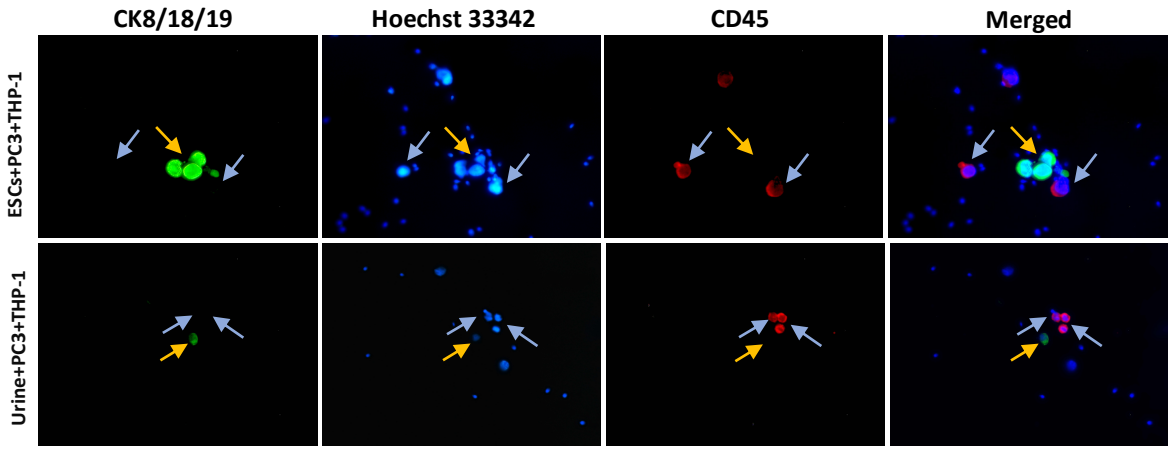

Figure. 3: Epithelial cells/PC3 cells and leukocytes/THP-1 cells can be distinguished in native ESCs and fresh urine samples. Epithelial cells/PC3 cells are CK 8/18/19+ and CD45-. Leukocytes/THP-1 cells are CD45+ and CK 8/18/19-. Yellow arrows: epithelial/ PC3 cells. Blue arrows: leukocytes/ THP-1 cells

As in homogeneous cultural conditions, epithelial cells/PC3 cells and leukocytes/THP-1 cells are able to be distinguished in native EJ and fresh urine samples (Figure 3). However, CKs and CD45 are general markers for epithelial cells and leukocytes, so the added cultural cells were difficult to be distinguished from epithelial cells and leukocytes from ESCs and somatic cells of fresh urine. Here, epithelial cells/PC3 cells and leukocytes/THP-1 cells are shown in the same field and can be distinguished. Consequently, the primary and secondary antibodies are practical and specific in native EJ and urine samples.

3.3. Detection of epithelial cells and leukocytes in EJ and ExU

Figure 4 demonstrates somatic cells in frozen EJ and ExU without adding cultured cells. Sperm cells of EJ were excluded as described above, and only the rest somatic cells were used for IF. As the IF results above show, epithelial cells with green and leukocytes with red signals. In ESCs and somatic cells from ExU, epithelial cells and leukocytes exist. In ExU, the number of somatic cells is more than ESCs after the elimination of sperms cells.

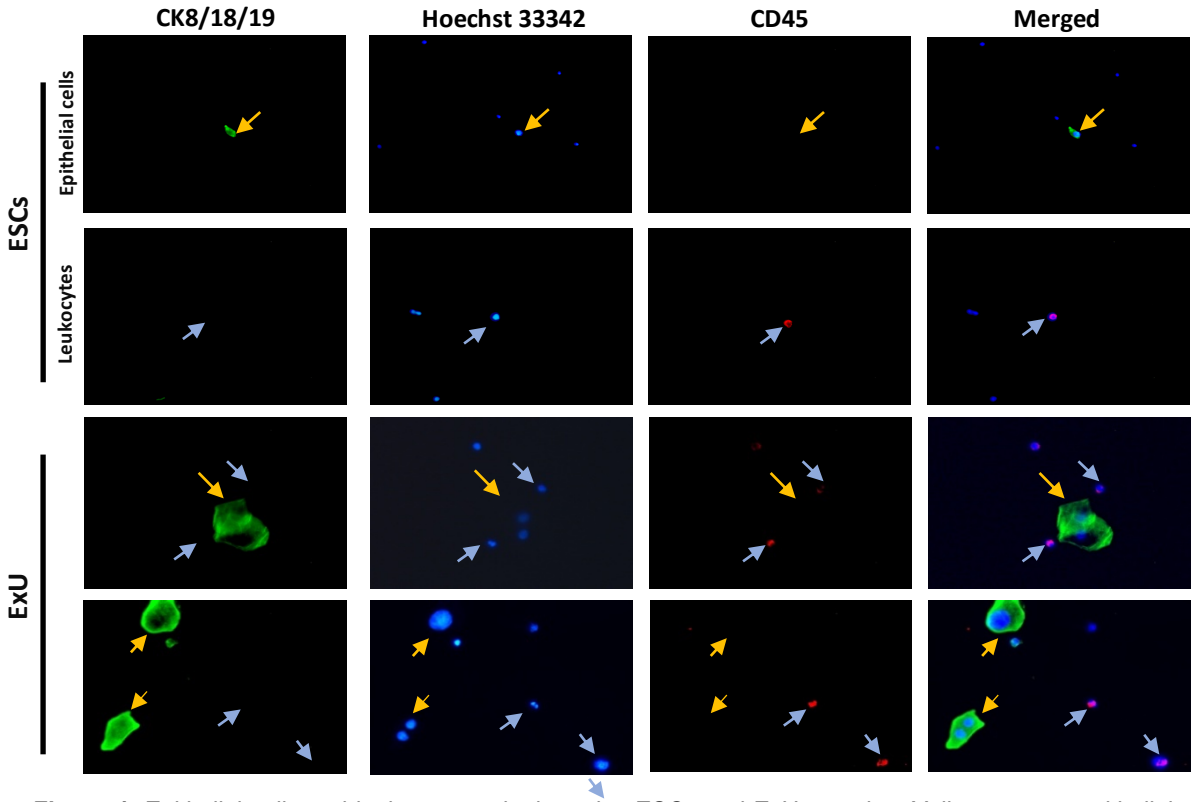

Figure 4: Epithelial cells and leukocytes exist in native ESCs and ExU samples. Yellow arrows: epithelial cells. Blue arrows: leukocytes.

3.4. Validation of pyrosequencing using methylated, unmethylated control DNA and prostate cancer cell lines

Before measuring the methylation ratio of the selected TSGs in ESCs and somatic cells from ExU, verification experiments were done to define the efficiency of pyrosequencing and test the feasibility of the handling procedures for subsequent experiments. Table 3 shows that methylation levels of selected TSGs were measured in methylated control, unmethylated control, PC3, LNCaP, and DU145 cell lines, respectively. Hypermethylation of each selected TGS could be detected in methylated controls. In the methylated control group, promoter methylation levels of each selected TSG are between 82.17%- 98.67%. The unmethylated group shows a significantly lower methylation level for all genes ranging from 0.6% to 7.29%, which is not above 8%.

Table 3: Methylation levels of selected TSGs in methylated control, unmethylated control and prostate cancer cell lines

Control groups	*EDNRB*	*CDKN2A*	*PITX2*	*BMP7*	*PTGS2*	*BMP4*
Methylated DNA	96.60%	82.17%	95.60%	98.67%	88.67%	98.20%
Unmethylated	0.60%	1.00%	1.00%	7.29%	3.33%	2.60%

PCa cell lines	*EDNRB*	*CDKN2A*	*GSTP1*	*PITX2*	*BMP7*	*PTGS2*	*BMP4*
PC3	84.60%	92.50%	26.6%	9.60%	49.67%	55.67%	97.40%
LNCaP	13.40%	1.50%	61.6%	56.80%	42.00%	60.67%	94.00%
DU145	64.00%	1.83%	64.0%	41.80%	26.33%	68.33%	9.40%

Methylation levels are heterogeneous in prostate cancer cell lines. The selected TSGs showed hypermethylation (>15%) in 16 out of 21 tests of all three cell lines. Methylation levels of *PTGS2, BMP7,* and *GSTP1* were from 26.33% to 68.33%, and these genes were hypermethylated in all three cell lines. *PITX2*, *EDNRB*, and *BMP4* showed hypermethylation in two cell lines ranging from 41.8% to 97.4%. *CDKN2A* showed a 92.5% of methylation level in the PC3 cell line.

3.5. The majority of somatic cells in EJ and ExU are leukocytes

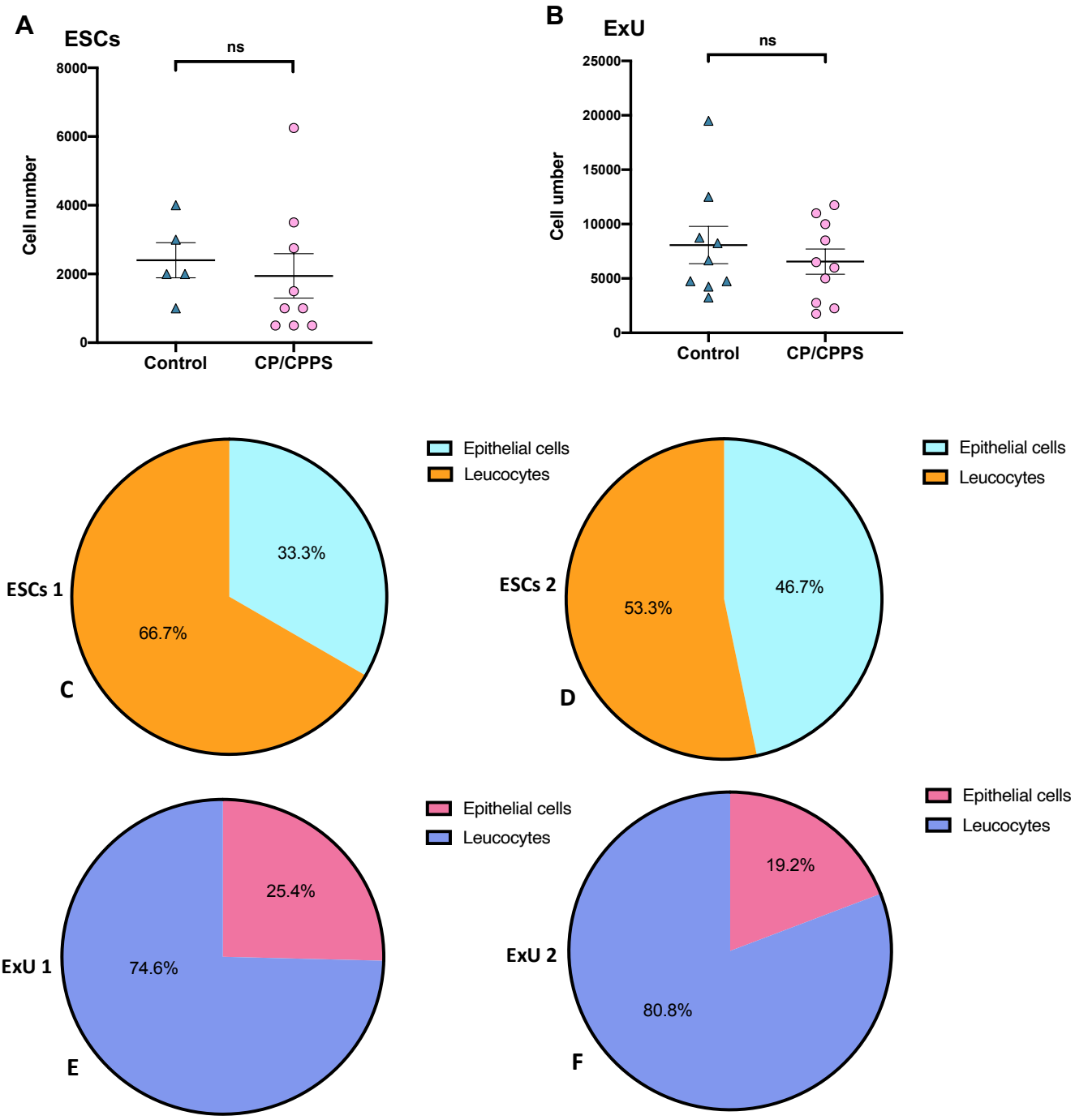

Figure 5: The number of somatic cells and the proportion of epithelial cells and leukocytes in ESCs and ExU samples were counted. (A) The ESCs in the 5 samples from healthy controls ranged from 1000 - 4000; in 9 samples from CP/CPPS patients, they were from 600 - 6200. (B) The numbers of somatic cells in 9 ExU samples from healthy controls ranged from 3000-20000, and in 10 samples from CP/CPPS patients, were from 1000- 12000. (C-D) In 2 frozen ESCs samples, leukocytes occupied the central portion of all cells (66.7% and 53.3%, respectively). (E-F) In 2 frozen ExU pellets, like in ESCs, leukocytes also occupy the central portion (74.6% and 80.8%, respectively).

The number of somatic cells in EJ and ExU samples is unknown and varies. Due to the volume variety of each sample, the cell amount may affect the efficiency of DNA/RNA extraction. Figure 5 shows the total number and composition of somatic cells in EJ and ExU samples. 5 EJ and 9 ExU samples from healthy controls, and 9 EJ and 10 ExU samples from CP/CPPS patients were enrolled. Overall, there are more karyocytes in ExU pellets compared to ESCs. In addition, in both ESCs and ExU pellets, leukocytes occupy the majority, and healthy control showed a slightly higher amount of cells than CP/CPPS patients.

3.6. Promoter hypermethylation of TSGs is observed in somatic cells in liquid biopsies of CP/CPPS patients

The DNA promoter methylation levels of selected TSGs in the CP/CPPS patient group and healthy controls in ESCs and ExU somatic cells were first evaluated. The characteristics, clinical exam parameters, average methylation and mRNA expression levels of selected TSGs of patients and healthy controls are summarized in Table 4-5 in the supplement. Heat maps of TSGs' average methylation levels in ESCs of each patient and healthy control are shown in Table 6-7 below. Actual sample numbers for pyrosequencing for each gene differed since PCR successfully amplified not each sample. For example, sample 1 showed a specific band with the correct product size after PCR of gene A which meant the sample was correctly amplified and could be used for pyrosequencing in gene A. However, sample 1 may not be successfully amplified for gene B. DNA fragments are forced into an aggressive reaction state during bisulfite treatment, which leads to abasic sites resulting in DNA cleavage of the DNA phosphodiester bond (i.e., DNA degradation). Therefore, the number of samples finally used for pyrosequencing was less than the total number of samples for each gene in both ESCs and ExU somatic cells.

Figure 6 illustrates that hypermethylation of TSGs was frequently shown in EJ samples from CP/CPPS patients. *EDNRB* ($p<0.0001$), *CDKN2A* ($p<0.0001$), *PTGS2* ($p=0.0469$), *BMP7* ($p<0.0001$), *BMP4* ($p=0.0132$) were higher methylated in CP/CPPS patients. Healthy controls show slight hypomethylation in *PITX2* and *GSTP1,* but there are no significant differences compared to CP/CPPS patients. Generally, patients show higher methylation levels than healthy controls. Especially for *CDKN2A,* half of

the enrolled samples show hypermethylation (16 of 31, metylation level >15%), with the highest average methylation (13.29%), and the general difference was significant.

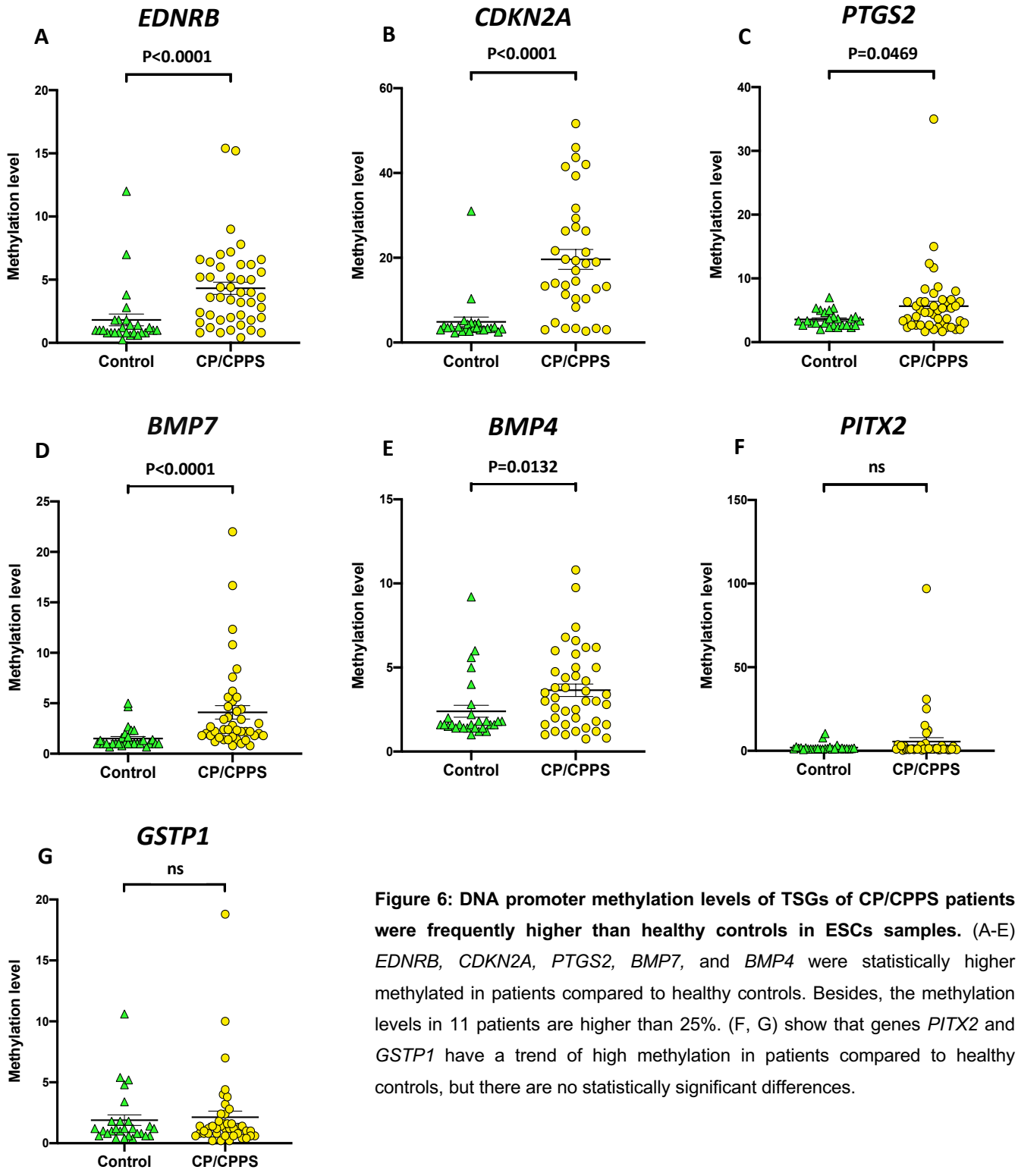

Figure 6: DNA promoter methylation levels of TSGs of CP/CPPS patients were frequently higher than healthy controls in ESCs samples. (A-E) *EDNRB, CDKN2A, PTGS2, BMP7,* and *BMP4* were statistically higher methylated in patients compared to healthy controls. Besides, the methylation levels in 11 patients are higher than 25%. (F, G) show that genes *PITX2* and *GSTP1* have a trend of high methylation in patients compared to healthy controls, but there are no statistically significant differences.

Table 6: Heat map of TSGs average methylation levels in ESCs (patients)

ESCs								
	BMP4_01	PTGS2_02	BMP7_01	PITX2_02	CDKN2A	EDNRB	GSTP1	Mean
P5-301	N/A	3.0	0.8	12.2	3.0	N/A	1.6	4.1
P5-317	3.2	5.0	2.0	1.0	19.3	6.4	1.2	5.4
P5-322	3.4	4.3	8.4	1.0	3.3	7.8	1.2	4.2
P5-323	6.2	6.3	2.0	1.2	N/A	3.4	N/A	3.8
P5-371	3.8	5.0	2.2	0.6	19.0	4.4	0.8	5.1
P5-375	1.4	2.3	N/A	15.2	2.7	6.6	0.2	4.7
P5-395	2.4	2.0	2.8	10.6	10.3	5.2	1.4	5.0
P5-397	4.4	N/A	16.7	30.8	N/A	5.2	18.8	15.2
P5-399	2.0	6.3	5.2	N/A	26.3	6.0	0.4	7.7
P5-401	1.2	1.7	1.4	1.2	N/A	1.0	N/A	1.3
P5-403	1.6	2.7	1.2	4.4	N/A	3.2	3.2	2.7
P5-407	2.0	11.7	1.4	2.0	3.0	7.0	2.4	4.2
P5-411	3.0	5.3	3.4	2.6	10.3	5.0	1.2	4.4
P5-413	2.6	2.3	N/A	97.0	4.7	6.6	N/A	22.6
P5-416	N/A	2.7	7.6	0.6	13.5	15.4	N/A	8.0
P5-423	N/A	4.0	N/A	1.2	N/A	3.6	0.8	2.4
P5-425	6.2	1.7	1.7	1.4	13.3	3.2	1.4	4.1
P5-426	4.2	15.0	0.8	0.4	27.3	5.0	1.2	7.7
P5-427	0.8	N/A	22.0	0.8	N/A	N/A	N/A	7.9
P5-428	10.8	5.7	2.2	0.8	N/A	4.0	0.2	3.9
P5-429	2.8	35.0	N/A	1.0	N/A	0.8	0.6	8.0
P5-432	1.6	N/A	N/A	N/A	N/A	2.2	1.4	1.7
P5-436	6.0	6.7	3.6	3.2	19.7	1.2	N/A	6.7
P5-450	9.8	5.3	4.4	2.8	42.0	N/A	4.0	11.4
P5-451	1.0	2.3	1.4	3.6	3.3	2.0	N/A	2.3
P5-452	6.6	3.3	1.8	3.0	39.3	4.0	1.6	8.5
P5-455	N/A	7.7	N/A	N/A	N/A	1.4	1.2	3.4
P5-458	4.8	8.0	2.3	0.8	41.5	1.0	0.2	8.4
P5-459	4.5	2.0	2.2	1.0	12.7	2.2	2.4	3.9
P5-463	3.0	12.3	12.3	N/A	N/A	2.8	1.8	6.5
P5-464	N/A	6.3	5.6	1.0	31.7	3.6	0.8	8.2
P5-465	N/A	5.7	4.2	N/A	21.3	N/A	1.4	8.2
P5-467	5.8	N/A	6.2	1.0	26.3	1.8	3.8	7.5
P5-473	1.2	2.0	1.0	1.0	14.5	0.8	1.0	3.1
P5-474	1.6	2.7	1.3	0.8	N/A	1.6	4.4	2.1
P5-476	2.5	3.0	1.8	0.8	N/A	N/A	1.0	1.8
P5-477	N/A	4.7	3.0	1.0	11.3	1.8	0.8	3.8
P5-479	1.2	3.3	N/A	1.0	17.0	6.2	0.6	4.9
P5-480	3.5	8.7	1.8	3.0	29.3	6.2	0.6	7.6
P5-486	5.0	8.3	2.7	1.0	43.7	0.4	0.4	8.8
P5-489	N/A	3.7	5.6	1.0	51.7	4.4	10.0	12.7
P5-495	6.8	5.7	10.8	1.4	13.3	9.0	1.6	6.9
P5-498	3.8	2.7	2.2	1.0	18.7	7.2	0.8	5.2
P5-504	1.0	6.3	2.4	N/A	N/A	15.2	7.0	6.4
P5-522	7.4	6.7	2.4	1.4	8.3	5.2	1.0	4.6

N/A: Not available.
Mean: Mean of methylations of each TSG

Table 7: Heat map of TSGs average methylation levels in ESCs (Healthy controls)

ESCs								
	BMP4_01	PTGS2_02	BMP7_01	PITX2_02	CDKN2A	EDNRB	GSTP1	Mean
P5G-85	1.5	N/A	1.6	N/A	N/A	1.0	4.8	2.2
P5G-88	1.2	3.7	1.0	1.0	31.0	3.8	N/A	6.9
P5G-90	1.8	N/A	N/A	N/A	4.7	N/A	10.6	5.7
P5G-91	1.6	3.7	1.4	7.8	4.3	0.8	1.4	3.0
P5G-92	1.4	2.7	1.0	10.4	3.3	1.8	1.2	3.1
P5G-93	4.0	2.3	1.0	1.2	4.0	0.3	1.2	2.0
P5G-95	2.2	2.0	1.0	1.0	3.7	0.6	1.0	1.6
P5G-96	2.0	2.3	1.0	1.6	3.2	1.4	1.0	1.8
P5G-97	1.6	5.0	0.8	1.2	10.3	7.0	0.6	3.8
P5G-98	1.2	3.3	0.7	1.2	3.0	1.0	1.2	1.7
P5G-99	1.6	4.0	1.0	1.4	2.3	0.8	1.8	1.8
P5G-101	5.6	3.0	1.0	1.0	3.3	1.8	1.8	2.5
P5G-102	9.2	4.0	1.0	1.2	2.7	1.8	3.4	3.3
P5G-103	1.0	3.3	0.7	1.4	3.7	1.2	5.4	2.4
P5G-104	1.8	7.0	1.0	1.0	N/A	1.2	1.0	2.2
P5G-105	2.8	5.3	1.0	1.4	N/A	1.4	5.2	2.9
P5G-106	1.6	3.3	2.0	1.4	N/A	N/A	1.8	2.0
P5G-107	N/A	3.0	4.7	1.4	3.0	0.8	0.8	2.3
P5G-109	1.4	3.7	2.7	1.6	3.5	N/A	N/A	2.6
P5G-120	1.6	4.7	1.0	2.2	3.7	0.8	0.4	2.0
P5G-121	N/A	N/A	2.3	1.2	3.5	2.8	0.6	2.1
P5G-122	1.4	2.7	1.0	1.2	4.7	0.8	0.8	1.8
P5G-123	1.4	5.3	1.0	3.4	3.3	1.0	1.2	2.4
P5G-124	1.6	2.7	2.3	1.0	3.0	0.8	0.8	1.7
P5G-125	1.8	2.7	5.0	1.8	4.3	0.8	0.6	2.4
P5G-126	1.8	2.3	1.0	1.8	3.3	1.0	0.6	1.7
P5G-127	6.0	N/A	1.3	1.2	5.2	1.0	1.2	2.7
P5G-61	1.6	2.7	1.7	0.8	2.5	12.4	0.4	3.1
P5G-112	1.4	3.0	1.3	1.6	N/A	0.8	N/A	1.6
P5G-113	5.0	5.0	1.0	2.4	2.7	0.6	0.4	2.4

N/A: Not available.
Mean: Mean of methylations of each TSG

Heat maps of TSGs' average methylation levels in ExU somatic cells of each patient and healthy control are shown in Table 8-9 below. Figure 7 compares methylation levels of the selected TSGs in ExU somatic cells in healthy controls and CP/CPPS patient groups. *EDNRB* (p=0.026) and *CDKN2A* (p=0.0027) were significantly hypermethylated in CP/CPPS patients compared to healthy controls. *PTGS2*, *BMP7*, *BMP4*, *PITX2,* and *GSTP1* did not show significant differences between CP/CPPS patients and healthy controls. Generally, TSGs in CP/CPPS patient group were hypermethylated. *PTGS2* and *CDKN2A* showed hypermethylation in most patient samples.

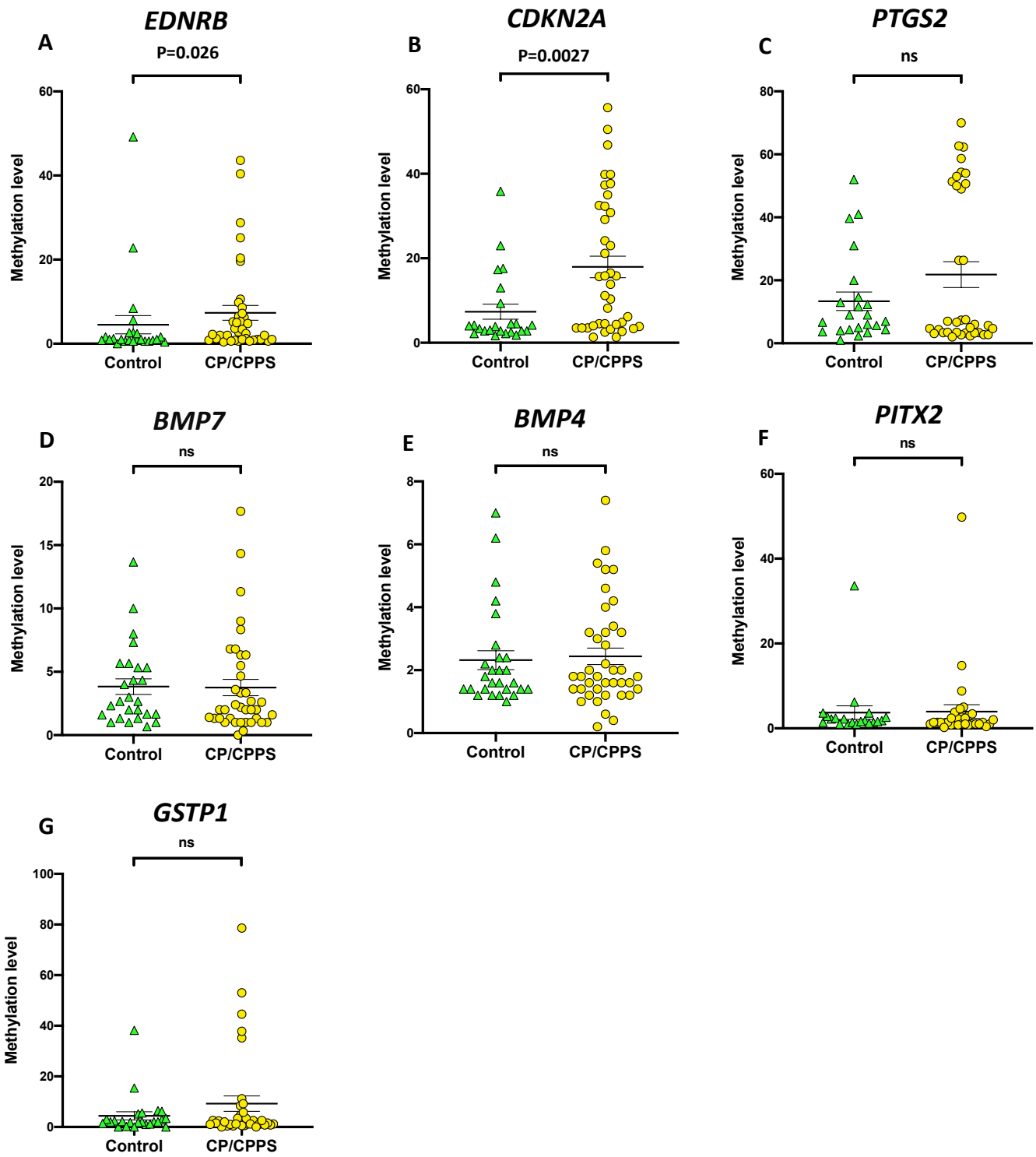

Figure 7: DNA promoter methylation levels of TSGs were measured in ExU samples of patients and healthy controls. (A, B) *EDNRB* and *CDKN2A* are statistically higher methylated in patients compared to healthy controls. 14 patients show >25% methylation level in *CDKN2A,* and the average methylation rate is the highest (20.01%) among other TSGs. (C-G) promoter methylation levels of genes *PTGS2, BMP7, BMP4, PITX2* and *GSTP1* are not statistically different between patients.

Table 8: Heat map of TSGs average methylation levels in ExU (patients)

ExU								
	BMP4_01	PTGS2_02	BMP7_01	PITX2_02	CDKN2A	EDNRB	GSTP1	MW
P5-301	1.2	3.3	2.6	N/A	N/A	0.6	0.6	1.7
P5-317	1.8	54.3	1.3	1.0	2.7	10.6	1.2	10.4
P5-322	3.2	3.3	2.0	1.0	39.8	N/A	1.2	8.4
P5-323	2.8	2.8	2.2	1.0	32.5	6.5	0.8	6.9
P5-371	N/A	N/A	1.3	1.4	4.8	0.6	4.6	2.6
P5-375	2.2	4.3	8.3	0.8	3.8	2.0	1.6	3.3
P5-395	0.2	N/A	1.0	2.6	50.5	0.4	1.6	9.4
P5-397	1.4	2.8	6.8	1.4	21.2	6.3	0.4	5.7
P5-399	5.4	49.0	17.7	49.8	24.2	9.8	8.4	23.5
PS-401	2.0	26.3	1.0	3.0	3.5	0.8	0.6	5.3
P5-403	5.2	51.3	14.3	N/A	29.2	N/A	2.6	20.5
P5-407	1.2	53.0	3.3	1.4	3.3	28.8	1.0	13.2
P5-411	1.4	62.3	0.0	N/A	15.8	1.0	44.6	20.9
P5-413	3.2	N/A	1.3	N/A	13.8	8.6	53.0	16.0
P5-416	1.8	6.0	2.0	1.4	10.3	5.2	N/A	4.5
P5-423	4.0	54.0	6.3	N/A	23.0	2.0	3.4	15.5
P5-425	5.8	N/A	1.3	N/A	N/A	5.3	78.6	22.8
P5-426	1.6	3.5	6.8	2.2	32.3	19.6	3.4	9.9
P5-427	1.8	7.3	N/A	N/A	11.2	N/A	N/A	6.8
P5-428	2.0	26.3	1.6	3.8	4.5	3.6	0.8	6.1
P5-429	0.6	62.7	1.0	14.8	37.3	1.0	0.4	16.8
P5-432	1.6	2.7	0.3	1.0	3.5	3.4	9.2	3.1
P5-436	2.0	7.5	2.0	0.8	16.5	4.8	2.6	5.2
P5-451	1.8	5.7	5.5	2.4	15.7	1.0	2.6	4.9
P5-452	4.2	4.7	9.0	3.4	4.0	7.2	2.4	5.0
P5-455	3.4	3.1	2.0	0.4	39.8	0.8	0.0	7.1
P5-459	1.2	2.0	N/A	4.6	15.8	43.6	N/A	13.4
P5-463	3.2	70.0	11.3	8.8	1.3	1.2	1.2	13.9
P5-464	1.4	2.3	2.0	0.2	2.5	0.6	5.8	2.1
P5-465	5.2	58.7	1.4	N/A	1.3	0.8	1.0	11.4
P5-473	0.4	4.7	6.3	1.8	4.5	2.4	1.6	3.1
P5-476	1.0	3.3	1.0	1.4	3.2	5.0	N/A	2.5
P5-477	1.6	5.0	4.7	1.0	35.0	1.2	1.0	7.1
P5-479	7.4	50.0	3.4	1.2	3.5	20.4	35.2	17.3
P5-480	4.6	50.7	1.0	N/A	55.7	40.4	37.8	31.7
P5-486	1.2	7.0	1.0	0.8	4.3	1.0	N/A	2.6
P5-495	1.6	6.7	2.7	2.4	46.8	25.2	2.0	12.5
P5-504	1.6	N/A	N/A	1.0	30.8	2.2	0.0	7.1
P5-522	1.0	N/A	1.0	N/A	37.7	0.6	1.2	8.3

N/A: Not available.
Mean: Mean of methylations of each TSG

Table 9: Heat map of TSGs average methylation levels in ExU (Healthy controls)

ExU								
	BMP4_01	PTGS2_02	BMP7_01	PITX2_02	CDKN2A	EDNRB	GSTP1	Mean
P5G-85	N/A	N/A	N/A	N/A	N/A	1.6	N/A	1.6
P5G-88	3.8	6.7	1.7	N/A	N/A	49.2	2.0	12.7
P5G-90	1.8	14.7	2.7	1.4	4.5	0.6	2.4	4.0
P5G-91	1.4	N/A	2.3	N/A	N/A	2.6	0.0	1.6
P5G-92	1.4	52.0	13.7	1.8	17.6	0.8	0.0	12.5
P5G-93	1.2	2.3	2.0	1.4	3.3	0.6	1.0	1.7
P5G-95	2.0	20.3	1.6	N/A	4.5	22.8	38.2	14.9
P5G-96	1.6	12.3	4.3	1.8	4.2	0.4	2.8	3.9
P5G-97	1.4	N/A	3.0	1.0	2.8	2.6	6.4	2.9
P5G-98	1.6	5.0	5.3	2.2	1.7	1.2	2.0	2.7
P5G-99	1.4	9.0	5.7	1.4	2.8	0.8	1.2	3.2
P5G-102	1.0	4.0	1.0	2.2	4.0	1.6	5.2	2.7
P5G-103	1.2	N/A	N/A	N/A	N/A	2.4	N/A	1.8
P5G-104	2.0	5.7	5.3	1.6	2.5	1.0	2.0	2.9
P5G-105	1.2	3.3	2.7	2.8	2.2	0.6	1.8	2.1
P5G-106	1.2	4.3	5.7	2.4	2.8	1.0	6.2	3.4
P5G-107	1.4	4.3	7.3	2.6	1.8	0.6	3.4	3.1
P5G-120	1.6	39.7	1.3	N/A	4.2	0.0	1.8	8.1
P5G-121	2.8	41.0	1.0	N/A	3.8	5.6	2.0	9.4
P5G-122	7.0	31.0	1.0	1.0	23.0	8.4	N/A	11.9
P5G-123	2.2	13.0	4.3	33.6	17.3	0.8	0.0	10.2
P5G-124	4.8	11.7	1.7	1.6	9.3	0.8	3.0	4.7
P5G-125	2.4	N/A	1.3	N/A	35.8	N/A	15.4	13.7
P5G-126	1.4	1.0	0.7	1.0	N/A	N/A	N/A	1.0
P5G-127	2.4	9.0	8.0	3.6	2.2	1.0	2.2	4.1
P5G-61	4.2	7.0	10.0	6.2	13.0	1.0	0.2	5.9
P5G-112	2.0	6.0	2.0	3.6	2.8	N/A	1.4	3.0
P5G-113	6.2	3.7	4.0	1.2	3.0	N/A	5.6	3.9

N/A: Not available.
Mean: Mean of methylations of each TSG

3.7. TSGs are frequently downregulated in somatic cells of liquid biopsies from CP/CPPS patients.

The selected TSG expression levels of the CP/CPPS patient group and healthy controls in ESCs and ExU somatic cells were also evaluated. Like promoter methylation analysis, not all samples gave proper Ct values or the right RT-PCR products for each TSG according to the melting curves. Therefore, the numbers of patients and healthy controls included in the analysis differed for each gene. Figure 8 compares mRNA expression levels of the selected TSGs between healthy controls and CP/CPPS patients in ESCs. Healthy controls showed higher mRNA expression levels in *CDKN2A* (p=0.0044) and *PTGS2* (p=0.0138) compared to CP/CPPS patients.

The expression level of *GSTP1* had a significant difference between CP/CPPS patients and healthy controls (p=0.0001), but oppositely CP/CPPS patients showed a higher expression level than healthy controls. There were no significant differences in mRNA expression levels in *EDNRB*, *BMP7*, *BMP4*, and *PITX2* between CP/CPPS patients and healthy controls.

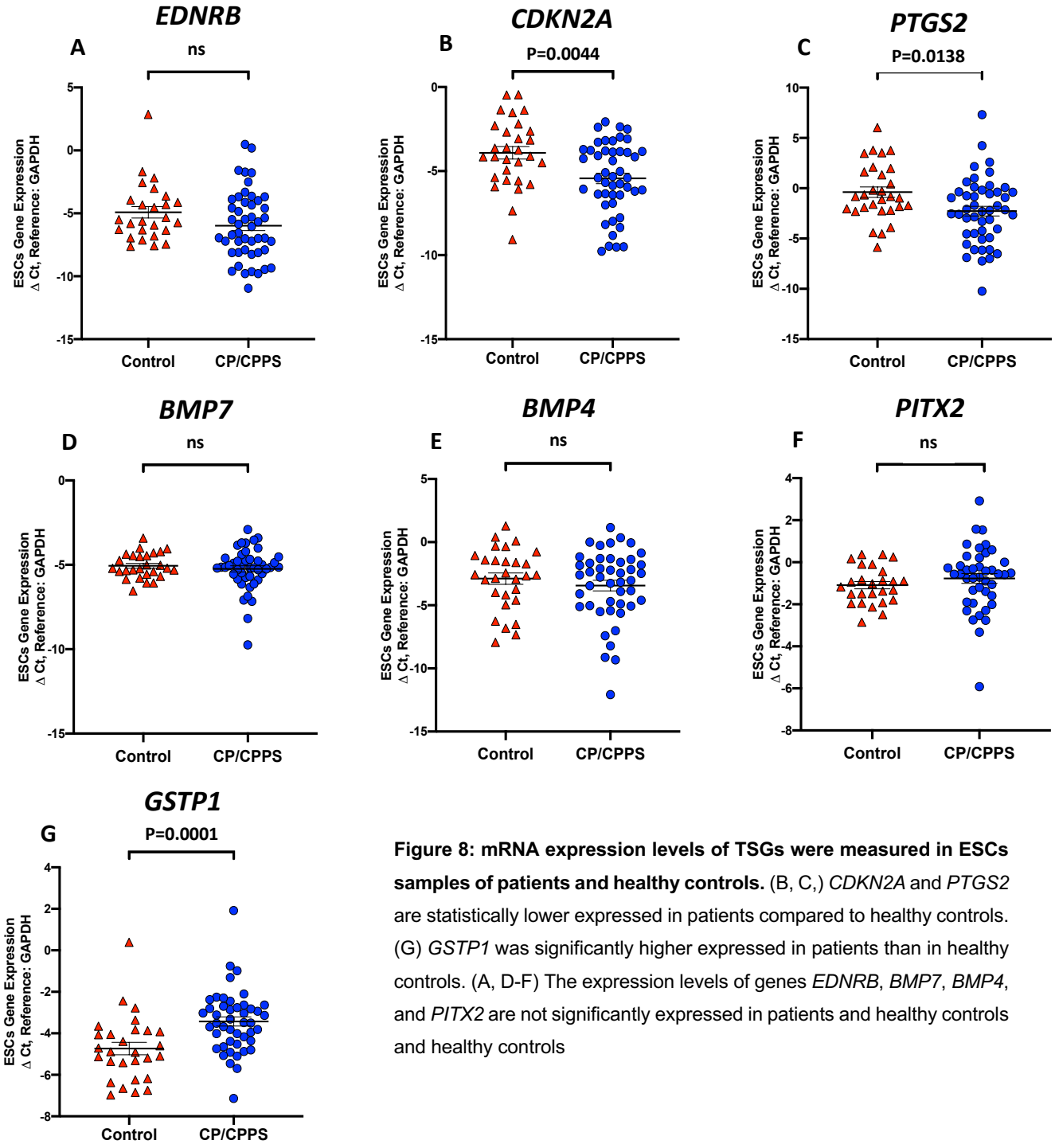

Figure 8: mRNA expression levels of TSGs were measured in ESCs samples of patients and healthy controls. (B, C,) *CDKN2A* and *PTGS2* are statistically lower expressed in patients compared to healthy controls. (G) *GSTP1* was significantly higher expressed in patients than in healthy controls. (A, D-F) The expression levels of genes *EDNRB*, *BMP7*, *BMP4*, and *PITX2* are not significantly expressed in patients and healthy controls and healthy controls

Figure 9 shows the mRNA expressions of the selected TSGs in ExU somatic cells compared to healthy controls and CP/CPPS patients. *CDKN2A* and *PTGS2* were statistically lower expressed in patients compared to healthy controls. On the other hand, expression levels of genes *EDNRB, BMP7, BMP4* and *PITX2* were not significantly different between patients and healthy controls. Gene *CDKN2A* showed a significantly higher methylation level and a lower mRNA expression level in patients than in healthy controls of both ESCs and ExU somatic cells. Therefore, *CDKN2A* may play a promising role in the prognosis of CP/CPPS developing into prostate cancer.

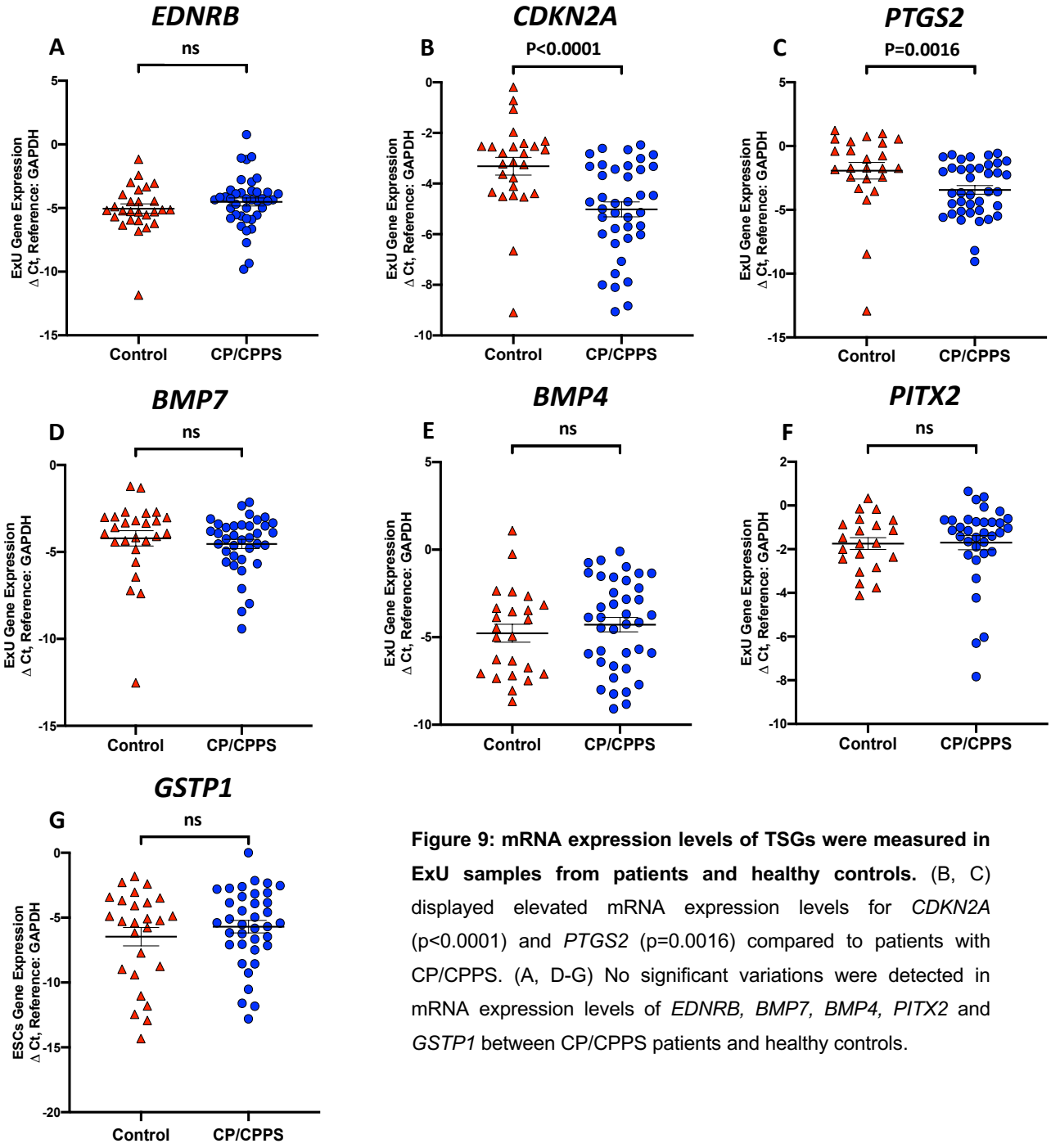

Figure 9: mRNA expression levels of TSGs were measured in ExU samples from patients and healthy controls. (B, C) displayed elevated mRNA expression levels for *CDKN2A* ($p<0.0001$) and *PTGS2* ($p=0.0016$) compared to patients with CP/CPPS. (A, D-G) No significant variations were detected in mRNA expression levels of *EDNRB, BMP7, BMP4, PITX2* and *GSTP1* between CP/CPPS patients and healthy controls.

3.8. Correlations exist among TSG methylation and expression levels in ESCs and ExU.

The results of our study demonstrate that multiple TSGs exhibit hypermethylation in patients with CP/CPPS. Our findings indicate that not only is a single TSG hypermethylated in CP/CPPS patients but multiple TSGs are affected. Additionally, our analysis revealed a correlation between methylation and mRNA expression levels, offering insight into the potential functional consequences of hypermethylation. The correlation analysis was conducted by incorporating the methylation values and mRNA expression levels from patients and healthy controls, and representative graphical illustrations of the results are provided for visual clarification.

3.8.1 Investigation of the inter-TSG correlation of methylation in the selected TSGs

The current analysis aimed to examine the correlation between the methylation levels of TSGs in EJ and ExU, as evidenced by a comprehensive overview of the correlations presented in the supplement (Table 10-11), highlighting 14 powerful combinations between different TSGs. Out of these 14 significant correlations, 12 aligned with our expectations. Here, 9 of the 14 correlations were demonstrated. Figure 10 suggests a statistically significant positive correlation exists between the methylation levels of *EDNRB* in ExU and EJ ($p = 0.0026$, $r = 0.4174$). In addition, positive correlations were found between the *EDNRB* methylation levels in EJ and *CDKN2A* in EJ ($p = 0.0159$, $r = 0.3464$), and *CDKN2A* in ExU ($p = 0.0049$, $r = 0.4000$). In ExU, the methylation levels of *BMP4* were also positively correlated with *EDNRB* ($p=0.037$, $r=0.290$) and *PTGS2* ($p=0.011$, $r=0.4352$). Furthermore, the methylation levels of *BMP7* in EJ showed a statistically significant correlation with *CDKN2A* in ExU ($p=0.0468$, $r=0.2855$) and *EDNRB* in EJ ($p=0.0039$, $r=0.3802$). Lastly, the methylation levels of *GSTP1* in EJ were positively correlated with *PITX2* in EJ ($p=0.0037$, $r=0.3951$). However, a negative correlation was observed between the methylation levels of *GSTP1 i*n EJ and *BMP4* in ExU ($p=0.0154$, $r= -0.3343$).

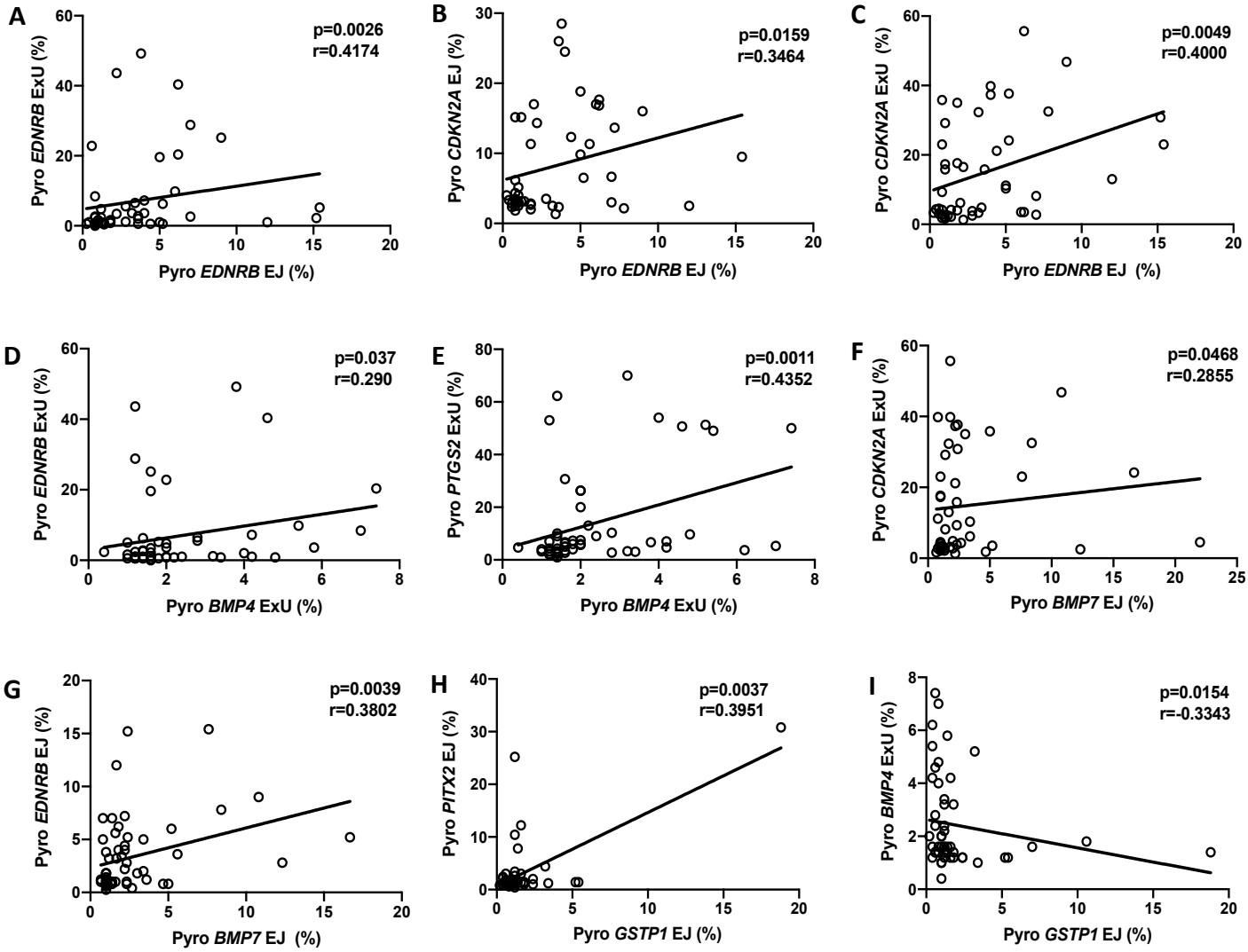

Figure 10: The results of our study indicate a positive correlation between the methylation levels of selected TSGs in both the EJ and the ExU samples. (A-C) *EDNRB* methylation levels were positively correlated between the EJ and ExU samples, and methylation levels of *EDNRB* in EJ showed positive correlations to *CDKN2A* methylation in both EJ and ExU. (D, E) In ExU samples, *BMP4* methylation positively correlated with *EDNRB* and *PTGS2*. (F, G) *BMP7* methylation in EJ showed a positive correlation with *CDKN2A* in ExU, as well as *EDNRB* in EJ. Conversely, (H-I) *GSTP1* methylation in EJ showed a significant positive correlation with *PITX2* in EJ but a negative correlation with *BMP4* in ExU.

3.8.2. Investigation of the inter-TSG correlation of mRNA expression in the selected TSGs

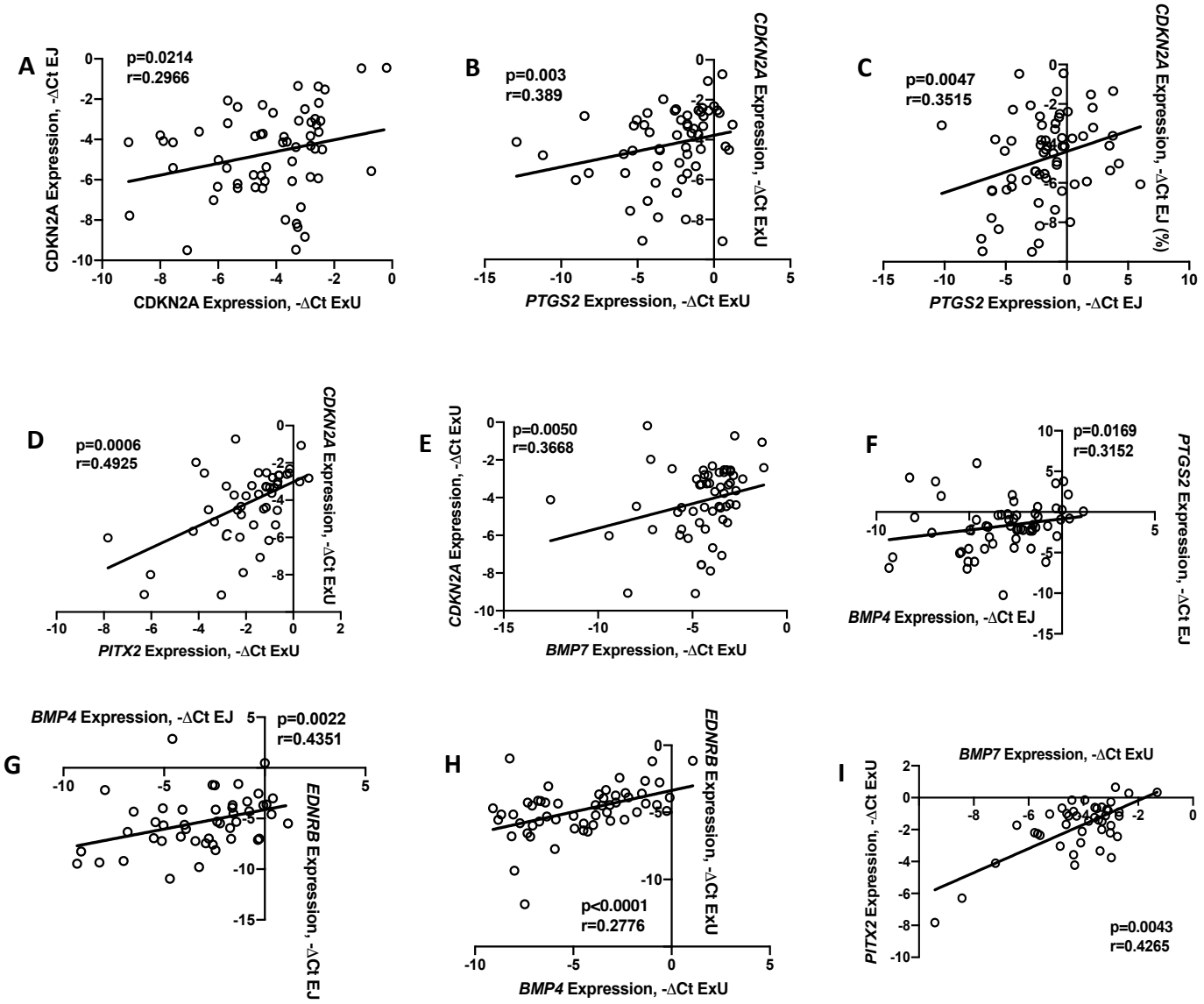

Figure 11: The mRNA expression levels of the selected TSGs exhibited similar trends of correlation. (A, C) Positive associations were observed between the expression levels of *CDKN2A* in the EJ and *CDKN2A* in the ExU, as well as between *CDKN2A* in EJ and *PTGS2* in EJ. (B, D, E) The expression of *CDKN2A* in ExU was found to have positive correlations with *PTGS2*, *PITX2*, and *BMP7* in ExU. (F-H) The expression of *BMP4* in EJ was significantly correlated with *PTGS2* in EJ and *EDNRB* in EJ. Furthermore, in the ExU, a positive correlation was observed between *BMP4* and *EDNRB*. Additionally, *BMP7* in ExU demonstrated a positive correlation with *PITX2* in ExU.

In this study, we investigated the correlations between the mRNA expression levels of selected TSGs. The results of the correlation analysis are summarized in the supplement (Table 12-13). Of the 91 correlations evaluated, 17 were identified as significant. Out of these 17 significant correlations, 12 aligned with our expectations.

9 of these expected correlations are depicted in Figure 11. We found that *CDKN2A* expression in ExU was positively correlated with *CDKN2A* expression in EJ ($p = 0.0214$, $r = 0.2966$), as well as with *PTGS2* in ExU ($p = 0.003$, $r = 0.389$), *PITX2* in ExU ($p = 0.0006$, $r = 0.4925$), and *BMP7* in ExU ($p = 0.0050$, $r = 0.3668$). In ExU, *BMP7* expression was also significantly correlated with *PITX2* ($p = 0.0043$, $r = 0.4265$). In addition, *PTGS2* expression in EJ showed a positive correlation with *CDKN2A* expression in EJ ($p = 0.0047$, $r = 0.3515$) and *BMP4* expression in EJ ($p = 0.0169$, $r = 0.3152$). Furthermore, *BMP4* expression in EJ and ExU was significantly correlated with *EDNRB* expression in EJ ($p = 0.0022$, $r = 0.4351$) and ExU ($p < 0.0001$, $r = 0.2776$), respectively. Interestingly, we observed that *GSTP1* expression in EJ had the most negative correlations with other TSGs, including *CDKN2A* in EJ, *PTGS2* in EJ, and ExU, which did not conform to our expectations.

3.8.3 Investigation of the inter-TSG correlation between methylation and mRNA expression levels in the selected TSGs

Here, we analyzed the relationship between mRNA expression and methylation levels of selected TSGs. The results of the correlation analysis are summarized in the supplement (Table 14-15), revealing negative correlations between the two variables. Specifically, as shown in Figure 12, we observed a significant negative correlation between the mRNA expression of *CDKN2A* in ExU and the methylation levels of *EDNRB* in both EJ ($p=0.0099$, $r=-0.3361$) and ExU ($p=0.0114$, $r=-0.3482$). Additionally, a significant negative correlation was found between *EDNRB* expression in EJ and the methylation of *CDKN2A* in ExU ($p=0.0106$, $r=-0.4153$). Furthermore, the expression of *EDNRB* in ExU was negatively correlated with the methylation of *PITX2* in EJ ($p=0.0259$, $r=-0.3059$) and *BMP7* in ExU ($p=0.0354$, $r=-0.2843$). Finally, we observed a correlation between the expressions of *GSTP1* in EJ and the methylation of *PITX2* ($p=0.013$, $r=-0.3328$) in EJ. In conclusion, our study demonstrates negative correlations between mRNA expression and methylation levels of selected TSGs. These correlation results suggest a potential link between epigenetic modifications and gene expression in the context of tumorigenesis.

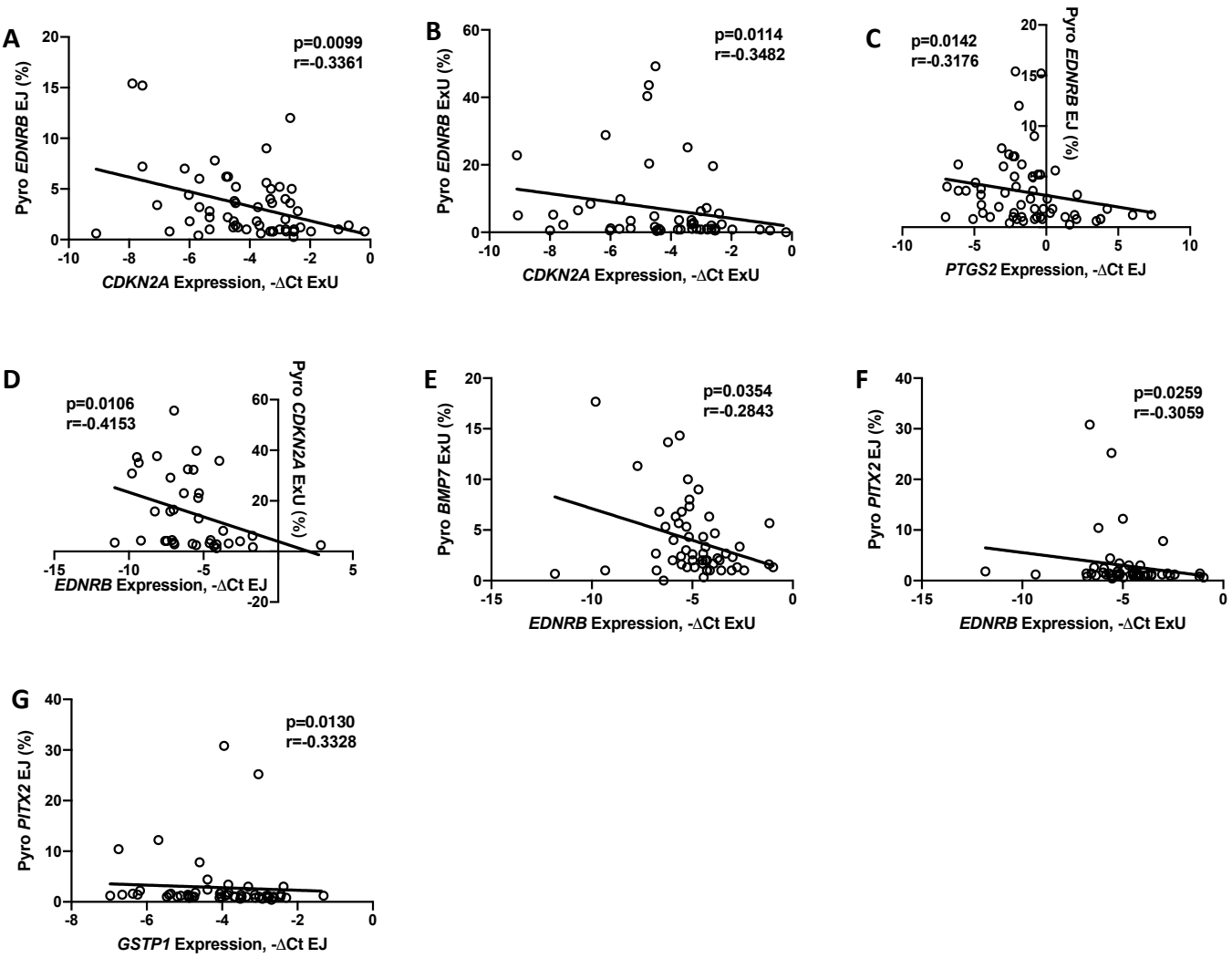

Figure 12: The study results indicated an interrelation between the mRNA expression and methylation levels of the selected TSGs. (A, B) The expression of *CDKN2A* in ExU showed a negative correlation with the methylation levels of *EDNRB* in both ExU and EJ. (C-F) In EJ, the methylation and expression levels of *EDNRB* were negatively correlated with the expression of *PTGS2* in EJ and the methylation of *CDKN2A* in ExU. Moreover, the expression of *EDNRB* in ExU had significant negative correlations with the methylation of *BMP7* in ExU and *PITX2* in EJ. (G) The methylation of *PITX2* in EJ was also negatively correlated with *GSTP1* expression in EJ.

3.9. Confirmation of isolation efficiency of MACS system

ESCs and ExU are primarily comprised of two major cell types, namely epithelial cells and leukocytes. Given the observed hypermethylation and concomitant decrease in expression levels of *CDKN2A* in CP/CPPS patients in both the ESCs and ExU somatic cells, it was selected as the target for MACS isolation experiments aimed at

investigating the methylation and mRNA expression levels in the epithelial cells and leukocytes of these cellular compartments.

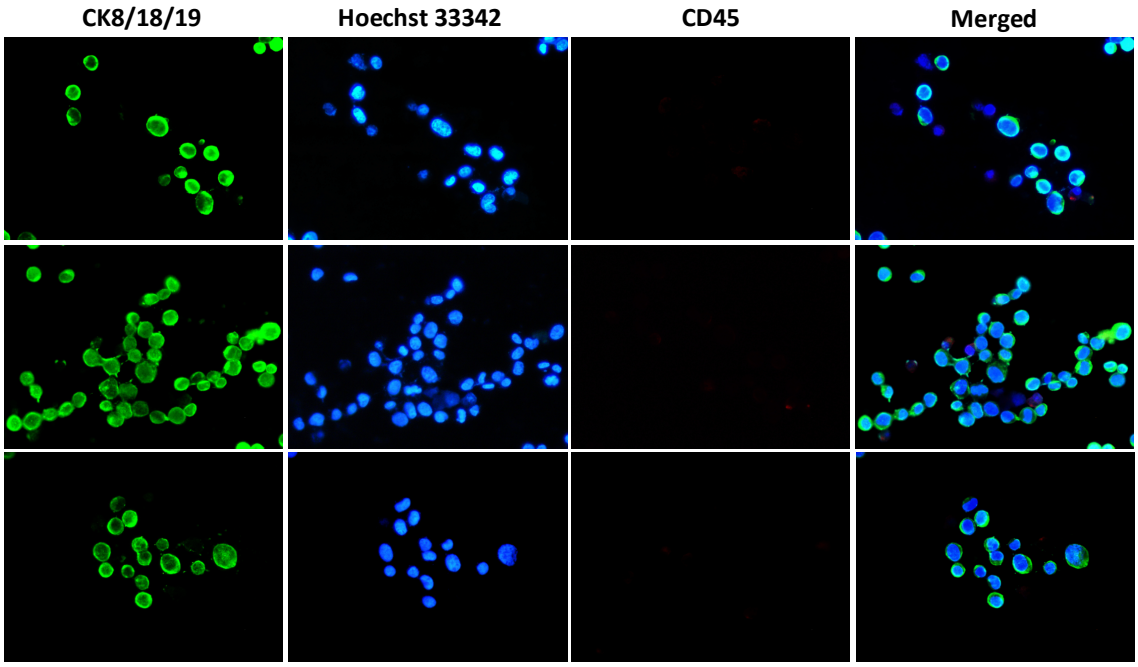

Figure 13: PC3 cells were detected after MACS isolation by EpCAM MicroBeads using IF. PC3 cells were only CK8/18/19+, which were indicated with a “green” signal, and THP-1 cells were only CD45+ and indicated with a “red” signal. No THP-1 cells were mixed in the isolated PC3 cells after the isolation.

PC3 cells as epithelial cells and THP-1 cells as leukocytes were chosen to be positive controls for testing the MACS system. PC3 and THP-1 cells were mixed at proportion 1:5 (2^ 10^5 : 1^ 10^6) according to the previous cell counting results. The PC3 and THP-1 cells were isolated by CD326 (EpCAM) MicroBeads, human, and subsequently CD45 MicroBeads, human. CK 8/18/19 and CD45 were used as primary antibodies, and Alexa Fluor 488 (Green signal) and Alexa Fluor 555 (Red signal) were used as corresponding secondary antibodies. PC3 cells were defined as CK8/18/19+, CD45- and Hoechst 33342+. THP-1 cells were defined as CD45+, CK8/18/19- and Hoechst 33342+. Particles, either CK 8/18/19+, CD45+ or Hoechst 33342 +, were not defined as cells. Figure 13 shows the isolated PC3 cells without residual THP-1 cells after MACS isolation.

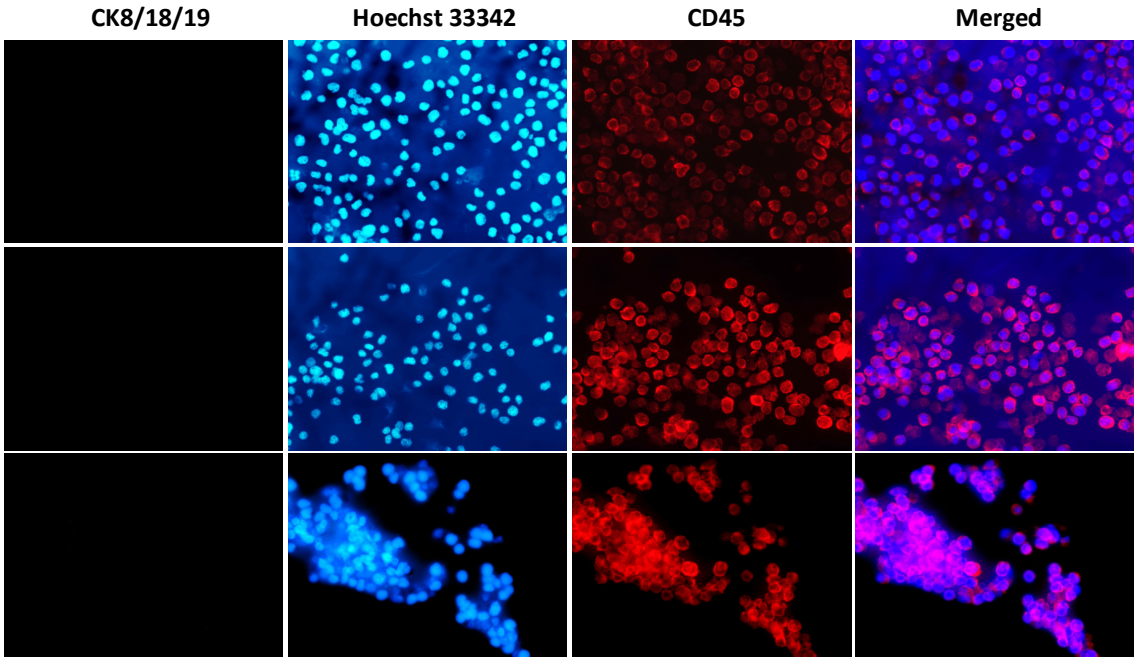

Figure 14: THP-1 cells were detected using IF after MACS isolation by CD45. THP-1 cells were CD45+ only and were indicated with a “red” signal. No PC3 cells were residual in the isolated THP-1 cells.

Figure 14 shows THP-1 cells isolated from the flow-through after PC3 cell isolation and validated by IF staining. CD45 MicroBeads, human, was used for the isolation. There were no residual PC3 cells after the isolation. In summary, the MACS system is highly effective and specific in sorting homogeneous cultured epithelial cells and monocytes.

Fresh EJ and ExU samples without adding PC3 cells and THP-1 cells were subsequently used for the MACS isolation efficiency test. For EJ samples, sperm cells were first eliminated after being depleted by MACSprep™ Forensic Sperm MicroBead Kit, human, to harvest pure ESCs. Subsequently, the epithelial cells and leukocytes from ESCs were sorted as described. CK 8/18/19 and CD45 were used as primary antibodies, and Alexa Fluor 488 (green signal) and Alexa Fluor 555 (red signal) were used as corresponding secondary antibodies. Figure 15 shows the epithelial cells and leukocytes from ESCs samples after the isolation. No epithelial cells were found in the isolated leukocytes; among the isolated epithelial cells, similarly, no leukocytes were interfused.

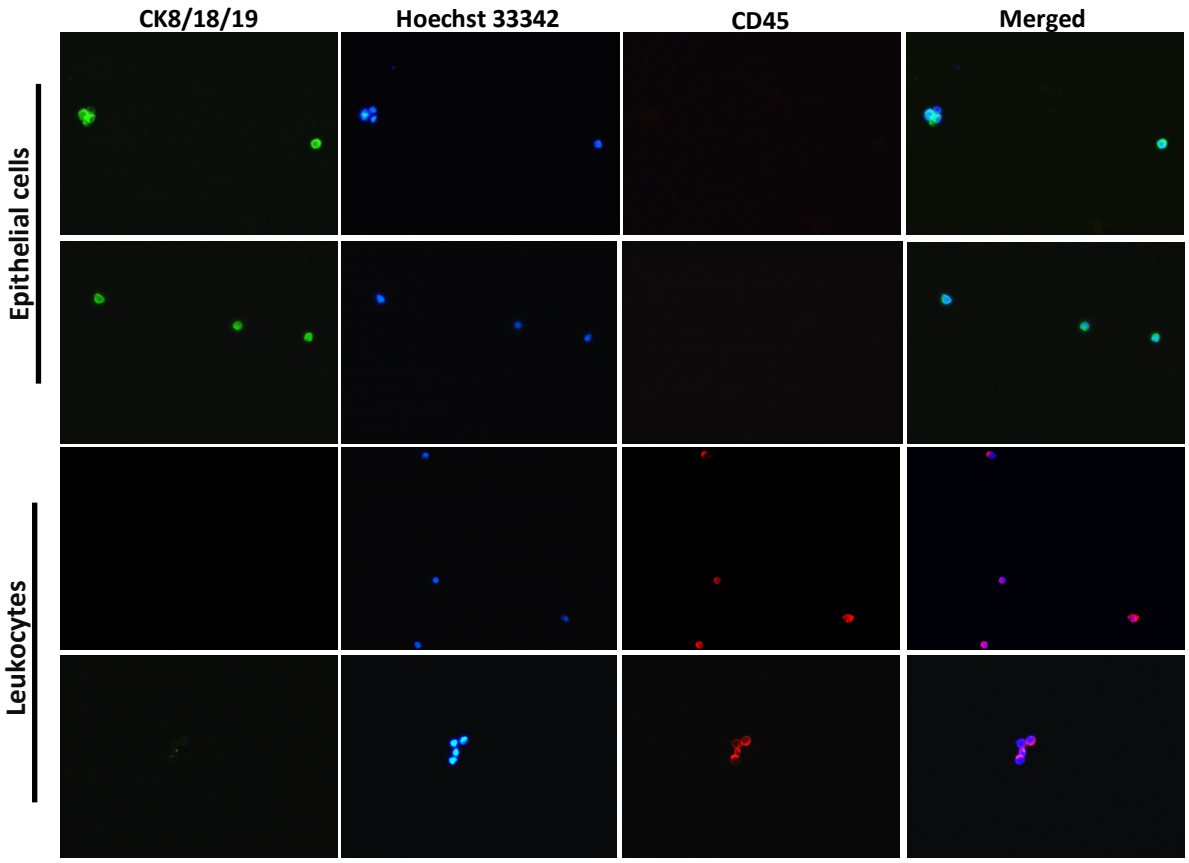

Figure 15: Epithelial cells and leukocytes from ESCs were successfully separated after MACS isolation. No leukocytes which show a “red” signal was found among the isolated epithelial cells. Likewise, no epithelial cells which showed a “green” signal were found after the isolation of leukocytes.

The procedures of sorting epithelial cells and leukocytes from ExU pellets were the same as EJ samples but without eliminating sperm cells. Figure 16 demonstrates the efficacy of the MACS system in separating the two cell populations. Like in EJ samples, no cells interfused with the other isolated cell groups. The isolation efficiency and specificity of the MACS system are promising in native EJ and ExU samples.

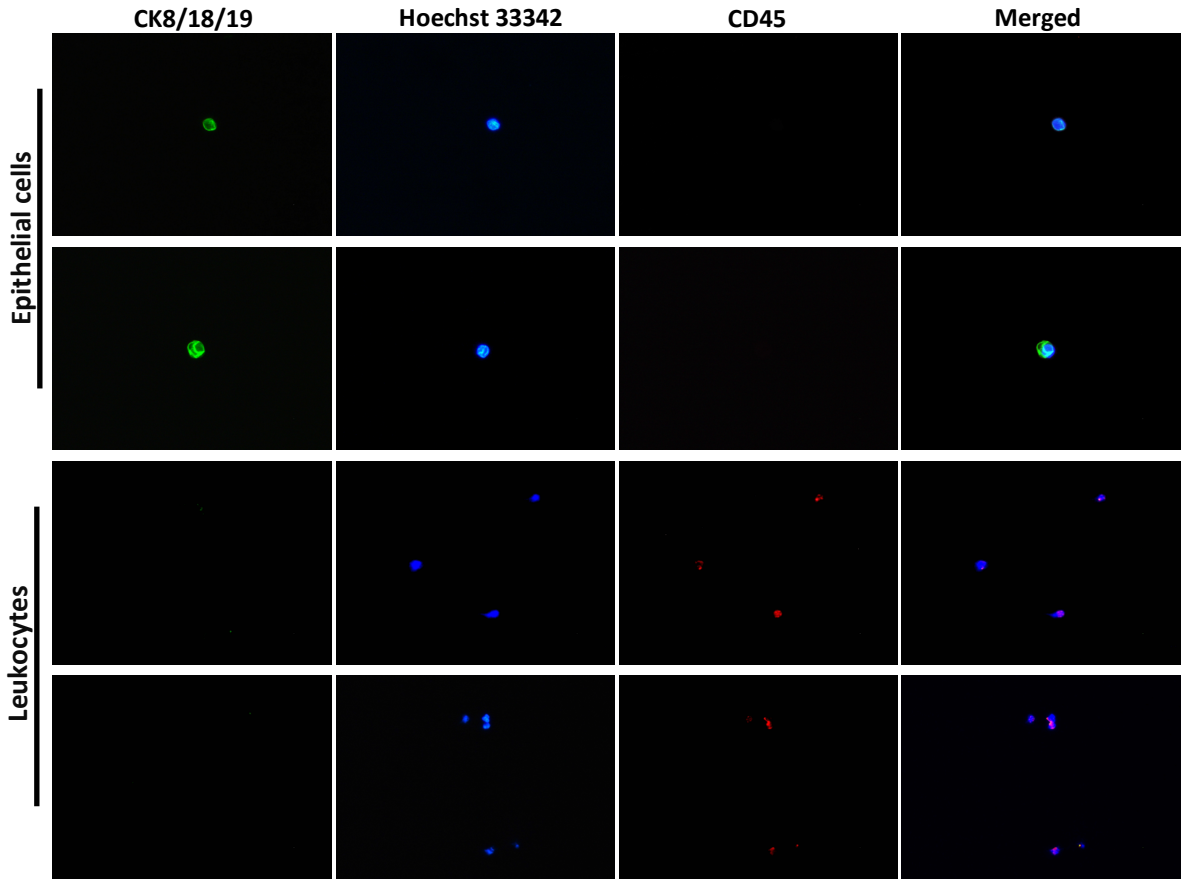

Figure 16: The MACS system successfully and accurately isolated the epithelial cells and leukocytes from ExU. The epithelial cell group comprised only those positive cells for CK/8/18/19 and displayed a "green" fluorescence signal. In contrast, leukocytes, identified by their CD45 expression and "red" fluorescence signal, were not present in the isolated epithelial cell group and only in the isolated leukocyte group.

The efficiency of the isolation procedure was further confirmed by RT-PCR analysis. Gene expression levels of *EpCAM* and *PTPRC*, specific markers for epithelial cells and leukocytes, respectively, were evaluated using RT-PCR with cDNA samples obtained from both epithelial cells and leukocytes in EJ and ExU samples from both patient and healthy control groups. The results, displayed in Figure 17, showed a significant and elevated expression of *EpCAM* in the sorted epithelial cell group compared to leukocytes ($p<0.0001$) and a higher expression of *PTPRC* in the sorted leukocyte group compared to epithelial cells ($p<0.0001$). These findings, combined with the results from the IF analysis, demonstrate the precise and effective isolation of the target cell populations using the MACS system in native liquid biopsy samples.

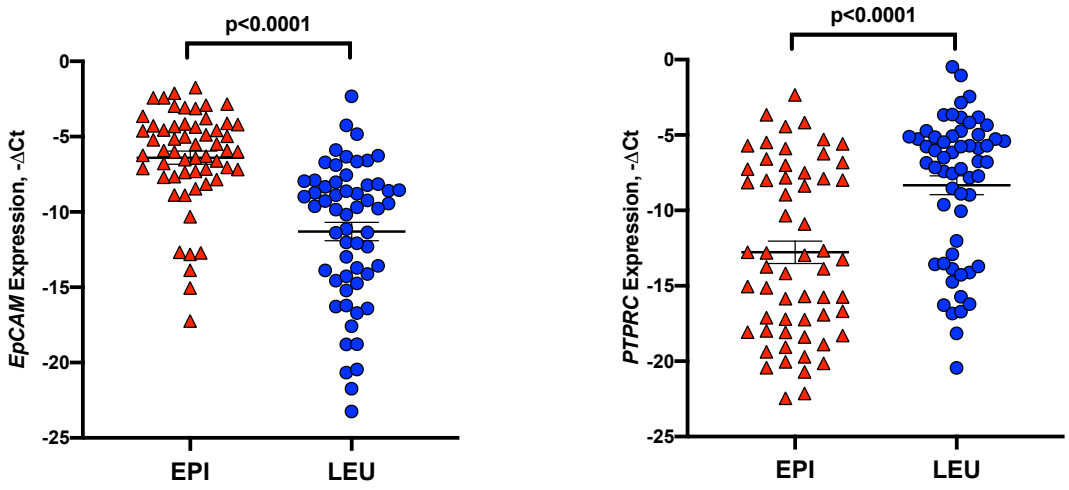

Figure 17: The mRNA expression levels of the genes *EpCAM* and *PTPRC* were analyzed in sorted epithelial cells and leukocytes. The results indicated that the epithelial cell group displayed a significantly higher expression of *EpCAM* when compared to leukocytes, as observed in both EJ and ExU samples. Conversely, the leukocytes demonstrated a significantly elevated expression of *PTPRC* compared to epithelial cells.

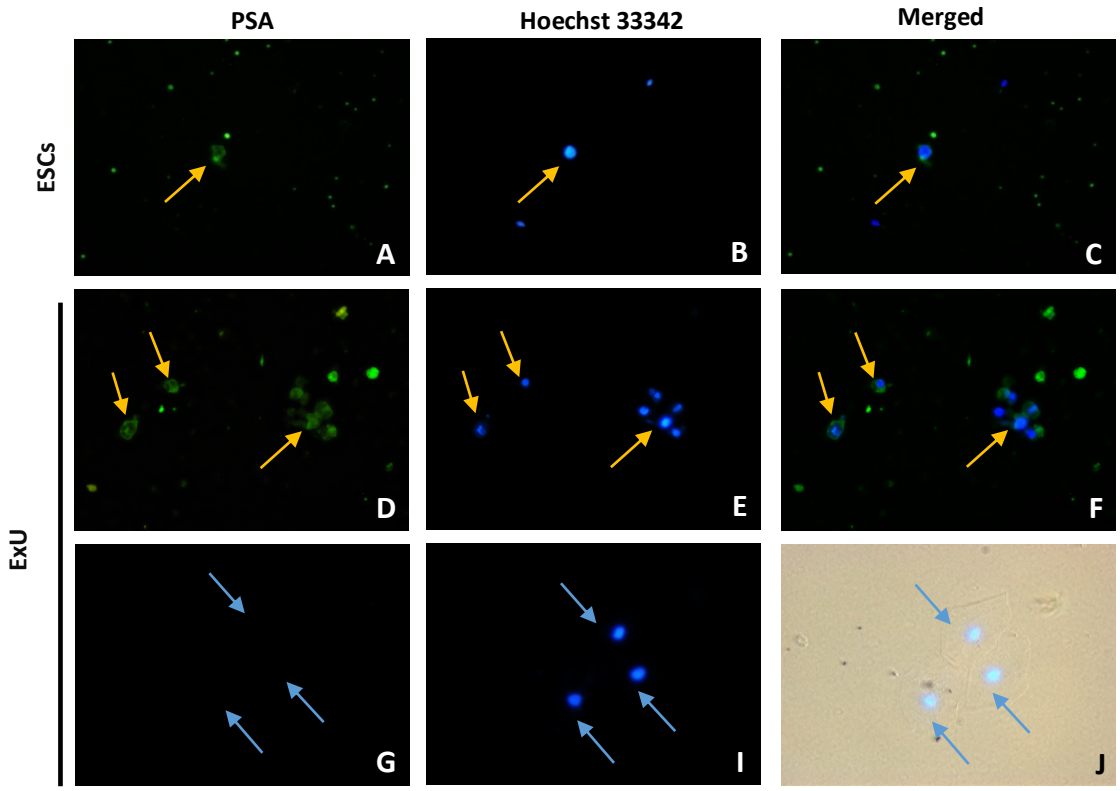

Figure 18: Prostatic epithelial cells in ESCs and ExU still exist after MACS isolation. (A-F) In both ESCs and ExU samples, prostatic epithelial cells can be found in the isolated epithelial cells. (G-J) Epithelial cells without a PSA signal were defined as non-prostate epithelial cells and were found in ExU samples after the isolation. Yellow arrows: Prostatic epithelial cells. Blue arrows: Transitional epithelium.

Prostatic epithelial cells can give insights into the prostate tissue, so they are the main research target in the isolated epithelial cells. Therefore, IF was used to prove the existence of prostatic epithelial cells after the MACS isolation. PSA is released by prostate gland and was utilized as a specific marker for prostatic epithelial cells, which were crucial in the investigation, given their significance in providing information on the prostate tissue. The experiment's results demonstrated the presence of prostatic epithelial cells identified as PSA+, and Hoechst 33342+ in both ESCs and ExU somatic cells, as indicated also by their morphological features (Figure 18). Furthermore, non-prostatic-origin epithelial cells were also observed: PSA - and Hoechst 33342 +. These results affirm the effectiveness of the MACS cell isolation process in preserving prostatic epithelial cells.

3.10. *CDKN2A* is hypermethylated and downregulated in the sorted epithelial cells and leukocytes

The promoter methylation levels of the *CDKN2A* were analyzed between CP/CPPS patients as well as healthy controls regarding both epithelial cells and leukocytes. The demographic data, clinical parameters of the study participants, and the experimental results for the sorted cell groups are shown in the supplement (Table 16-17). Results from the analysis of ESCs showed no significant difference in the methylation levels of *CDKN2A* in both epithelial cells and leukocytes. Conversely, in ExU, a significant increase in the promoter methylation levels of *CDKN2A* was observed in both epithelial cells ($p=0.0019$) and leukocytes ($p=0.0346$) in patients compared to healthy controls (Figure 19).

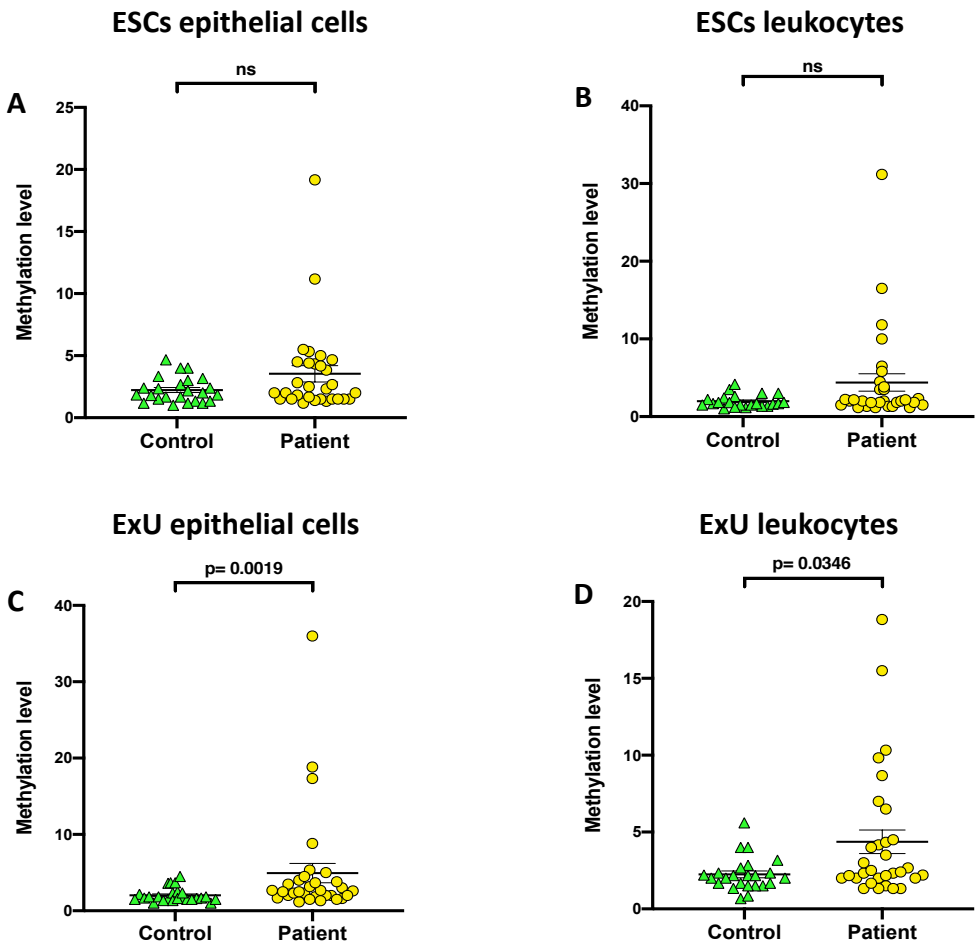

Figure 19: The promoter methylation levels of the *CDKN2A* were determined in sorted epithelial cells and leukocytes derived from ESCs and ExU samples. Results indicated no statistically significant elevation in the methylation levels of *CDKN2A* in both epithelial cells and leukocytes isolated from ESCs. However, a significant increase in the promoter methylation levels of *CDKN2A* was observed in both epithelial cells and leukocytes obtained from the ExU samples of the patient groups compared to those of the healthy controls.

Figure 20 compares the promoter methylation levels of *CDKN2A* in epithelial cells and leukocytes obtained from ESCs and ExU samples of both patient and healthy control groups. The results failed to demonstrate a statistically significant difference between the methylation levels of *CDKN2A* in epithelial cells and leukocytes in both ESCs and ExU groups. However, a slight elevation in the methylation levels of *CDKN2A* was observed in epithelial cells compared to leukocytes in the ESCs samples. Conversely, slight hypermethylation of *CDKN2A* was observed in leukocytes compared to epithelial cells in the ExU samples.

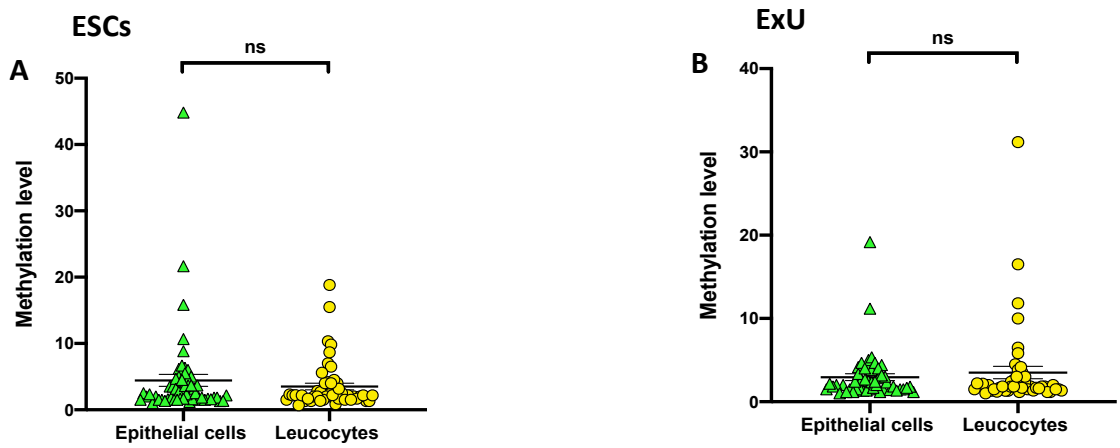

Figure 20: The promoter methylation levels of *CDKN2A* were analyzed in isolated epithelial cells and leukocytes derived from ESCs and ExU of patients and healthy controls. The comparison results revealed an absence of a statistically significant difference in the promoter methylation levels of *CDKN2A* between the isolated epithelial cells and leukocytes in both ESCs and ExU groups.

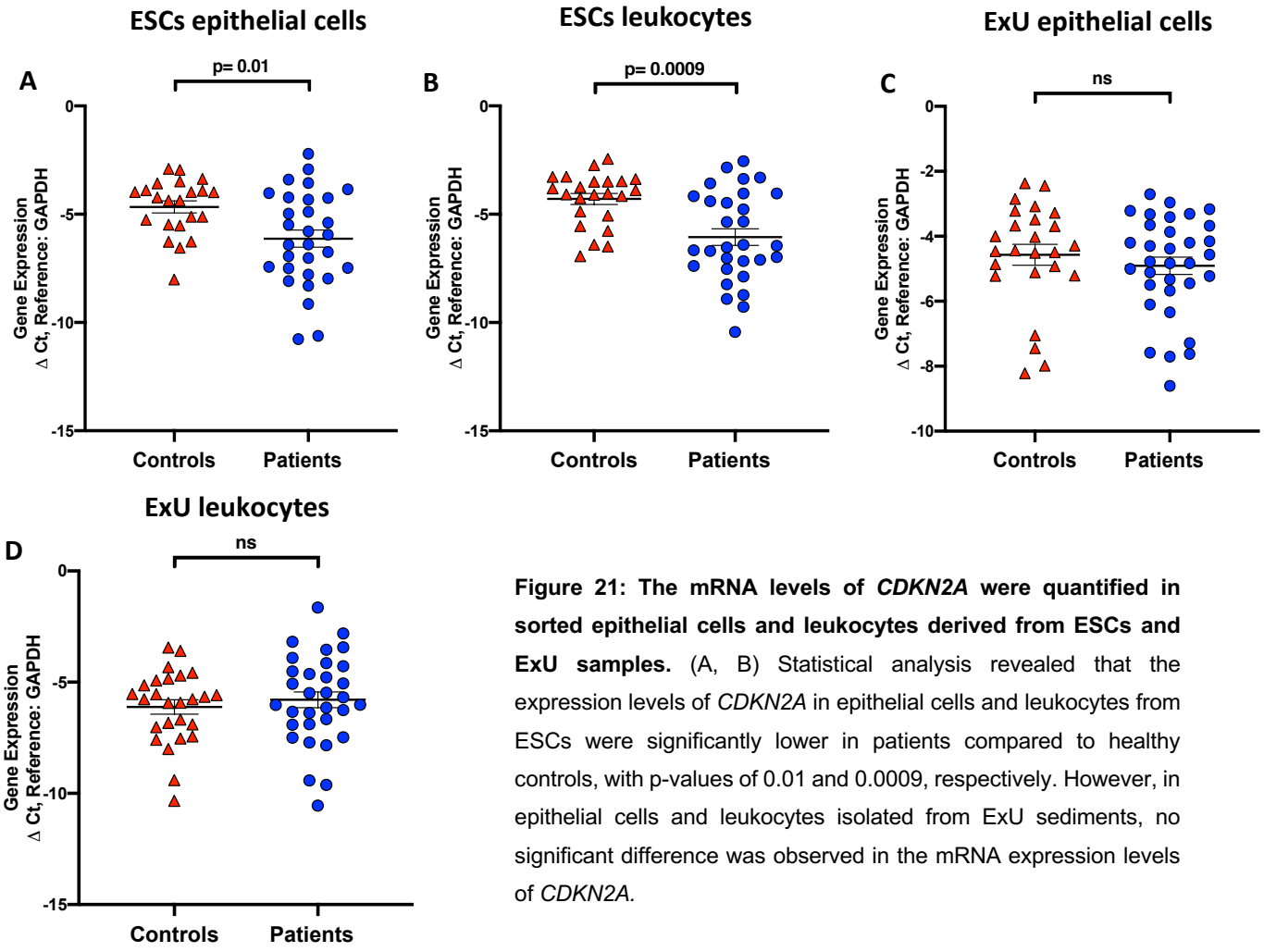

Figure 21: The mRNA levels of *CDKN2A* were quantified in sorted epithelial cells and leukocytes derived from ESCs and ExU samples. (A, B) Statistical analysis revealed that the expression levels of *CDKN2A* in epithelial cells and leukocytes from ESCs were significantly lower in patients compared to healthy controls, with p-values of 0.01 and 0.0009, respectively. However, in epithelial cells and leukocytes isolated from ExU sediments, no significant difference was observed in the mRNA expression levels of *CDKN2A.*

The mRNA expression levels of *CDKN2A* were quantified in isolated epithelial cells and leukocytes populations derived from ESCs and ExU of patients and healthy controls. Figure 21 presents the *CDKN2A e*xpression levels in both patient and control groups. Results indicated *CDKN2A* expression was significantly lower in epithelial cells (p=0.01) and leukocytes (p=0.0009) of patients with CP/CPPS in ESCs. However, there was no statistical difference in *CDKN2A* expression levels between patients and healthy controls in epithelial cells and healthy controls in ExU.

A comparative analysis assessed the differential expression of *CDKN2A* mRNA between epithelial cells and leukocytes. The results of this study are depicted in Figure 22. The data for this analysis was collected from epithelial cells and leukocytes sorted from the EJ and the ExU of patients and healthy controls. The results indicated a lack of significant difference in *CDKN2A* expression between epithelial cells and leukocytes in the EJ samples. Conversely, in the ExU samples, the epithelial cells showed a statistically significant higher expression level of *CDKN2A* (p=0.0007) when compared to leukocytes. These findings align with the trend of methylation of *CDKN2A* observed in epithelial cells and leukocytes in both the EJ and ExU.

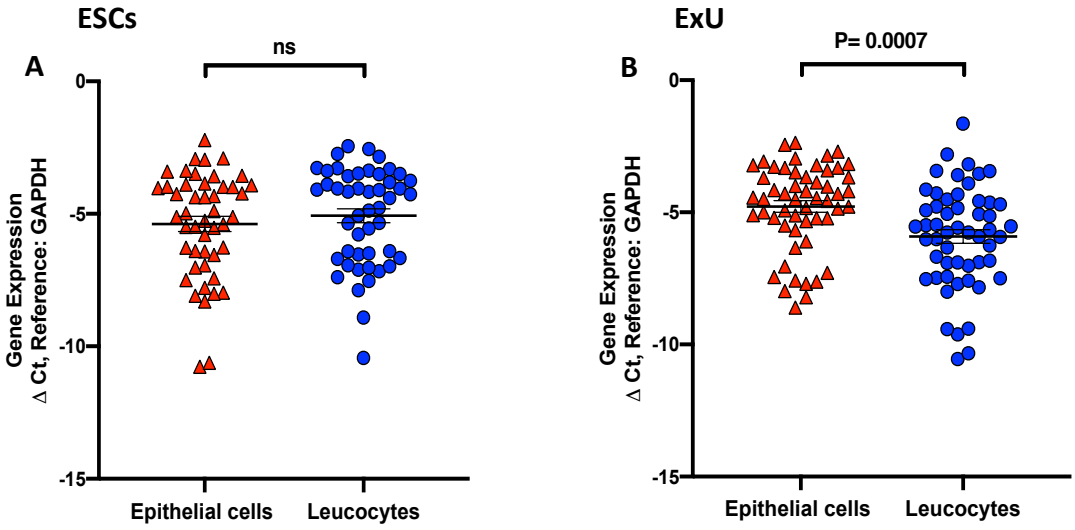

Figure 22: The mRNA expression levels of *CDKN2A* were compared in isolated epithelial cells and leukocytes from ESCs and ExU in both CP/CPPS patients and healthy individuals. The results showed that in ExU samples, the isolated epithelial cells demonstrated statistically significant hypermethylation compared to the leukocytes. In the ESCs, while the leukocytes exhibited a slight hypermethylation in comparison to the epithelial cells, this difference was not found to be statistically significant.

3.11. Liquid biopsy-based analysis of methylation and mRNA expression levels of TSGs demonstrates promising prognostic potential in CP/CPPS

The objective of the present study was to examine the relationship between the outcomes obtained from laboratory and ultrasonographic examinations and the levels of methylation and mRNA expression of selected TSGs, which can contribute to advancing our understanding and potentially inspire future research regarding the correlations between the utilization of liquid biopsy and clinical parameters in the context of CP/CPPS. As Figure 23 shows, the results revealed significant correlations between the study participants' age, PSA value, prostate volume, and the TSGs' methylation and mRNA expression levels. In the first instance, the analysis showed that the age of the participants had significant positive correlations to the levels of *EDNRB* (p=0.0074, r=0.3426) and *BMP7* (p=0.0387, r=0.2698) methylation in EJ. In addition, a negative correlation was established between the age of the participants and the expression of *CDKN2A* in the ExU samples (p=0.007, r=-0.3392). The findings of the study suggest that there is a positive correlation between increasing age and hypermethylation, leading to a corresponding decrease in mRNA expression levels.

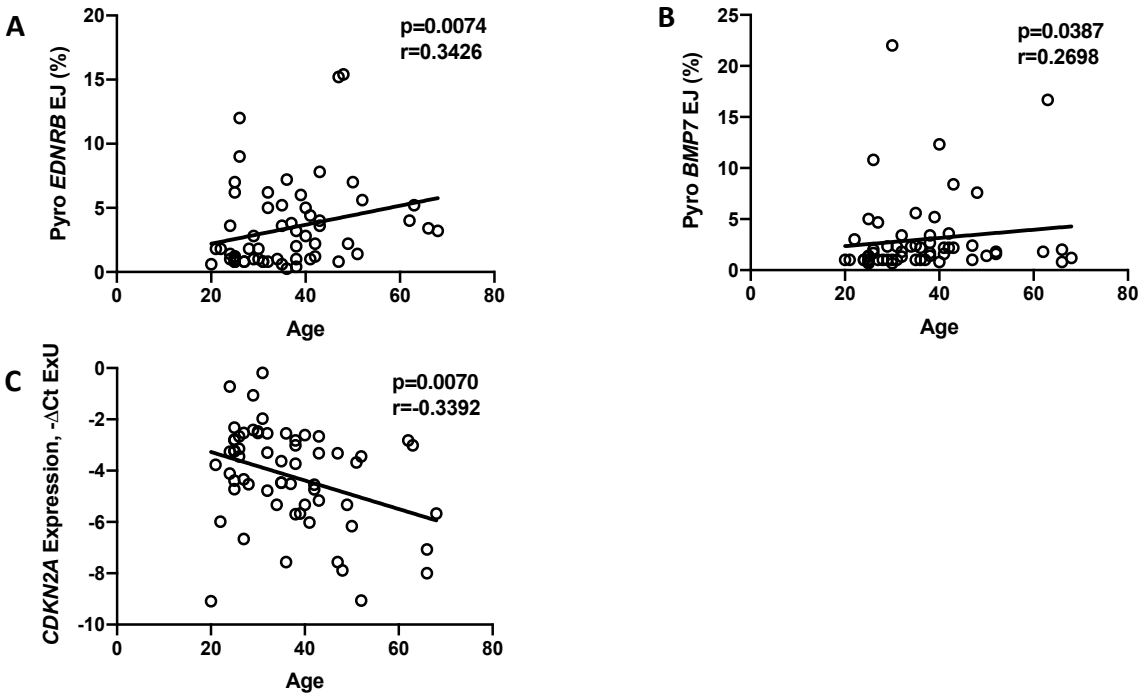

Figure 23: Higher methylation and lower mRNA expression levels are associated with increased age. (A, B) Positive correlations were established between age and the methylation levels of *EDNRB* and *BMP7* in EJ. (C) A negative correlation was observed between age and the expression level of *CDKN2A* in the ExU sample.

Our subsequent examination, as shown in Figure 24, revealed a significant inverse correlation between PSA levels and the expression of *CDKN2A* in ExU (p=0.0202, r=-0.3804) and *GSTP1* in EJ (p=0.00458, r=-0.3449). These findings imply that elevated PSA levels in patients with CP/CPPS may be associated with reduced expression of prostatic TSGs in liquid biopsies, thus serving as a potential predictor of an unfavorable prognosis and an increased likelihood of PCa development.

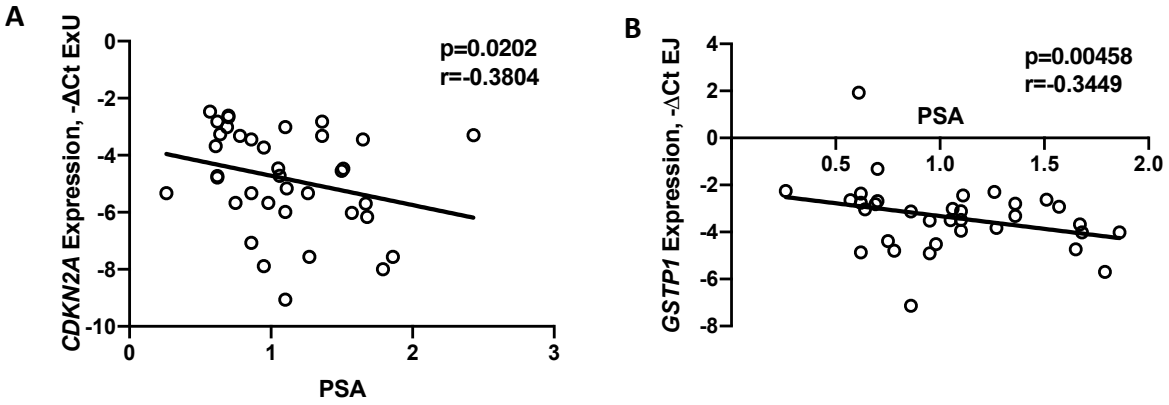

Figure 24: PSA had a significant inverse association with the mRNA expression of TSGs. As indicated, there were negative correlations between PSA values and the mRNA expression of *CDKN2A* in ExU and *GSTP1* in EJ.

As depicted in Figure 25, our analysis indicated a positive correlation between prostate volume and the methylation levels of TSGs. However, due to limited data availability, this analysis was limited to only the patient group and excluded healthy controls. In EJ, the methylation levels of *EDNRB* (p=0.0259, r=0.4447) and *GSTP1* (p=0.0196, r=0.4730) were found to have positive correlations with prostate volume. These results suggest that the methylation levels of TSGs related to the prostate may serve as a biomarker for the severity of urination symptoms in patients with CP/CPPS.

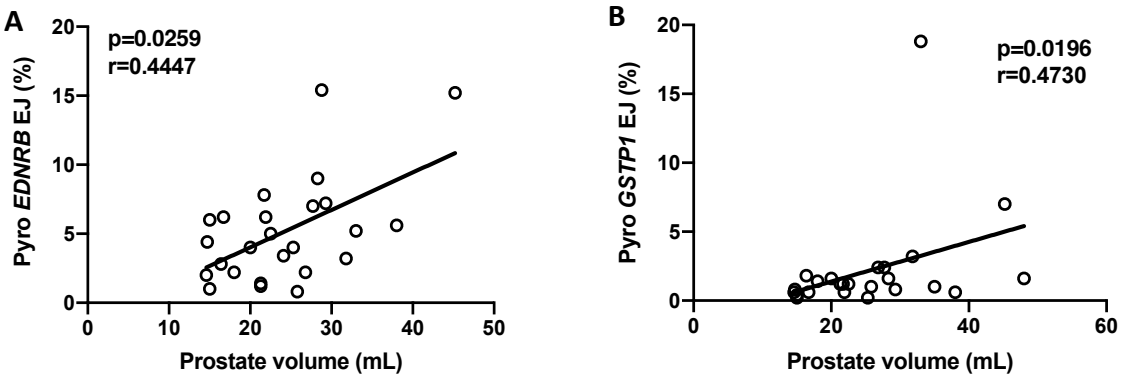

Figure 25: The correlation between prostate volume and methylation levels of *EDNRB* and *GSTP1* was investigated. The results showed a positive association between prostate volume and the methylation levels of *EDNRB* in EJ and *GSTP1* in EJ.

The subsequent study examined the correlation between the IPSS and CPSI scores to the mRNA and methylation levels of selected TSGs. The overview of correlations of IPSS and CPSI scores to TSGs methylation and expression levels are shown in the supplement (Table 18-19). Here, the graphs below show only the correlations of *CDKN2A* with IPSS and CPSI scores. The correlations of *CDKN2A* with IPSS are explicitly shown in Figure 26. The results indicate a significant positive correlation between IPSS and the methylation level of *CDKN2A* in the EJ sample (p=0.0327, r=0.3122). Furthermore, a significant negative correlation was observed between *CDKN2A* expression in EJ and IPSS (p=0.0138, r=-0.3274). In the ExU sample, the results showed a positive correlation between the methylation level of *CDKN2A* and IPSS (p=0.0021, r=0.4474).

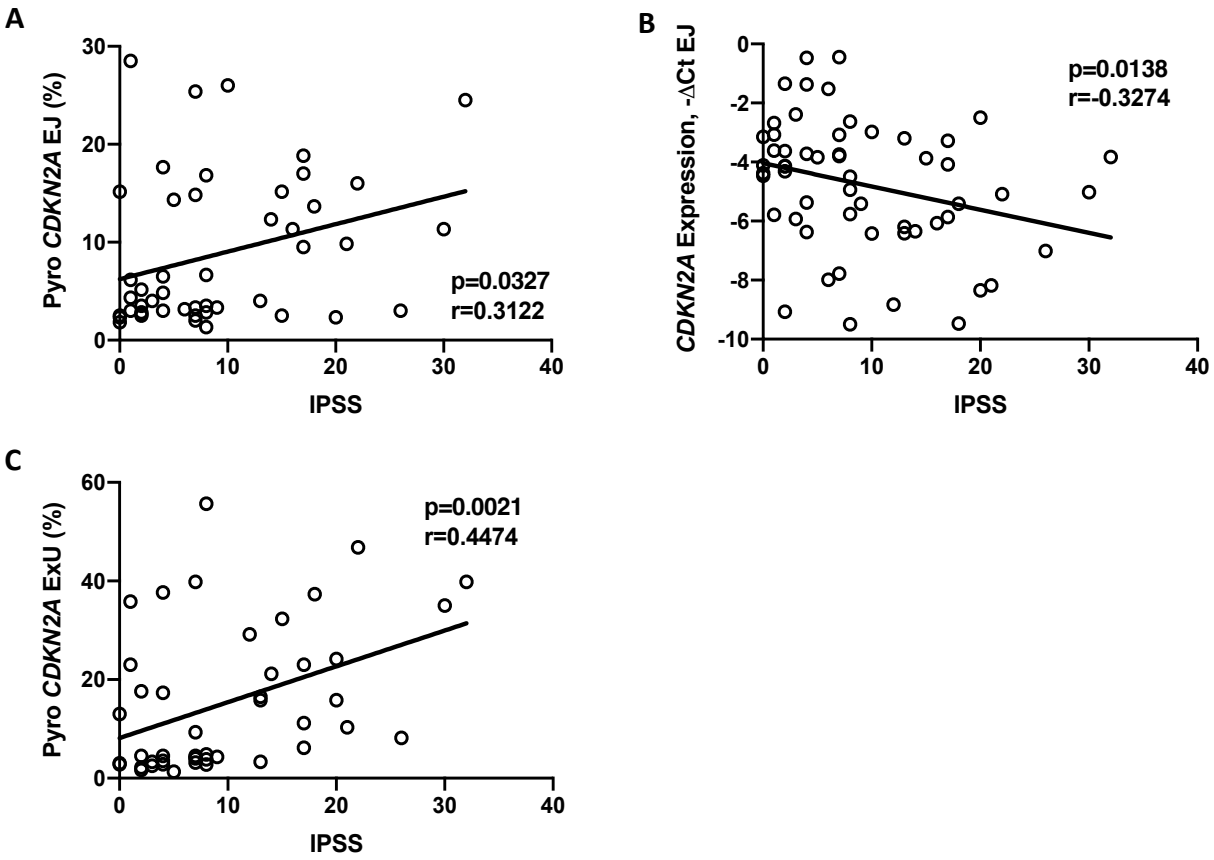

Figure 26: The study results indicate significant correlations between the methylation status and mRNA expression levels of *CDKN2A* with IPSS. (A, B) In EJ, the level of methylation of *CDKN2A* was found to be positively correlated with IPSS, while the trend of methylation was negatively correlated with expression levels, which in turn were negatively correlated with IPSS. (C) In ExU, IPSS was found to be positively correlated with *CDKN2A* methylation.

The CPSI is a tool to assess pain and discomfort associated with CP/CPPS. One component of CPSI, CPSI I, was first analyzed concerning methylation and mRNA expression levels of *CDKN2A* in both the EJ and the ExU. Figure 27 indicates a positive correlation between CPSI I and *CDKN2A* methylation and expression levels in both EJ (p=0.034, r=0.3133) and ExU (p=0.0062, r=0.4060). Conversely, expression levels of *CDKN2A* in both EJ (p=0.0045, r=-0.3779) and ExU (p=0.0032, r=-0.3939) showed negative correlations with CPSI I. These findings contribute to a better understanding of the complex relationship between CPSI I and *CDKN2A* in the context of CP/CPPS.

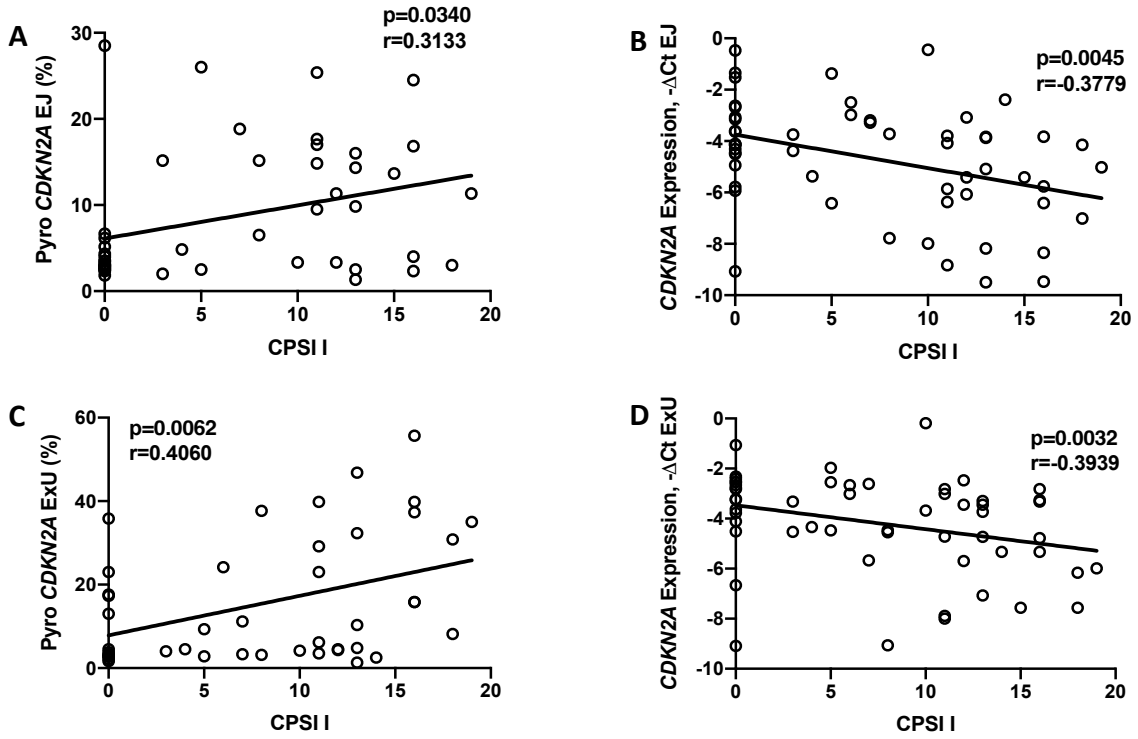

Figure 27: Methylation and mRNA expression levels of *CDKN2A* correspond to CPSI I. (A-B) Higher methylation of *CDKN2A* in EJ predicated higher CPSI I scores, and correspondingly, higher *CDKN2A* expression level showed a lower CPSI I score. (C-D) In ExU, the same trend of the methylation and expression levels of *CDKN2A* was observed as in EJ.

Next, we investigate the association between CPSI II, a tool for evaluating CP/CPPS patients' urinary symptoms, and methylation levels in the *CDKN2A* (Figure 28). Data analysis revealed a significant positive correlation between CPSI II and *CDKN2A* methylation levels in the ExU (p=0.0139, r=0.3684). Furthermore, in EJ, CPSI II was significantly negatively correlated with *CDKN2A* expression level (p=0.0465, r=-0.2696).

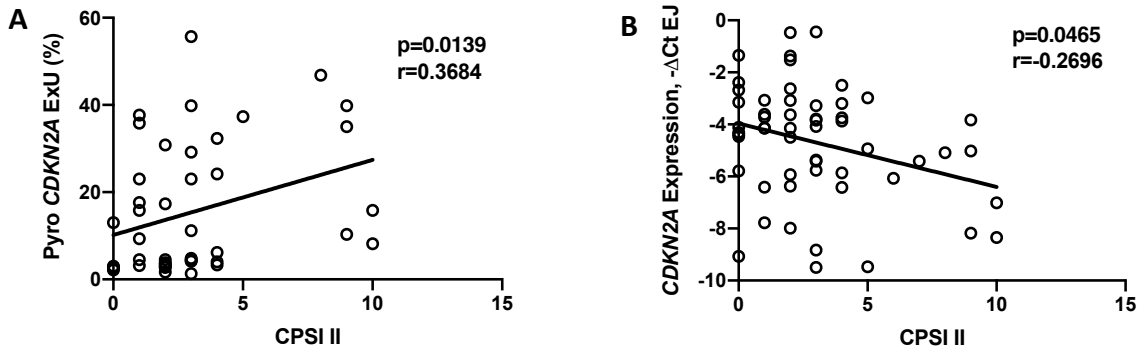

Figure 28: The results of CPSI II analysis revealed significant associations between the methylation and mRNA expression levels of *CDKN2A*. Specifically, CPSI II was positively correlated with the methylation levels of *CDKN2A* in the ExU. In contrast, CPSI II negatively correlated with the *CDKN2A* expression level in EJ.

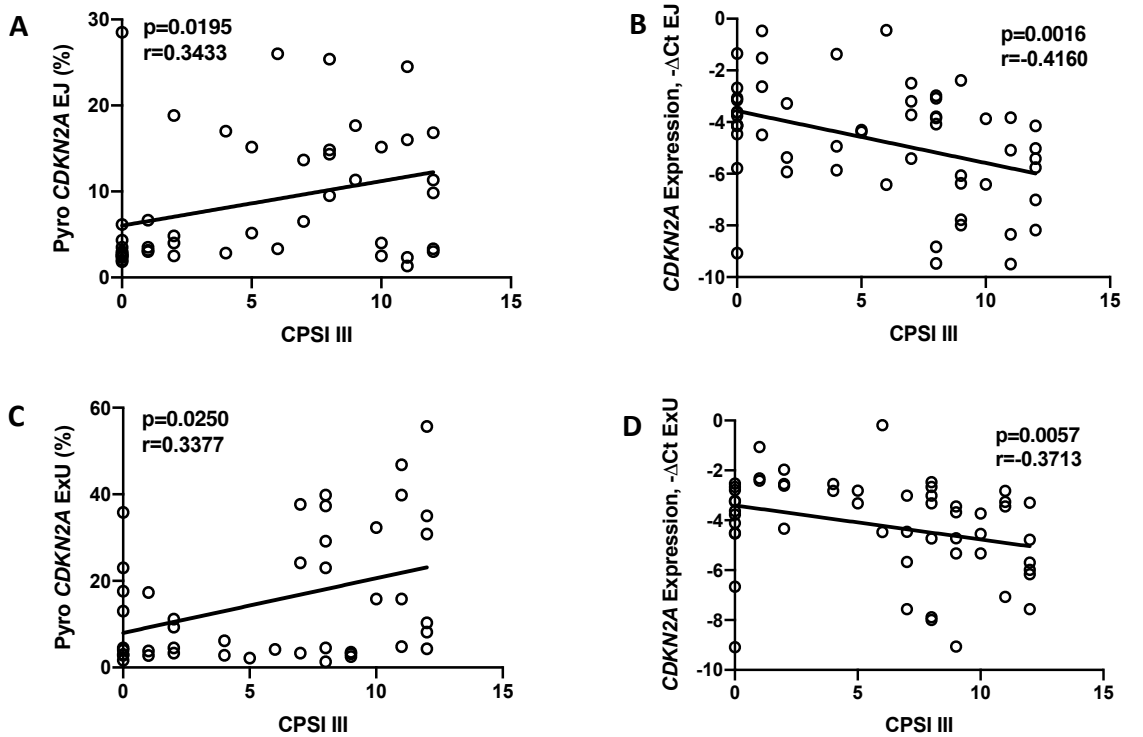

Figure 29: The results of the study revealed significant associations between the methylation status and mRNA expression levels of *CDKN2A* and CPSI III. (A-B) In the EJ, CPSI III exhibited a significant positive correlation with the methylation of *CDKN2A*, while a significant negative correlation was observed between CPSI III and the expression levels of *CDKN2A*. (C-D) Analogously, in the ExU, a similar trend was apparent as in EJ.

Evaluating life quality in patients with CP/CPPS is essential to clinical management. CPSI III, a widely used instrument, has been employed for this purpose. The present study investigated the correlation between methylation and expression levels of *CDKN2A* with a particular focus on EJ and ExU and CPSI III. Figure 29 shows the

study's findings and indicates a significant positive correlation between *CDKN2A* methylation levels in EJ (p=0.0195, r= 0.3433) and ExU (p=0.0025, r=0.3377) to CPSI III. Furthermore, a negative correlation between mRNA expression levels of *CDKN2A* and CPSI III was observed in both EJ (p=0.0016, r=-0.416) and ExU (p=0.057, r=-0.3713).

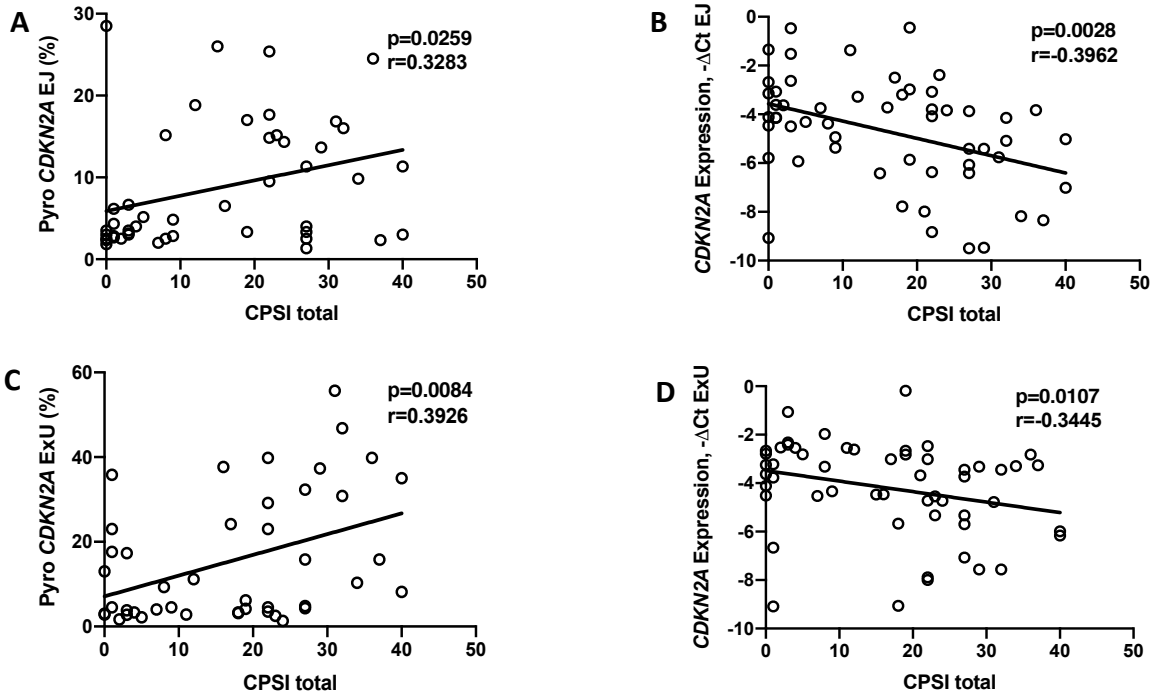

Figure 30: Significant correlations were observed between CPSI total score and *CDKN2A* methylation and mRNA expression levels. (A, C) In both EJ and ExU cohorts, CPSI total displayed a significant positive correlation with *CDKN2A* methylation levels. (B, D) We observed a significant negative correlation between CPSI total score and *CDKN2A* expression levels in both cohorts.

In this study, the CPSI total score, which is the sum of CPSI I, CPSI II, and CPSI III, was examined for its potential association with the methylation and expression status of *CDKN2A*. As presented in Figure 30, the results demonstrated significant positive correlations between CPSI total score and *CDKN2A* methylation levels in both EJ (p=0.0259, r=0.3283) and ExU (p=0.0084, r=0.3926). Additionally, negative correlations were observed between *CDKN2A* expression levels and CPSI total score in EJ (p=0.0028, r=-0.3926) and ExU (p=0.0107, r=-0.3445).

Except for *CDKN2A*, other selected TSGs, such as *EDNRB*, *PTGS2*, and *BMP4*, were also shown in association with CPSI evaluation. However, *CDKN2A* showed more

significant correlations between methylation and mRNA expression levels to CPSI scores in both EJ and ExU samples than other TSGs, suggesting its potential use as a biomarker for CP/CPPS. These findings provide important insights into the underlying connections between CP/CPPS and PCa, and highlight the potential role of TSGs in the prognosis of CP/CPPS and the possibility of liquid biopsies as a biomarker for this condition. Furthermore, the observed positive and negative correlations between CPSI scores and the methylation and mRNA expression levels of prostatic TSGs suggest a possible involvement of epigenetic modifications in developing CP/CPPS. In particular, *CDKN2A*, with its efficiency and specificity, has emerged as a promising candidate for future biomarker development.

Recent studies have reported that CP/CPPS can harm male fertility, affecting sperm motility, viability, and concentration[112,113]. It is important to note that the evaluation of sperm motility is one of the essential parameters in male fertility assessment, as impaired motility can lead to difficulties in achieving conception. To better understand the potential role of liquid biopsies in CP/CPPS, correlations between sperm motility and the methylation and mRNA expression levels of selected TSGs were investigated. Besides, examining the methylation and mRNA expression of these genes in somatic cells of liquid biopsies of CP/CPPS may indirectly help to measure the percentage of motile and immotile spermatozoa and to conjecture fertility. Specifically, the clinicians distinguished sperm motility in straight moving (motility a), zig-zag moving (motility b), vibrating (motility c), and immotile (motility d), with sperm motility total being the summation of motility a+b+c.

Progressive motility is a commonly used parameter for assessing the motility of spermatozoa in semen analysis. It refers to the proportion of spermatozoa that exhibit forward movement with a rapid, linear, or large-circular trajectory. This type of motility is crucial for sperm to reach the site of fertilization and penetrate the oocyte. Non-progressive motility, on the other hand, refers to the proportion of spermatozoa that exhibit some movement, such as swimming in small circles or having erratic movement. Finally, immotile spermatozoa are those that show no movement at all. Table 20-21 in the supplement provides an overview of the correlations between various sperm motilities and the methylation and expression levels of TSGs. The observed correlations generally align with our expectations. Figure 31, for example,

illustrates negative correlations between sperm motility a and the methylation levels of *EDNRB* in EJ (p=0.0143, r=-0.3147) and *BMP7* in EJ (p=0.0201, r=-0.3019), as well as positive associations with mRNA expression levels of *CDKN2A* in ExU (p=0.0187, r=0.2978), and *PTGS2* in ExU (p=0.0025, r=0.3932).

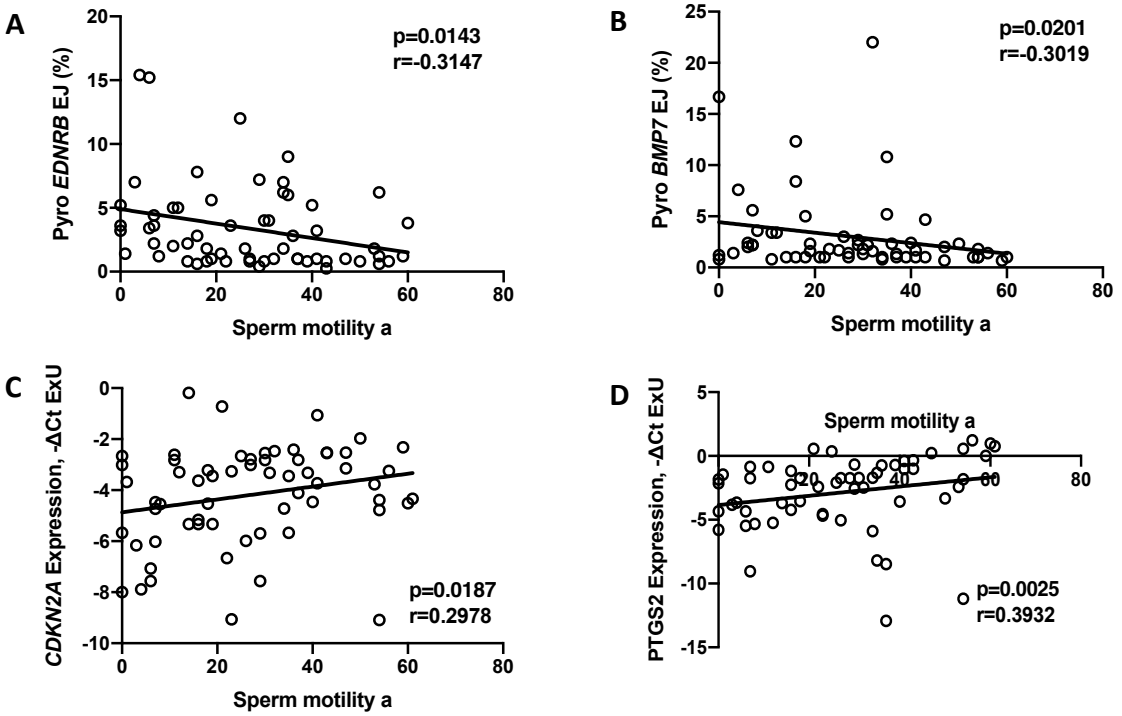

Figure 31: The study investigated the potential association between methylation and mRNA expression levels of TSGs with sperm motility a in EJ and ExU. (A-B) The results revealed a negative correlation between sperm motility a in the EJ and methylation levels of *EDNRB* and *BMP7*. (C-D) In the ExU, the expression levels of *CDKN2A* and *PTGS2* were positively correlated with sperm motility a.

In the investigation of the relationship between sperm motility b and experimental data, we observed a significant negative correlation between the methylation of *BMP7* in ExU (p=0.0095, r=-0.3466) and *GSTP1* in EJ (p=0.0438, r=-0.2657) and sperm motility b (Figure 32).

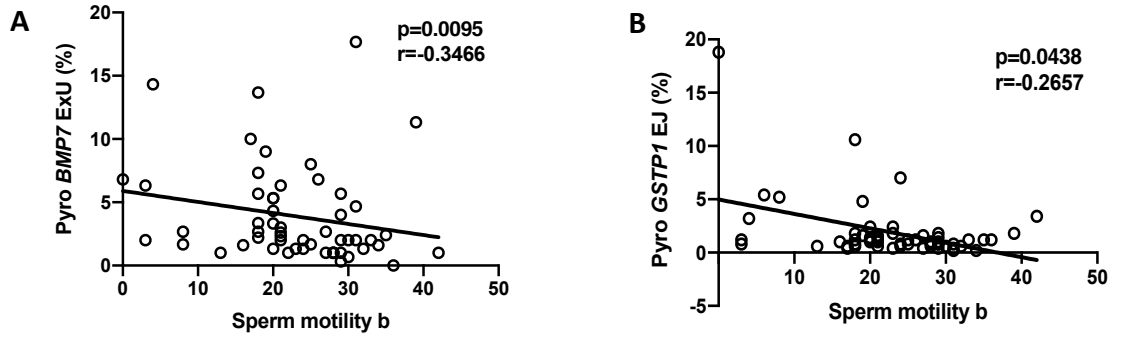

Figure. 32: Sperm motility b was negatively correlated to methylation levels of *BMP7* in EJ and *GSTP1* in ExU.

Non-progressive motility (motility c) was included in the calculation of total motility. As Figure 33 shows, we noticed that the methylation of *BMP7* in EJ (p=0.012, r=-0.4129) showed a negative correlation to motility c.

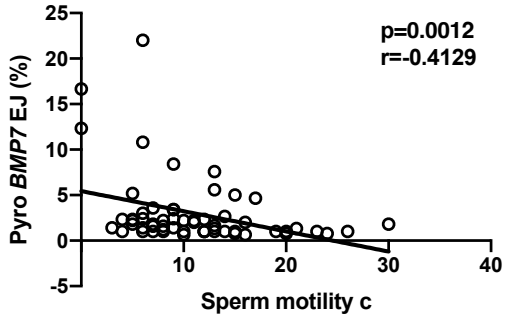

Figure. 33: Sperm motility c was negatively correlated to methylation levels of *BMP7* in EJ.

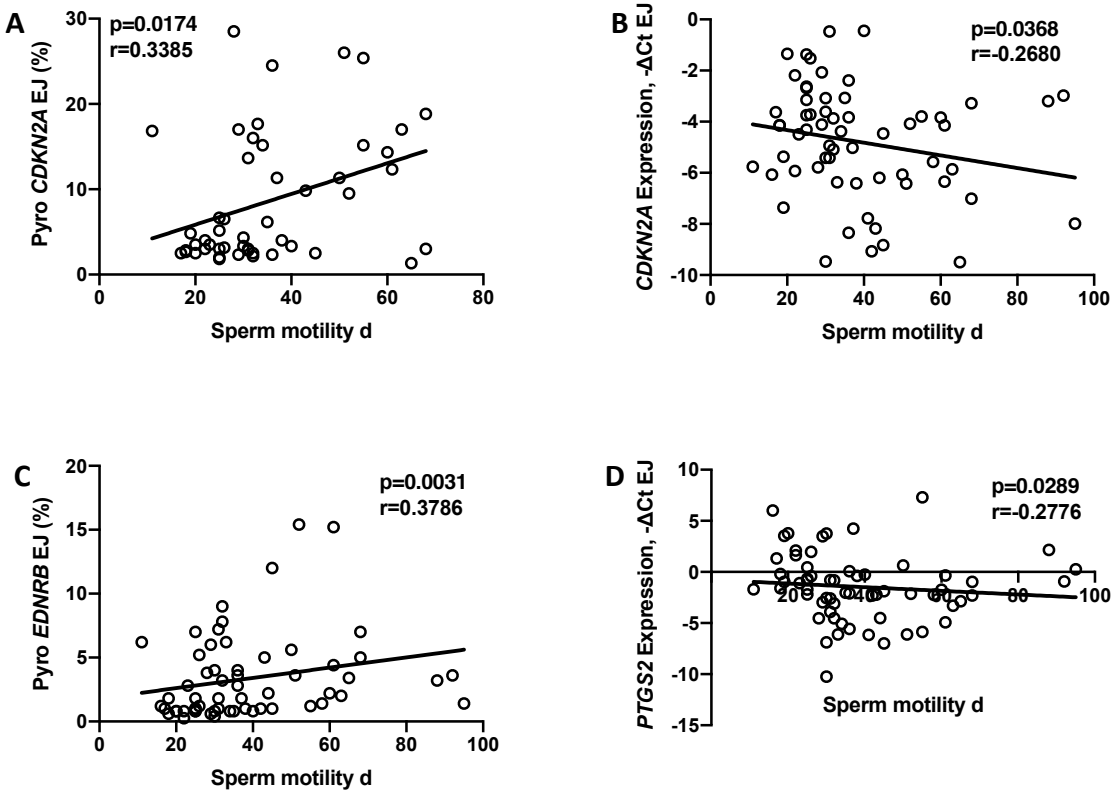

Figure. 34: The relationship between the methylation and mRNA expression levels of TSGs with sperm motility d was investigated. (A, B) The study's findings indicated a positive correlation between sperm motility d and the methylation levels of *CDKN2A* in EJ. Correspondingly, a negative correlation was observed between the expression of *CDKN2A* in EJ and sperm motility d. (C, D) A positive correlation between the methylation of *EDNRB* in EJ and sperm motility d was revealed, while the expression of *PTGS2* in EJ showed a negative correlation with sperm motility d.

As the term suggests, immotile spermatozoa are sperm cells that exhibit no movement. These spermatozoa are considered non-functional and are unable to contribute to fertility. Our research has shed light on the potential utility of analyzing the methylation and mRNA expression patterns of TSGs to assess the percentage of immotile spermatozoa. Notably, Figure 34 displays the positive correlation between the methylation levels of *CDKN2A* (p=0.0174, r=0.3385) in EJ and *EDNRB* (p=0.0031, r=0.3786) in the EJ and sperm motility d. In addition, the mRNA expression levels of *CDKN2A* in EJ (p=0.0368, r=-0.268) and *PTGS2* in EJ (p=0.0289, r=-0.2776) were found to be negatively correlated with sperm motility d.

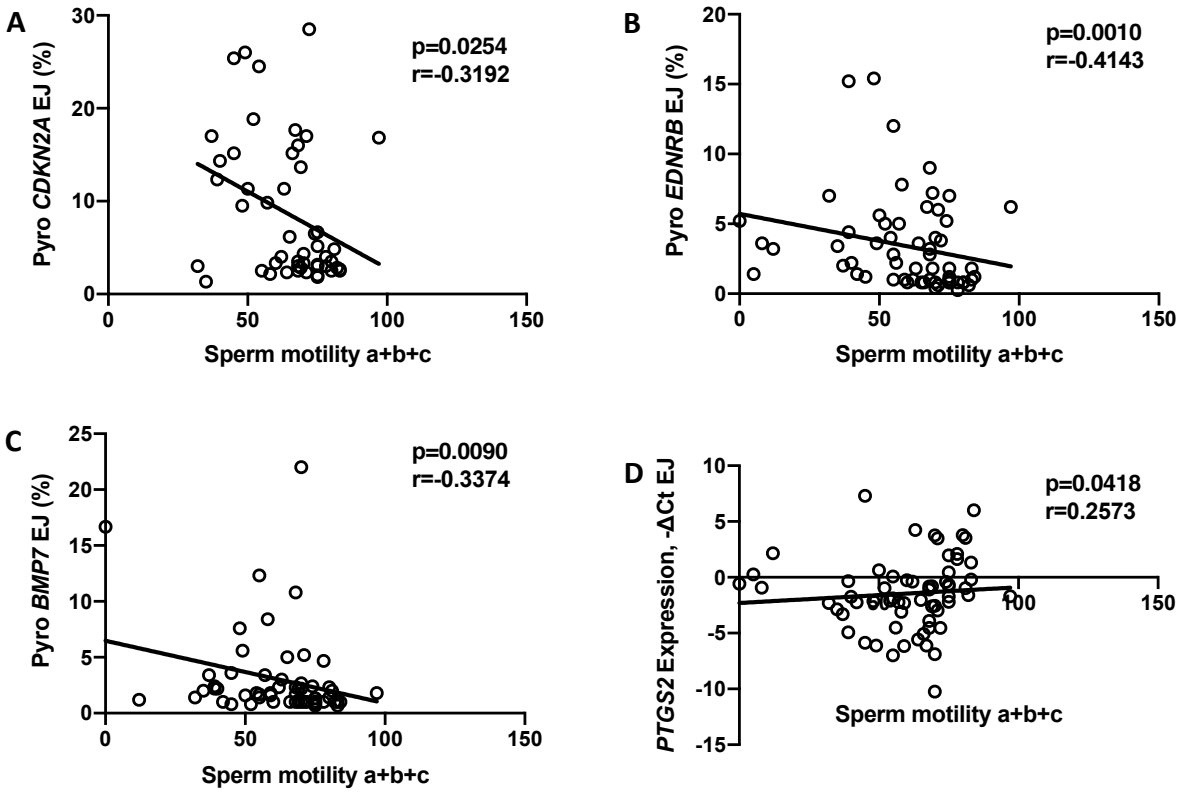

Figure 35: The study aimed to investigate the potential associations between total sperm motility and the methylation and mRNA expression levels of selected TSGs. (A-C) In EJ, negative correlations were observed between sperm total motility and the methylation levels of *CDKN2A*, *EDNRB*, and *BMP7*. (D) A positive correlation was found between total sperm motility and the expression of *PTGS2* in EJ.

The total sperm motility, which encompasses all types of sperm movement, was determined by the summation of sperm motility a+b+c. As presented in Figure 35, the study's results revealed a significant association between the methylation and mRNA expression levels of TSGs and total sperm motility. Specifically, a negative correlation was observed between the methylation levels of *CDKN2A* (p=0.0254, r=-0.3192),

EDNRB (p=0.001, r=-0.4143), and *BMP7* (p=0.009, r=-0.3374) in the EJ and total sperm motility. Correspondingly, a positive correlation was found between the mRNA expression level of *PTGS2* in EJ and total sperm motility (p=0.0418, r=0.2573). These findings provide valuable insight into the potential use of TSG methylation and mRNA expression analysis as a non-invasive tool for evaluating male infertility.

3.12. Correlation of *CDKN2A* expression levels between sorted epithelial cells and leukocytes

In this study, we sought to investigate the correlations between methylation and mRNA expression in sorted epithelial cells and leukocytes, as well as the relationship between experimental data and clinical parameters. Our analysis focused on *CDKN2A* as a target for methylation and mRNA expression level analysis, as it was the only gene that showed corresponding relations between methylation and expression in both ESCs and ExU somatic cells.

In Figure 36, our study demonstrated a significant positive correlation between *CDKN2A* expression in leukocytes isolated from EJ and the *CDKN2A* expression in epithelial cells of EJ (p<0.0001, r=0.7906) and ExU (p=0.0256, r=0.3254). Although no significant correlation was observed between methylation and mRNA expression levels in these two cell cohorts, these results imply a potential association between *CDKN2A* methylation status and its expression in the aforementioned liquid biopsy cell types. Furthermore, our findings suggest that both epithelial cells and leukocytes may contribute to the hypermethylation of *CDKN2A* in EJ and ExU.

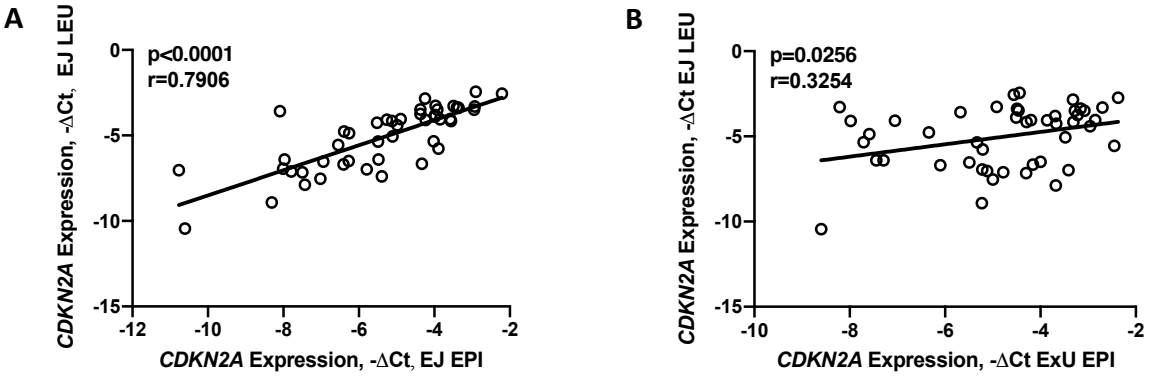

Figure 36: The correlations between methylation and mRNA expression levels of *CDKN2A* in isolated cell groups were analyzed. Our results indicated a positive correlation between *CDKN2A* expression in leukocytes of EJ and the expression of *CDKN2A* in the epithelial cells of both EJ and ExU.

3.13. *CDKN2A* methylation and expression levels in sorted epithelial cells and leukocytes play a role in CP/CPPS management

Significant positive correlations between the methylation level of PSA and age with the methylation value of *CDKN2A* in epithelial cells of EJ were revealed (Figure 37), with p-values of 0.0273 and 0.0227, respectively. In addition, the correlation coefficients were found to be 0.4411 and 0.3125, respectively, indicating a moderate to strong positive correlation.

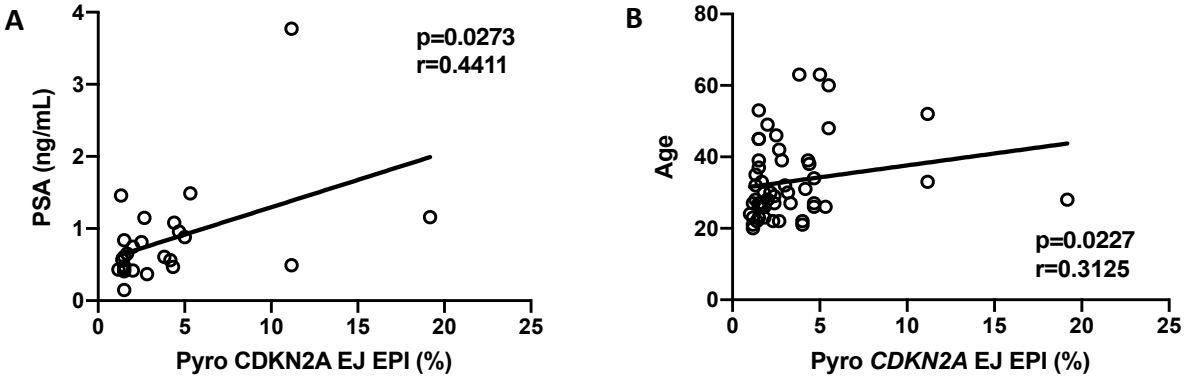

Figure 37: Methylation levels of *CDKN2A* in epithelial cells of EJ were positively correlated to both PSA and age.

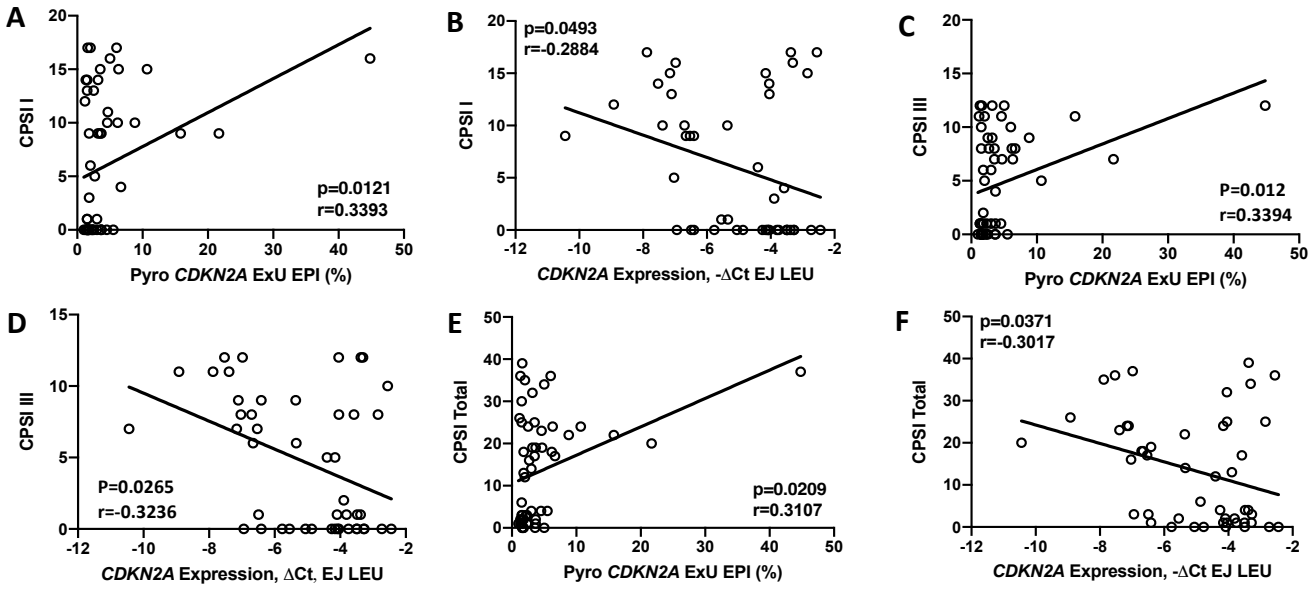

Figure 38: The study investigated the associations between the various CPSI values with the methylation and mRNA expression levels of *CDKN2A* in sorted epithelial cells and leukocytes. (A, C, E) Notably, the results revealed a positive correlation between *CDKN2A* methylation levels in ExU epithelial cells with CPSI I, CPSI III, and CPSI total scores. (B, D, F) Negative correlations were observed between the expression of *CDKN2A* in leukocytes of EJ and CPSI I, CPSI III, and CPSI total, respectively.

Examining the reciprocity of CPSI scores to sorted epithelial cells and leukocytes from EJ and ExU samples can provide valuable insights into the severity of CP/CPPS, and aid in evaluating the current condition of the disease. For example, Figure 38 shows significant positive correlations between CPSI I (p=0.0121, r=0.3393) and CPSI III (p=0.012, r=0.3394) with the methylation level of *CDKN2A* in ExU epithelial cells. Conversely, negative correlations were observed between CPSI I (p=0.0493, r=-0.2884) and CPSI III (p=0.0265, r=-0.3236) and the expression of *CDKN2A* in EJ leukocytes. Moreover, the methylation level of *CDKN2A* in ExU epithelial cells exhibited a significant positive correlation with CPSI total (p=0.0209, r=0.3107), while the expression of *CDKN2A* in EJ leukocytes was negatively correlated with CPSI total (p=0.0371, r=-0.3107).

Methylation patterns and expression levels of *CDKN2A* were also found that may serve as indicators of non-progressive sperm motility. For example, Figure 39 illustrates that sperm motility c exhibited a negative correlation with *CDKN2A* methylation levels in EJ leukocytes (p=0.038, r=-0.3138), as well as in both epithelial cells (p=0.0101, r=-0.3641) and leukocytes of ExU (p=0.0072, r=-0.3909).

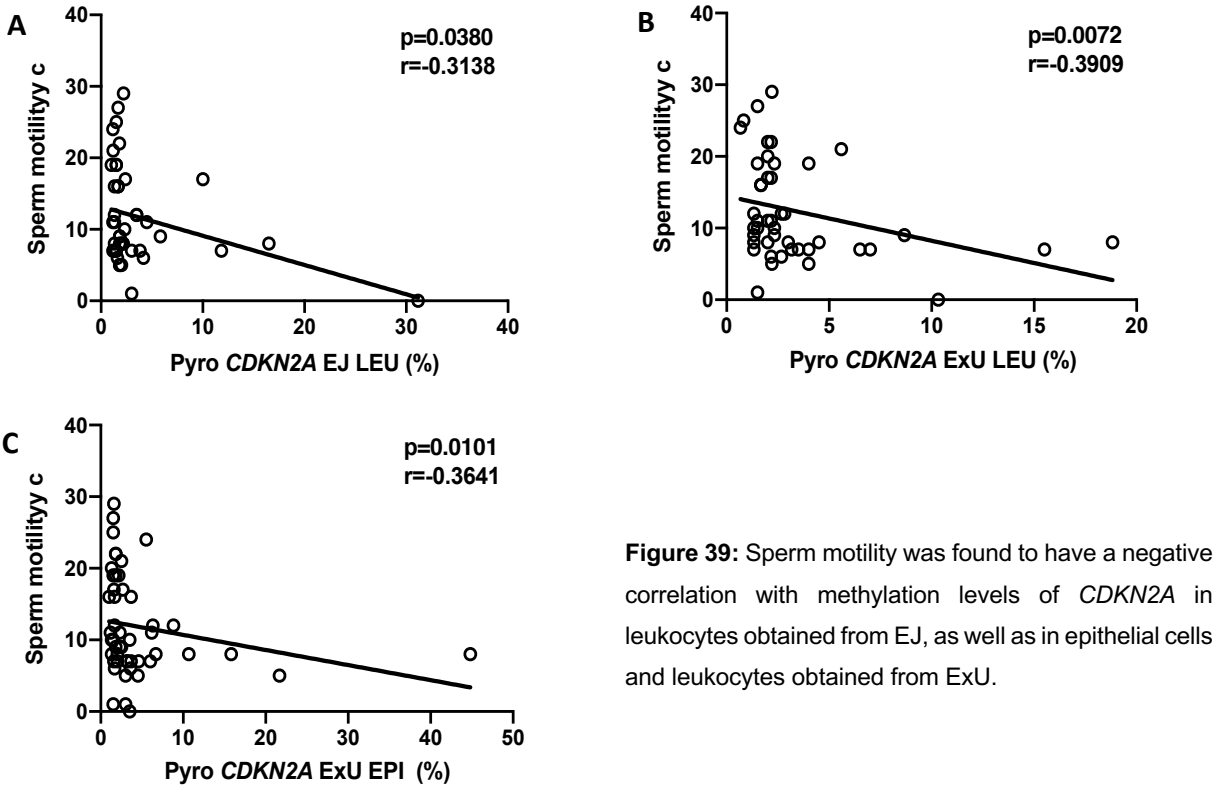

Figure 39: Sperm motility was found to have a negative correlation with methylation levels of *CDKN2A* in leukocytes obtained from EJ, as well as in epithelial cells and leukocytes obtained from ExU.

3.14. Polarization of THP-1 cells with whole exosomes isolated from ExU supernatant

Monocytes are white blood cells that are crucial to the immune response. Upon activation, monocytes can rapidly migrate to sites of inflammation, differentiate into macrophages and dendritic cells, and perform their functions. The THP-1 cell line is a widely used model of human monocytes that has been extensively studied to understand their behavior and functions. Exosomes, conversely, are small extracellular vesicles secreted by cells and involved in intercellular communication. They contain a range of constituents, including proteins, DNA, RNA, lipids, and cytosol of the cells that secreted them[114]. Exosomes have been implicated in various diseases, including cancer, neurodegeneration, and inflammatory diseases, where they can affect cell function and behavior.

To investigate the effect of exosomes on the differentiation of M0 macrophages, THP-1 cells were first treated with PMA to induce differentiation into M0 cells. The M0 cells were then treated with exosomes extracted from ExU. The mRNA expression levels of M1 macrophage markers (TNF-a, IL-1ß), M2 macrophage markers (CD206, CCL22, CCL18, and IL-10), and *CDKN2A* were analyzed using RT-PCR.

This study aimed to understand how exosomes can influence the differentiation of M0 macrophages into either M1 or M2 macrophages. The study's results will help us understand the role of exosomes in regulating the immune response and potentially lead to the development of new treatments for inflammatory diseases.

3.14.1. Polarization of THP-1cells to M0 macrophages using PMA after 0h, 24h and 48h

In Figure 39, we present the morphological changes of THP-1 cells upon treatment with 20 µg/mL PMA for 24 and 48 hours, 1.25 million THP-1 cells were seeded in each well of 6-well plates as observed under bright field microscopy. Following PMA treatment, THP-1 cells exhibited adhesion to the cell culture plate and gained polarity, transforming their round morphology to an irregular polygonal shape, a characteristic feature of M0 cells.

In the 24-hour incubation group, approximately 50-55% of the THP-1 cells showed adhesion, whereas 70-75% exhibited adhesion after 48 hours of incubation. The M0 cells that differentiated after 48 hours of incubation were chosen for further experimentation.

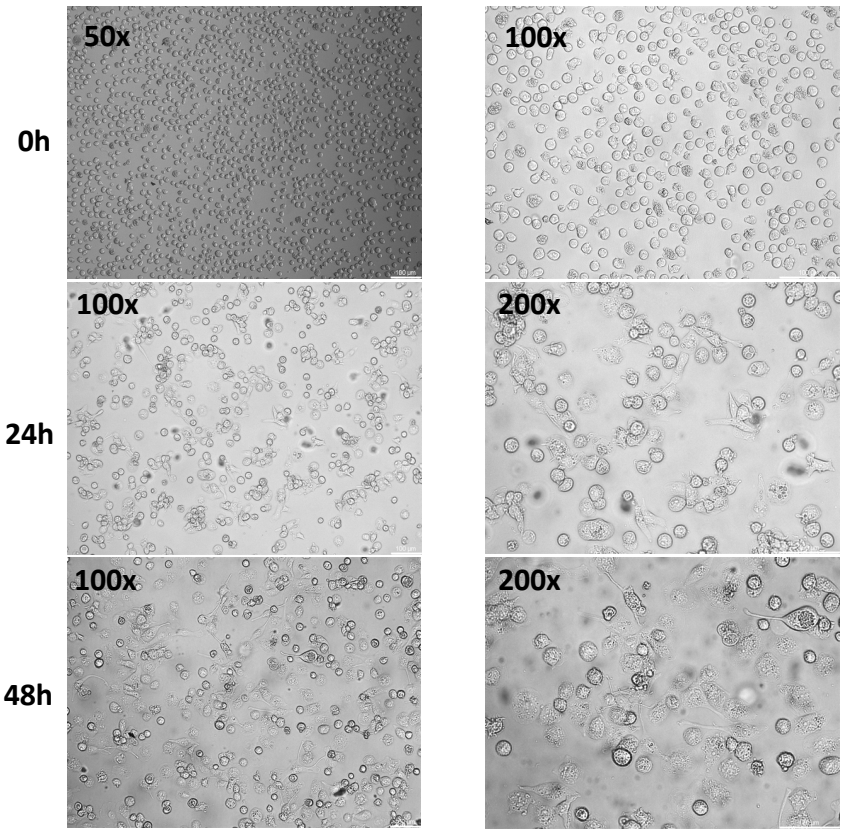

Figure 39: Prior to PMA treatment, THP-1 cells exhibited a non-polarized morphology. However, following PMA exposure for 24 and 48 hours, the cells displayed an adhesive and polarized phenotype. Specifically, in the 48-hour group, a significant proportion (70-75%) of the cells adhered firmly to the culture plate and demonstrated clear polarity.

3.14.2. Infiltration of exosomes into M0 macrophages after 24h treatment

Here, the efficacy of exosome infiltration treatment was evaluated utilizing IF, as depicted in Figure 40. Exosomes extracted from ExU samples of one patient and one healthy control were used at a concentration of 1.25% for a 24-hour incubation period in polarized M0 cells, after which the cells were subjected to IF processing. CD81 (1:100, Alexa Fluor 488 as a corresponding secondary antibody), a known exosome marker, was used to detect exosomes that had entered the cells. To serve as an

untreated control, DMSO at a concentration of 1.25% was used. The target cells were defined as CD81 + and Hoechst 33342 +.

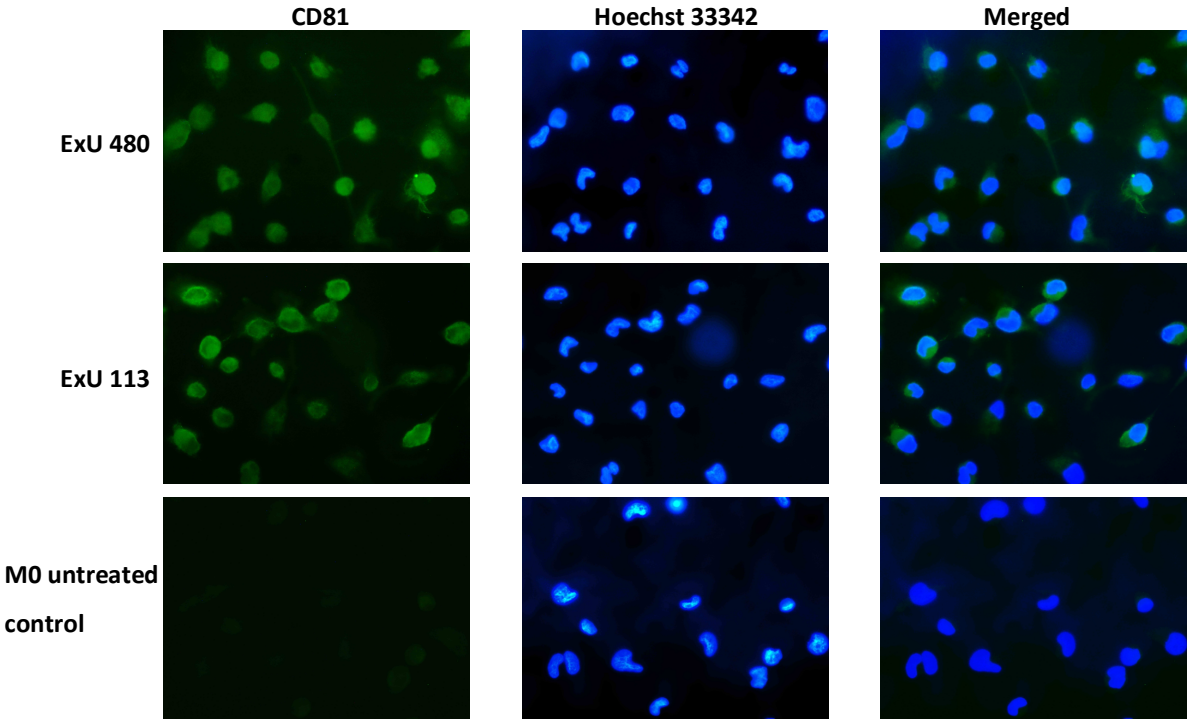

Figure 40: IF detected CD81 in cells after 48 hours of exosome incubation. The results showed that both patient-derived exosomes (ExU 480) and healthy control-derived exosomes (ExU 113) induced the detection of green signals by IF in their respective treated groups. In contrast, the untreated control group (M0) exhibited no significant CD81 signals. These findings suggest that exosomes from both patient and healthy control sources could penetrate the cells and induce a CD81 response, while untreated cells did not show any such response. Such insights can help in the development of new therapeutic strategies for the treatment of various diseases.

3.14.3. mRNA expression levels of TNF-α and IL-1β after 24h and 48h exosome treatment

Tumor necrosis factor-α (TNF-α) and interleukin 1 beta (IL-1β) are essential cytokines in inflammatory and autoimmune diseases[115]. TNF-α is a member of the TNF superfamily, and its expression has been linked to the pathogenesis of various inflammatory and autoimmune disorders. Similarly, IL-1β is a member of the interleukin 1 family of cytokines, which are known to promote inflammatory responses in tissue injury caused by pathogen-associated molecular patterns released from damaged cells[116,117]. These cytokines are predominantly expressed in M1-like macrophages, characterized by their pro-inflammatory properties[118].

In this context, Figure 41 shows the mRNA expression levels of *TNF-α* and *IL-1β* in various conditions. These conditions include M0 macrophage controls, M1 macrophage controls (M0 macrophages incubated with IFN-γ /LPS), M2 macrophage controls (M0 macrophages incubated with IL-4 /IL-13), M0 macrophages incubated with patients' exosomes, and M0 macrophages incubated with healthy controls' exosomes. The expression levels of *TNF-α* and *IL-1β* were measured at two time points: 24h and 48h.

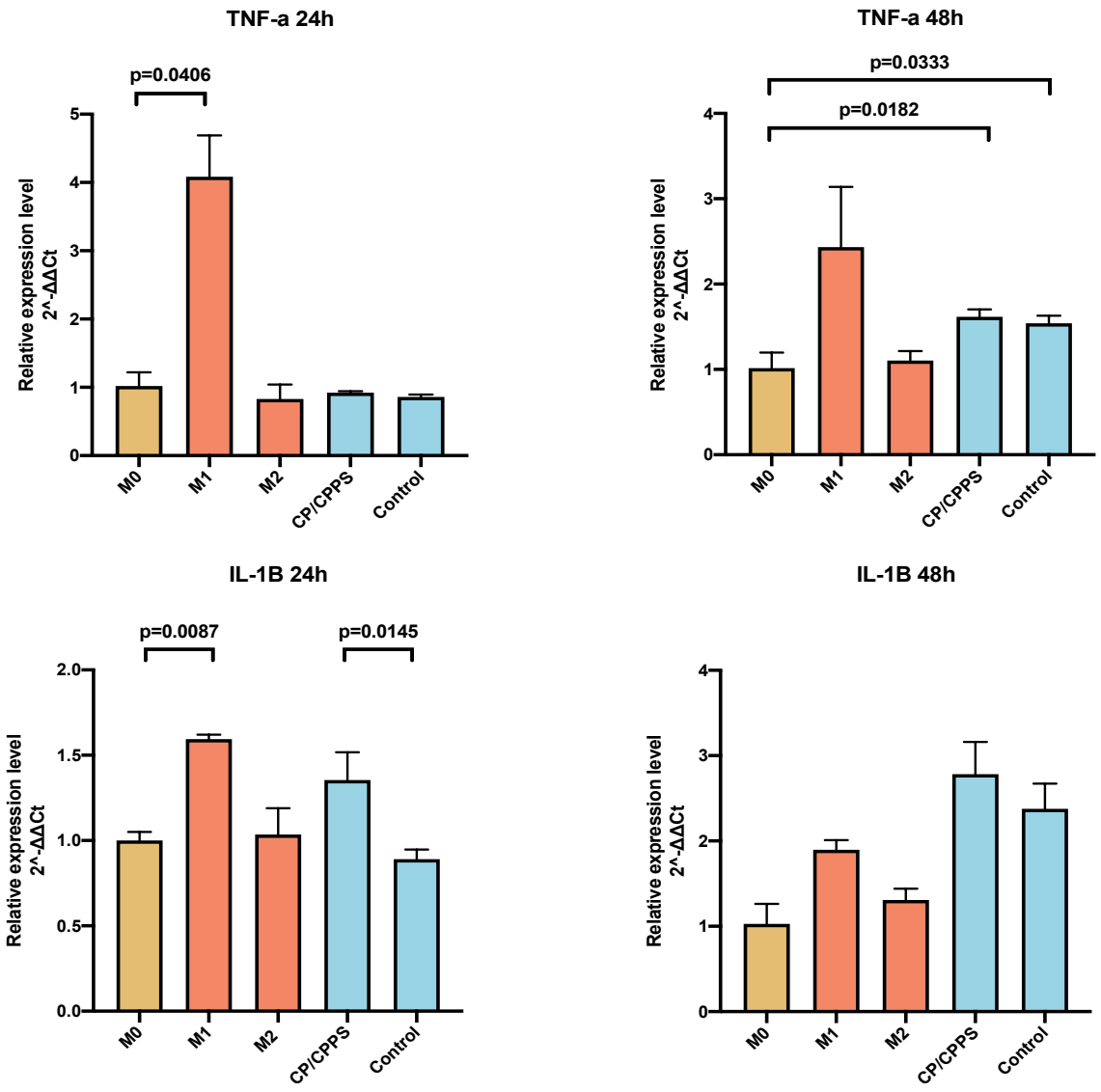

Figure 41: Expression levels of *TNF-α* and *IL-1β* were measured in M0, M1, M2, CP/CPPS, and healthy control ExU exosome-treated groups. The *TNF-α* expression level was significantly increased in the M1 control group compared to M0 after 24 h incubation. Nevertheless, for 48 h incubation, *TNF-α* was higher expressed in the M1 group but not significant. In both CP/CPPS patients and healthy controls, *TNF*-α was significantly higher expressed than M0, and expressions in CP/CPPS patients group were slightly higher than in healthy controls after 24 h incubation. In the 24 h incubation group, the *IL-1β* expression level was significantly higher expressed in the M1 control compared to M0, and CP/CPPS patient group was also higher expressed than in the healthy control.

The expression levels of *TNF-α* and *IL-1β* were measured in different macrophage conditions, and the results were compared. The expression levels of *TNF-α* were significantly higher in M1 controls than in M0 controls after 24 h (p=0.0406). In addition, the mRNA levels of *TNF-α* have been highly expressed in both patient (p=0.0182) and healthy control (p=0.0333) groups compared to the M0 controls after 48 h of incubation. After 24 h incubation, *IL-1β* expression was significantly higher in M1 controls than in M0 controls (p=0.0087). Moreover, the patients' group showed significantly higher expression levels of *IL-1β* than the healthy controls (p=0.0145). No significant differences were observed in the expression levels of *IL-1β* between patients and controls after 48 h of incubation. However, patient groups still showed a trend of higher *IL-1β* expression levels than healthy controls. These findings have important implications for understanding the function of exosomes from ExU in the polarization of M0 macrophages. Especially the higher expression levels of *IL-1β* in the patient group compared to healthy controls suggest that M1 macrophages may play a more critical role in CP/CPPS pathogenesis.

3.14.4. mRNA expressions of *IL-10*, *CD206*, *CCL18* and *CCL22* after 24h and 48h exosome treatment

The immune system is crucial in the body's defense against pathogens and other foreign agents. Interleukin 10 (IL-10), a type of cytokine, is known for its anti-inflammatory properties, as it can inhibit the synthesis of pro-inflammatory cytokines such as IFN-γ, IL-2, and IL-3. In addition to IL-10, other markers have been identified as essential indicators of macrophage polarization, including Cluster of Differentiation 206 (CD206), primarily on the surface of macrophages and contribute to immune homeostasis through its involvement in manna glycoproteins and endocytosis[119]. Furthermore, Chemokine (C-C motif) ligand 18 (CCL18) and C-C motif chemokine 22 (CCL22) are additional markers involved in immune regulation and inflammatory processes. These markers are predominantly expressed in M2 macrophages and are used to distinguish them from other macrophage subtypes[120–123].

To investigate the expression levels of these markers, mRNA expression was measured in various samples, including M0 control, M1 macrophages control, M2 macrophages controls, patients' exosomes incubated M0 macrophages, and healthy

controls' exosomes incubated M0 macrophages after 24 h and 48 h incubation. Specifically, Figure 42 illustrates the expression levels of *CD206* after 24h and 48h of incubation. The results showed that *CD206* expression levels in the M2 control were lower than M0 control after 24 h (p=0.0243). However, *CD206* expression levels were significantly higher in M2 macrophages than in the M0 control after 48 h (p=0.0004).

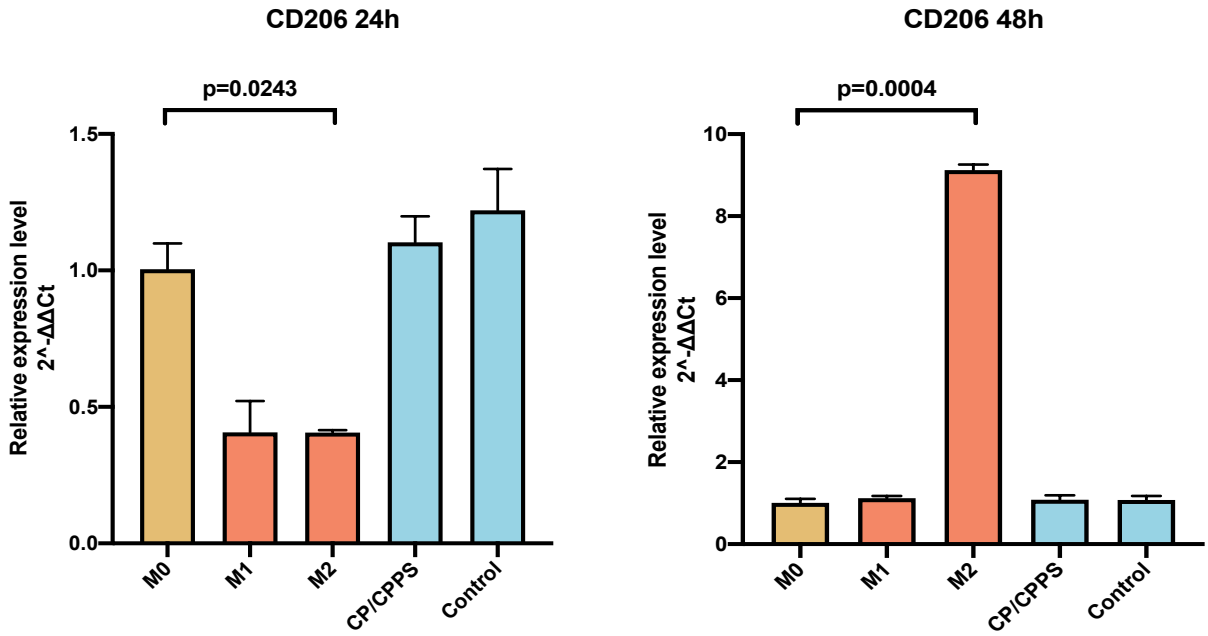

Figure 42: The expression levels of *CD206* in M0, M1, and M2 macrophages and in patients with CP/CPPS and healthy controls were investigated after treatment with exosomes isolated from ExU. After 24 h of incubation, the expression level of *CD206* was significantly lower in the M2 group compared to the M0 group. However, the *CD206* expression level was significantly higher in the M2 group than in the M0 group after 48 h of incubation. Notably, there were no significant differences in the expression levels of *CD206* in the CP/CPPS patient and healthy control groups compared to the M0 macrophages in both the 24 h and 48 h incubation groups.

The results in Figure 43 indicate a significant increase in the RNA expression levels of *CCL22* in M2 macrophages compared to M0 controls in the 24 h incubation group (p=0.0268). Furthermore, in the 48 h incubation group, *CCL22* expression levels in M2 macrophages were significantly increased compared to M0 controls (p=0.0019). Conversely, M1 macrophages exhibited decreased expression levels of *CCL22* (p=0.0069), as did both patients (p=0.0021) and healthy controls (p<0.0001) when compared to M0 controls. Notably, CP/CPPS patients demonstrated a higher expression level of *CCL22* than healthy controls (p=0.0452).

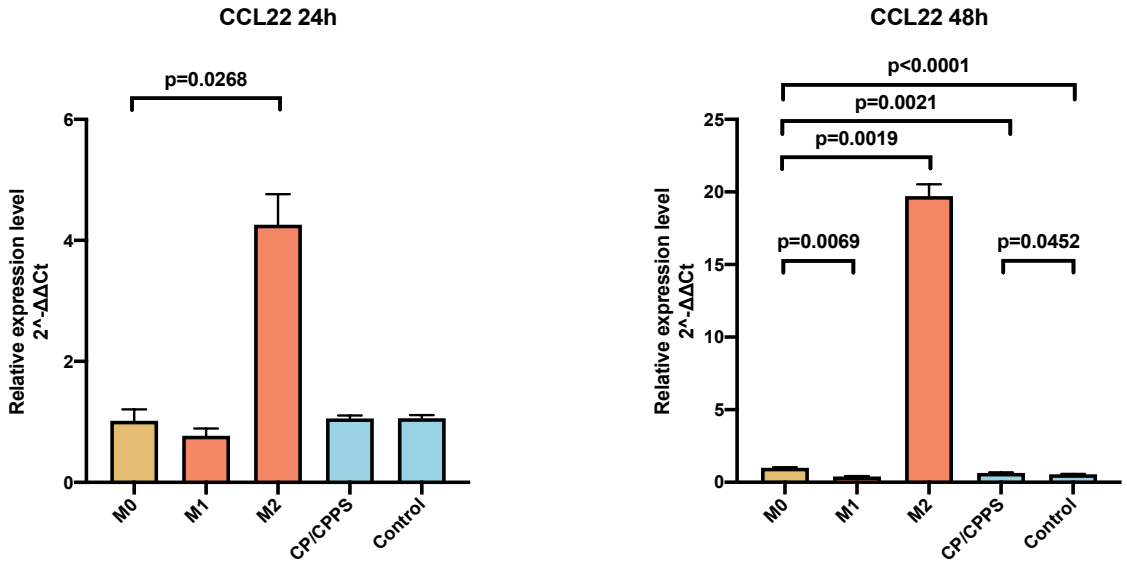

Figure 43: Expression levels *CCL22* in M0, M1, M2, CP/CPPS, and healthy control ExU exosome treated groups. *CCL22* was significantly more expressed in M2 macrophages than the M0 macrophages after 24 h and 48 h incubation. In the 48 h incubation group, *CCL22* expression was significantly decreased in M1 macrophages, CP/CPPS patients group, and healthy control group compared to M0. CP/CPPS patients had a significantly higher expression of *CCL2* than healthy controls in the 48 h incubation group.

The results presented in Figure 44 indicate no significant difference in the expression levels of *IL-10* among M0 control, M1 macrophages, M2 macrophages, patient, and healthy control groups after a 24 h incubation. However, after 48 hours of incubation, the expression of *IL-10* in M2 macrophages was significantly decreased compared to the M0 control (p=0.0297), and there was no significant difference in patients and healthy controls compared to M0 macrophages.

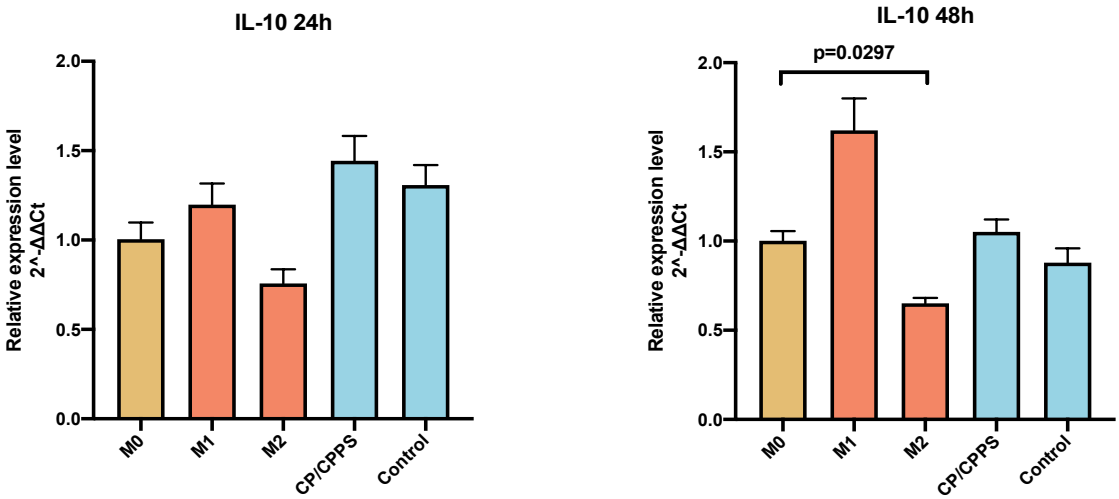

Figure 44: There was no statistically significant difference in mRNA expression for *IL-10* following a 24 h incubation of exosomes. However, after 48 h incubation, the expression of *IL-10* in M2 control cells was significantly lower than in M0 control cells.

Under the 24 h and 48 h incubation conditions, we investigated the expression levels of *CCL18* in different treatment groups. As shown in Figure 45, our results revealed that the expression of *CCL18* was significantly higher in the patient group than in the M0 control group after the 24 h incubation (p=0.0368). Moreover, the patient group showed significantly lower expression levels of *CCL18* than the healthy control group (p=0.0388). After the 48 h incubation, the expression levels of *CCL18* significantly increased in the M2 macrophage group (p<0.0001), patient group (p=0.0056), and healthy control group (p=0.0219) compared to the M0 macrophage control group. Conversely, the expression of *CCL18* was significantly lower in the M1 macrophage group than in the M0 control group (p=0.0006).

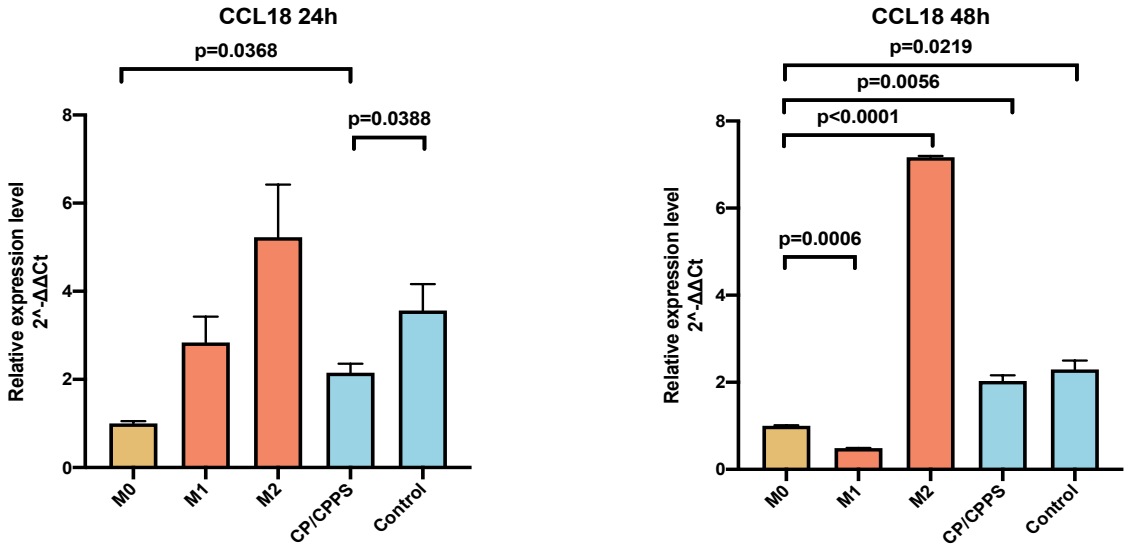

Figure 45: The expression levels of *CCL18* in various treatment groups were compared. *CCL18* was significantly higher expressed in CP/CPPS patients than in M0 macrophages after 24 h of incubation. Moreover, CP/CPPS patients had a significantly lower expression of *CCL18* than healthy controls. In the 48 h incubation group, the expression levels of *CCL18* in M1 controls showed a significant decrease compared to M0 controls. In contrast, *CCL18* expression in M2, CP/CPPS patients, and healthy controls was significantly higher than in M0 controls.

3.15. mRNA expressions of *CDKN2A* after exosome treatment for 24h and 48h

The objective of the present study was to investigate the potential short-term impact of exosomes on the expression of TSG. To this end, the levels of *CDKN2A* mRNA were measured in patient and healthy control samples after 24 h and 48 h of incubation,

and the results were compared to those of the M0 controls. The data, shown in Figure 46, revealed a significant reduction in *CDKN2A* expression levels in both patient and healthy control groups after 24 and 48 hours of incubation, as evidenced by statistical analysis (p=0.0151 for the patient group at 24h, p=0.0048 for the patient group at 48h, p=0.0157 for the healthy control group at 24h, and p=0.0091 for the healthy control group at 48h). It should be noted, however, that the difference in *CDKN2A* expression levels between the patient and healthy control groups after 48 hours of incubation did not attain statistical significance.

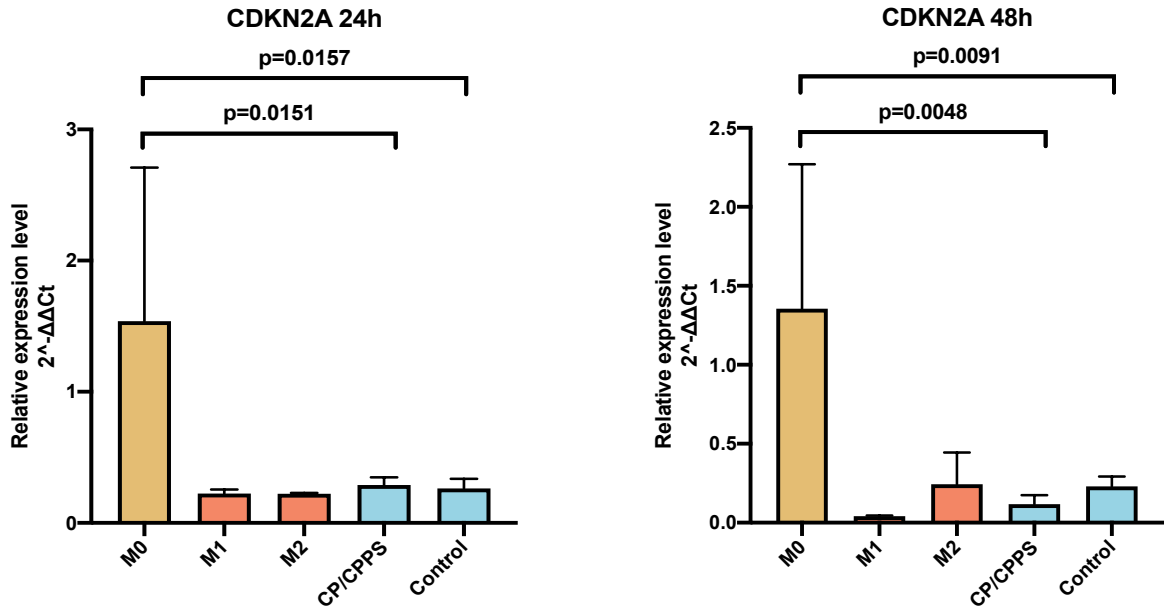

Figure 44: The investigation of the expression levels of *CDKN2A* in various groups, including M0, M1, M2, CP/CPPS, and healthy control ExU exosome-treated groups, in both the 24 h and 48 h incubation periods was conducted. The expression levels of *CDKN2A* were significantly lower in CP/CPPS patients and healthy controls compared to M0 macrophages in both incubation periods. Interestingly, after 24 h of incubation, CP/CPPS patients demonstrated a slightly higher expression level of *CDKN2A* compared to the healthy control group. However, in the 48 h incubation group, the trend was reversed, and the healthy control group displayed a slightly higher expression level of *CDKN2A* than the CP/CPPS group.

4. Discussion

Inflammations could contribute to carcinogenesis and the development of malignant tumors[124]. Rudolph Virchow first presented the hypothesis in 1863 when he demonstrated the presence, infiltration, or accumulation of leukocytes in tumor tissues. Other researchers have furtherly proved this finding. Moreover, epidemiological studies have shown that several types of cancer, such as bowel-, esophageal-, or stomach cancer, significantly correlated to inflammation[125–128]. Chronic prostate inflammation has been regarded as a trigger of prostate carcinogenesis and contributes to progression[129–131]. However, no studies have investigated potential biomarkers evaluating the potential risk for CP/CPPS patients to develop PCa in a later stage. Therefore, the underlying mechanism and the long-term prognosis of CP/CPPS are still unclear. In this study, we investigated DNA promoter methylation levels and mRNA expression levels of selected prostate cancer-related TSGs in the liquid biopsies of CP/CPPS patients, and compared them to the same type of samples from healthy controls. Clinical examination results were also embraced for investigating the correlation to our experimental results. Besides, the influence of exosomes isolated from ExU supernatant of CP/CPPS patients and healthy controls on monocytes cell line THP-1 was also investigated. CP/CPPS patients showed very different or unusual TSGs methylation levels and mRNA expression levels compared to healthy controls, and consistent correlations between clinical exams and our experimental results were also observed. Cell culture experiments showed that exosomes isolated from ExU could influence the M0 macrophages and trigger their polarization to M1 macrophages.

Our data lead to the following observations:

4.1. Epigenetic dysregulation of PCa-associated TSGs was observed in CP/CPPS

The limited availability of tissue samples constrains the study of CP/CPPS since prostate tissue biopsies are not commonly used in clinical practice. Thus alternative sources of starting material, such as EJ and ExU, have been proposed. EJ and ExU can be obtained non-invasively and contain somatic cells, including prostatic epithelial cells and leukocytes, which reflect the pathological conditions of the prostate gland. Our study investigated the methylation and expression levels of TSGs *CDKN2A*, *EDNRB*, *PTGS2*, *PITX2*, *BMP4*, *BMP7*, and *GSTP1* in somatic cells from EJ and ExU. These TSGs are associated with PCa and were chosen as candidate markers. We found that *EDNRB*, *CDKN2A*, *PTGS2*, *BMP7*, and *BMP4* were significantly hypermethylated in EJ from CP/CPPS patients, and *CDKN2A* and *PTGS2* showed lower expression levels. In ExU, *EDNRB* and *CDKN2A* showed increased methylation, while *CDKN2A* and *PTGS2* had significantly lower expression levels. *BMP7* exhibited significantly increased promoter CpG methylation in EJ samples from CP/CPPS patients, which aligned with the previous study of our group, even though the differences observed were not statistically significant.

The source of somatic cells collected is diverse and may originate from various organs and tissues such as the bladder, kidney, ureter, and urinary tract. This diversion could influence the final results, and the TSG methylation levels of these cells may differ from prostatic cells. Nonetheless, our results suggest that TSGs may play a role in the prognosis of CP/CPPS, and promoter hypermethylation of prostate-correlated TSGs is a feature of this condition. The downregulated mRNA expression levels in CP/CPPS patients correspond to the pyrosequencing results. In addition, the differences in methylation and mRNA expression between CP/CPPS patients and healthy controls were observed. Moreover, our findings support a potential correlation between CP/CPPS and PCa, considering the inflammatory microenvironment in CP/CPPS may lead to TSG methylation and silencing, resulting in uncontrolled regulation of cancer. Furthermore, our results indicate that liquid biopsies can reveal valuable information about the prostate microenvironment and potentially be used as ideal materials for future CP/CPPS research.

Our preliminary investigation found that *CDKN2A* exhibited notable sensitivity and specificity in detecting differences in methylation and mRNA expression levels between individuals diagnosed with CP/CPPS and healthy controls. Furthermore, considering its established association with prostate cancer, *CDKN2A* was utilized as a biomarker for subsequent cell-sorting experiments.

CDKN2A is a well-known TSG that encodes for two crucial proteins, p16 and p14arf. The p16 protein has been shown to play a crucial role in regulating the cell cycle by inhibiting cyclin-dependent kinases 4 (CDK4) and 6 (CDK6), which are critical regulators of the G1 to S-phase transition. In addition to its role in cell cycle regulation, the p14arf protein also plays a critical role in tumor suppression. Precisely, it activates the p53 tumor suppressor, which regulates cell cycle progression and apoptosis. Despite the essential roles that the *CDKN2A* and its associated proteins play in tumor suppression, there is growing evidence that aberrant methylation and reduced expression of this gene contribute to developing certain types of cancer, including prostate cancer[132–134]. Furthermore, it has been demonstrated that there is a significant association between hypermethylation of the *CDKN2A* and worse clinicopathological outcomes in prostate cancer, highlighting the potential value of *CDKN2A* hypermethylation as a prognostic biomarker for cancer progression[135].

Epigenetic dysregulation of *CDKN2A* can arise from multiple mechanisms, including histone modifications and DNA promoter hypermethylation[136]. For instance, the transcription factor Forkhead Box A1 (FOXA1) has been demonstrated to exert a unique ability to modulate chromatin accessibility through interactions with other transcription factors[137,138]. By binding to cis-regulatory elements within the *CDKN2A* promoter, FOXA1 can stimulate promoter-enhancer communication and nucleosome remodeling, leading to increased expression of *CDKN2A* in the senescence of cells[139]*.* Enhancer of zeste homolog 2 (EZH2) is a vital component of polycomb group genes (PcGs) and serves as the catalytic subunit of the Polycomb repressive complex 2 (PRC2)[140]. One of the primary mechanisms through which EZH2 exerts its repressive function on transcription is by binding to lysine 27 on histone three and catalyzing its trimethylation, resulting in the formation of H3K27me3[141]. Notably, dysregulated EZH2 activity has been associated with the development of various malignancies, and it has been reported that the upregulation of H3K27me3 frequently correlates with the

repression of *CDKN2A* in malignant tumors. In this regard, the use of selective EZH2 inhibitors has been shown to reverse *CDKN2A* downregulation *in vitro* environments[142,143]. In addition to EZH2, both natural and artificial small molecule modifiers have been reported to have epigenetic effects on the expression of *CDKN2A*. For instance, genistein has been demonstrated to increase the acetylation of histones three and four at the *CDKN2A* promoter region[144]. Furthermore, the repression of *CDKN2A* transcription can also be attributed to the binding of Chromobox homolog 7 (CBX7) of Polycomb repressive complex 1 (PRC1) with antisense noncoding RNA in the INK4 locus (ANRIL) and H3K27me3. The interaction between CBX7 and ANRIL/H3K27me3 results in a repressive chromatin structure that prevents the transcription of *CDKN2A*[145]. The repression of *CDKN2A* has been demonstrated to impair the p53 and Rb pathways, which are essential regulators of cell cycle progression and are involved in preventing cancer development[146]. One study has indicated that macrophage migration inhibitory factor (MIF) could potentially play a role in carcinogenesis by upregulating the methylation level of *CDKN2A*[147]. The chronic nature of CP/CPPS suggests that inflammation could have long-term consequences, including the methylation of TSGs in their DNA promoters and subsequent cancer development. Our research corroborates this hypothesis, as *CDKN2A* was the only gene displaying significantly elevated methylation levels, leading to a downregulation in ESCs and somatic cells in ExU samples from CP/CPPS patients. These findings suggest that *CDKN2A* could serve as a reliable biomarker for monitoring the progression and prognosis of CP/CPPS while highlighting a possible association between this condition and prostate cancer. However, further research is necessary to elucidate the precise mechanisms by which *CDKN2A* methylation may contribute to PCa development from CP/CPPS and progression and to confirm the potential utility of *CDKN2A* as a prognostic biomarker for CP/CPPS.

4.2. EJ and ExU are promising sources for biomarker development in CP/CPPS and MACS system is suitable for cell sorting in liquid biopsies

Initially, nucleated cell counts were obtained to provide an overview of the quantity of input material available for subsequent experimental procedures. In EJ samples,

somatic cell numbers ranged between 600 and 6,200, while ExU samples exhibited a range of 1,000 to 20,000 cells. Although healthy control groups tended to exhibit marginally higher cell counts than patient groups in both sample types, these differences were not statistically significant. Despite the relatively low total cell numbers, sufficient material was available for further pyrosequencing and expression analyses, given the inherent involvement of the PCR process in both methods. IF staining was employed to confirm the presence of target cells, with epithelial cells and leukocytes identified in both EJ and ExU samples through CK 8/18/19 and CD45 staining, respectively. Thus, target cell groups were identified and available for subsequent pyrosequencing and mRNA analysis.

However, given the possibility of cell loss during isolation and the relatively low total quantity of input cells, and as a result, it was not immediately clear if isolated cell groups contained the target cells of interest. IF staining was utilized to confirm the presence of epithelial cells and leukocytes after cell sorting to address this concern. In this experiment, MACS was used to isolate the target cell populations by employing specific markers, with EpCAM and CD45 utilized to isolate epithelial cells and leukocytes, respectively. EpCAM, a 40 KDa transmembrane glycoprotein initially discovered in colon tumor cells from mice in 1979[148–150], is expressed at the basolateral membrane of various normal epithelial cells[151]. Numerous studies have shown that EpCAM is highly expressed in a range of epithelial cancers, including prostate adenocarcinoma, which exhibits one of the highest *EpCAM* expression levels[152]. CD45, on the other hand, is a member of the protein tyrosine phosphatase family and is encoded by the *PTPRC*. It is a type I transmembrane protein expressed in all hematopoietic cells except erythrocytes and platelets. EpCAM and CD45 are commonly employed in CTC isolation research to distinguish between target cancer cells and leukocytes.

After EJ and ExU samples were collected, epithelial cells and leukocytes were initially detected in their respective groups using CK 8/18/19 and CD45, respectively. However, a few epithelial cells and leukocytes were observed in the incorrectly sorted groups. Despite this, the number of "mispositioned" cells was insignificant compared to the total cell cohort, and thus their influence can be deemed negligible. To further evaluate the efficiency of cell isolation, RT-PCR was used to measure the expression

levels of *EpCAM* and *PTPRC* in both sorted cell groups. EpCAM was significantly upregulated in the epithelial cell cohort ($p<0.0001$), while *PTPRC* was highly expressed in the leukocyte cohort ($p<0.0001$), consistent with expectations. These findings indicate that epithelial cells and leukocytes can be retained in unsorted cell groups even with low total quantities and that the MACS cell sorting system functions effectively in low cell count conditions. Furthermore, this system is sensitive and specific for isolating epithelial cells and leukocytes in EJ and ExU samples.

Identifying and isolating specific cell types from complex tissues are essential for investigating various physiological and pathological processes. EpCAM is a well-known marker for normal epithelial cells, although it does not provide information regarding the source of these cells. In this regard, using PSA as a marker enables the detection of prostate-origin epithelial cells following isolation. PSA, a glycoprotein enzyme encoded by *KLK3* and a member of the kallikrein-related family, is predominantly secreted by the epithelial cells of the prostate gland. While PSA levels are typically low in the blood, ranging from 0 ng/mL to 4 ng/mL, they can increase in the presence of prostate inflammation or malignant disease. Therefore, with the digital rectal examination (DRE), PSA is essential for diagnosing early-stage PCa and predicting prognosis.

Using markers such as EpCAM and CD45 provides powerful means of characterizing specific cell types, essential for understanding the cellular heterogeneity and functional diversity in various disease conditions. Liquid biopsies have emerged as a promising tool to capture various diseases' molecular and cellular characteristics. Notably, prostatic epithelial cells and leukocytes in the isolated cell suspension represent a significant advancement in liquid biopsy-based diagnostics, enabling the study of the prostate microenvironment. Moreover, using isolated epithelial cells and leukocytes in pyrosequencing and gene expression analyses offer an opportunity to investigate the molecular mechanisms underlying the pathogenesis of CP/CPPS and may also contribute to developing novel diagnostic and therapeutic strategies.

4.3. *CDKN2A* methylation and mRNA expression in the sorted cells are heterogeneous

To the best of our knowledge, there is a lack of studies investigating the methylation status and mRNA expression levels of TSGs in somatic cells isolated from native ExU and EJ in CP/CPPS research. Mahbub et al. reported isolating renal proximal tubular cells from urine using dynabeads crosslinked with CD13 and Sodium-glucose linked transporter-2 (SGLT2)[153]. However, no studies have utilized MACS to isolate specific cell populations from liquid biopsies to investigate CP/CPPS.

Characterizing TSG methylation and mRNA expression profiles in isolated cell populations plays a role in elucidating the molecular mechanisms underlying various diseases. In particular, CP/CPPS is a complex disorder involving multiple cell types and signaling pathways, plus the limitation of biopsy materials, necessitating efficient and sensitive techniques for research. Flow cytometry has been utilized for cell sorting in urine samples. For some studies, the primary culture of urine-derived cells was first conducted in specific urine cell sorting studies. Subsequently, targeted cell groups were identified and sorted using Fluorescence-Activated Cell Sorting (FACS) and flow cytometry[154,155]. In one study, telomerase activity's impact on somatic stem cells' regenerative capacity was examined through the isolation and subsequent cultivation of urine-derived stem cells, followed by their identification utilizing flow cytometry[156]. Rao *et al.*[157] developed a comprehensive protocol for conducting single-cell level transcriptomics analysis from renal tissue and cryopreserved urine samples of patients with lupus nephritis. The urine cells were incubated with a customized antibody cocktail consisting of CD45, CD19, CD11c, CD10, CD14, CD3, CD4, CD8, CD31, and PD-1, followed by identification of epithelial cells and leukocytes using an 11-color flow cytometry panel. Another study investigated the diagnostic potential of flow cytometry analysis for urinary tract infections using 281 midstream urine samples. In order to identify bacteria and all particles present in the urine samples, each sample was independently stained and analyzed by flow cytometry[158].

MACS has emerged as a widely employed method for isolating specific cell subsets, relying on the expression of cell surface markers. The approach has gained considerable popularity in research due to its capacity for rapid, cost-effective, and

straightforward cell separation, enabling the processing of a large number of samples simultaneously. Furthermore, MACS provides several advantages, including its ability to attain high purity levels, with cell isolation purity reaching up to 90%[159]. As a result, it has proven to be a valuable tool for researchers seeking homogeneous cell populations for subsequent downstream applications. Therefore, applying MACS to isolate epithelial cells and leukocytes from ESCs and ExU somatic cells may provide new insights into the CP/CPPS research.

The MACS sorting system is restricted to membrane antigens as its sole basis for cell sorting, thus presenting a limitation in its capability to sort multi-subtype cells simultaneously effectively. Prostate-specific membrane antigen (PSMA), a zinc metalloenzyme located in the membranes, exhibits upregulation in PCa cells, thus making it a potential marker for the MACS system in PCa patients. However, one significant limitation of this approach is that PSMA is either absent or moderately expressed in benign and hyperplastic tissues[160]. This drawback may hinder the effective sorting of target cells from non-target cells using PSMA as a marker in combination with magnet-based cell sorting techniques. Therefore, using PSMA as a marker may result in losing target cells in CP/CPPS liquid biopsies. Furthermore, PSMA MicroBeads are not available in the market.

FACS provides possibilities for a more specific cell sorting because various epithelial cells and leukocyte subtypes can be isolated for a deeper investigations. FACS sorts based on markers which are located on membrane and plasma. FACS is a widely used technique for cell sorting based on the presence of specific markers on cell membranes and plasma. For example, in prostate cancer, PSA can be utilized as a marker for sorting prostate epithelial cells, while markers such as TNF-α and CD86 can distinguish between M1 macrophages and CD11c, CD206, and CCL22 for M2 macrophages. Using multiple markers enables the sorting of specific epithelial cells and subtypes of leukocytes based on their unique molecular characteristics. Such subtype-specific sorting can provide valuable information for understanding the complex role of different immune cell populations in CP/CPPS and may help develop novel therapeutic strategies.

During our experiment's optimization process of the MACS system, cryopreserved EJ and ExU samples presented challenges in cell sorting. Specifically, compared to their fresh counterparts, a decrease in karyocytes was observed in cryopreserved EJ and ExU samples before and after IF staining. This phenomenon was also observed in the MACS-isolated epithelial cells and leukocyte cohorts. Consequently, subsequent RT-PCR analysis of sorted epithelial cells and leukocytes revealed high Ct values (above 30) for the housekeeping gene (*GAPDH*) and even higher Ct values (between 35 and 40) for the genes of interest (GOI). These findings indicate that only fresh samples are suitable for MACS sorting experiments, as cryopreservation may lead to cell rupture and so that lower DNA and mRNA quality and quantity, which can negatively impact downstream analysis. Thus, fresh samples are recommended to ensure optimal results and minimize experimental variability.

Our results indicated that the promoter methylation level of *CDKN2A* did not differ significantly between CP/CPPS patients and healthy controls in epithelial cells and leukocytes of EJ samples. However, in ExU samples, patients with CP/CPPS exhibited higher levels of *CDKN2A* promoter methylation compared to healthy controls in both epithelial cells and leukocytes. Moreover, no significant difference was observed in *CDKN2A* methylation levels between epithelial cells and leukocytes in either EJ or ExU samples. Nonetheless, leukocytes showed slightly lower methylation levels than epithelial cells in EJ samples, while the opposite was observed in ExU samples. Additionally, our RT-PCR analysis demonstrated a significant downregulation of *CDKN2A* expression in epithelial cells and leukocytes isolated from patients' EJ samples compared to healthy controls, while no significant difference was observed in ExU samples. Furthermore, no significant difference was found in *CDKN2A* expression levels between epithelial cells and leukocytes in EJ samples. However, a significant upregulation of *CDKN2A* expression was observed in epithelial cells compared to leukocytes in ExU samples, consistent with the trend of promoter methylation levels between the two cell types in ExU.

Our study revealed that the regulation of *CDKN2A* in CP/CPPS is a complex process that can be influenced by several factors, such as the sample type and cell type. The results involved the analysis of sorted epithelial cells and leukocytes, which concur with prior studies that had not employed cell sorting techniques. Specifically, the study

showed the presence of DNA promoter methylation of TSGs, particularly *CDKN2A*, in CP/CPPS. Interestingly, *CDKN2A* methylation levels of the epithelial cells and leukocytes were discordant in EJ and ExU samples. However, the significant downregulation of *CDKN2A* in the leukocytes of ExU samples suggests that leukocytes may be more affected than epithelial cells in the microenvironment of the prostate gland in CP/CPPS patients.

To further advance our understanding of the regulation of *CDKN2A* in CP/CPPS, future studies should consider using FACS to sort the cells from both the epithelial and leukocyte groups in the EJ and ExU samples. This approach will enable a more detailed investigation of the specific cell types affected by *CDKN2A* regulation in CP/CPPS. Ultimately, a better understanding of the complex regulation of *CDKN2A* in CP/CPPS may lead to the development of new therapeutic strategies for this condition.

4.4. Methylation and mRNA expression of TSGs in liquid biopsies represent the status and prognosis of CP/CPPS

Our study aimed to investigate the potential interrelationships between DNA promoter methylation and mRNA expression levels of various TSGs. 91 combinations were evaluated for methylation levels, of which 14 demonstrated significant correlations. Notably, positive correlations were observed between methylations of *EDNRB* and *CDKN2A* in both EJ and ExU and between *EDNRB* in ExU and *EDNRB* in EJ. In terms of mRNA expression levels, 17 out of 91 combinations were found to exhibit significant correlations. Notably, *CDKN2A* expression in ExU significantly correlated with *CDKN2A* in EJ, and *PTGS2* regulation levels in ExU and EJ were positively correlated with *CDKN2A* in ExU and *CDKN2A* in EJ, respectively. Furthermore, *PITX2* expression was positively correlated with *CDKN2A* in ExU. Additionally, 18 out of 196 combinations showed significant correlations between methylation and mRNA expression levels. Expressly, *CDKN2A* expression in ExU indicated negative correlations with methylations of *EDNRB* in both EJ and ExU, respectively. In addition, *EDNRB* in ExU and EJ were negatively correlated with *BMP7* in ExU and *CDKN2A* in ExU.

The present correlation analyses demonstrate consistent correlations among methylations and mRNA expressions of most TSGs, which enhance the reliability of the findings for the DNA hypermethylation and downregulated mRNA of TSGs presented earlier. Noteworthy, when the methylation level of one TSG displayed positive correlations with methylations of other TSGs and led to a decrease in mRNA levels, it suggests that hypermethylation of multiple TSGs and corresponding depressed mRNA expression may occur in liquid biopsies of CP/CPPS patients rather than being incidental cases. Furthermore, the observed elevated methylation levels that corresponded with mRNA levels suggest that epigenetic dysregulation of DNA promoters of TSGs has occurred in CP/CPPS patients. To expand on these findings, future research may involve high-throughput DNA methylation analysis for the liquid biopsies of CP/CPPS using methods such as array-based analysis (Infinium Methylation Assay) and Next-generation sequencing-based analysis (Whole-genome bisulfite sequencing, WGBS). These methods can detect up to 870,000 to 28 million CpG sites[161], providing more comprehensive information on genome-wide methylation at a single base resolution. It enables the identification of epigenetic biomarkers and clinical applications such as tumor classification[162–165]. Besides, in the case of CP/CPPS research, whole-genome methylation analysis can cover more target genes related to PCa and genes associated with the immune system, such as IL10 and IL1B[166].

Diagnosing and evaluating CP/CPPS relies on various clinical assessments, including a thorough medical history, comprehensive physical examination, and diagnostic tests such as urine and EPS tests. The UPOINT(S) system is a valuable tool for defining clinical phenotypes of CP/CPPS, which can aid in selecting appropriate multimodal therapies[167]. In particular, the EPS midstream massage urine and post-prostate massage urine tests are crucial for accurately diagnosing CP/CPPS. The National Institutes of Health Chronic Prostatitis Symptom Index (NIH-CPSI) was developed in 1993 and remains a widely used questionnaire-based tool for evaluating the severity of symptoms in CP/CPPS patients. The NIH-CPSI questionnaire, in particular, provides a standardized and comprehensive approach to evaluating symptom severity and tracking treatment progress over time. The questionnaire consists of 13 items, each scored on a scale of 0-10 (1 item), 0-6 (1 item), 0-5 (3 items), 0-3 (2 items), and

0-1 (6 items)[168]. These items assess pain severity, frequency, and location, as well as urinary symptoms and the impact of symptoms on the patient's daily life[19,169].

Here, we explored potential associations between clinical parameters, DNA methylation, and expression levels of TSGs in the prostate. Our findings indicate significant correlations between participants' age and DNA methylation and mRNA expression levels, specifically the negative correlation between the expression of *CDKN2A* in the ExU and age. Additionally, negative correlations were observed between PSA levels and expression levels of *CDKN2A* in ExU and *GSTP1* in EJ. Moreover, we found significant positive correlations between prostate volume and methylation levels of *EDNRB* and *GSTP1* in EJ. Concerning the CPSI scores, which encompass pain score (CPSI I), urinary symptoms score (CPSI II), and life quality score (CPSI III), significant correlations with methylation and mRNA expression levels were also found. For instance, *CDKN2A* methylation levels in ExU positively correlated with CPSI I, CPSI II, and CPSI III scores. In contrast, *CDKN2A* expression levels in EJ exhibited negative correlations with CPSI I and CPSI III scores. The same trend happened in IPSS as well.

Our study investigated the potential of isolated epithelial cells and leukocytes from liquid biopsies of patients with CP/CPPS for prognosis and severity evaluation. Consistent with our previous findings, *CDKN2A* methylation levels in EJ epithelial cells exhibited significant positive correlations with participants' age and PSA levels. In ExU epithelial cells, we also observed significant positive correlations between *CDKN2A* methylation levels and CPSI I, CPSI III, and CPSI total scores. In contrast, we found significant negative correlations between *CDKN2A* expression levels in leukocytes from EJ and CPSI I, CPSI III, and CPSI total scores.

The results revealed that patients with advanced age and higher PSA levels displayed higher promoter methylation and lower mRNA expression levels of prostatic TSGs in somatic cells collected from liquid biopsies and isolated epithelial cells and leukocytes. Additionally, our findings revealed that TSG methylation and mRNA expression levels were significantly associated with CPSI scores and IPSS in CP/CPPS patients, indicating that TSGs may serve as potential biomarkers for evaluating symptom severity and guiding therapy in these patients. Furthermore, the significant association

between experimental parameters and clinical outcomes suggests that age and symptom severity could potentially predict the prognosis of CP/CPPS. Our results support the hypothesis that chronic inflammation-induced irritation can lead to pre-carcinogenesis. The observed hypermethylation and downregulation of TSGs in CP/CPPS patients with worse symptom indexes indicate an increased risk for cancer at later stages.

The gene *CDKN2A* has exhibited significant and noteworthy correlations with CPSI I, CPSI II, CPSI III, and CPSI total in both EJ and ExU samples, suggesting its potential utility as a more reliable and sensitive marker in the development of CP/CPPS markers. Assessment and prediction of the CP/CPPS process can be facilitated by the evaluation of isolated epithelial cells and leukocytes. Both cohorts of liquid biopsies from CP/CPPS patients display aberrant methylation and expression levels of *CDKN2A* and reflect changes in clinical parameters. Moreover, the present study highlights the age-related correlation of prostate volume, IPSS, CPSI I, CPSI II, CPSI III, and CPSI total, indicating that older CP/CPPS patients tend to exhibit more severe symptoms. This relationship may also suggest that older age and more severe symptoms may bidirectionally contribute to the risk of developing prostate cancer. However, further investigations with larger cohorts of CP/CPPS patients are warranted to validate the utility of these biomarkers.

CP/CPPS has been observed to be significantly associated with sexual dysfunction, which can negatively impact male fertility[170]. For instance, a case-control study has reported a higher likelihood of CP/CPPS diagnosis history in patients with erectile dysfunction (ED) compared to a randomly selected group (8.6% vs. 2.5%, $p<0.001$)[171]. Additionally, semen quality has been reported to be significantly affected in CP/CPPS patients. Sperm motility, defined as the percentage of sperms with moving tails and is regarded as an indicator of semen quality, is a crucial factor in male fertility. A meta-analysis indicated that the concentration of sperm, proportions of normal sperm, and progressively motile sperm in CP/CPPS patients are significantly lower than in healthy controls[113]. Similarly, a previous study by our group found a significant decrease in the amount of normal morphological sperm, sperm total amount, and progressive motility in CP/CPPS patients. Moreover, an increase in sperm DNA fragmentation and protamine mRNA ratios was also observed in these patients[172]. Semen pH, with a

standardized range of 7.2 to 8.0, can be affected by chronic bacterial prostatitis, urethritis, epididymitis, and blockage of seminal vesicles[173,174]. Our group's previous investigation revealed a significant decrease in semen pH in CP/CPPS patients[101,172]. The abnormality of semen pH can further decrease the motility and capacitation of sperm, potentially leading to male infertility[175].

Our investigation explored the relationship between sperm motility, epigenetic changes, and gene expression alterations in EJ and ExU from CP/CPPS patients. We categorized sperm motility into five groups, including straight moving (motility a), zigzag moving (motility b), vibrating (motility c), non-motile (motility d), and total motility (motility a+b+c). Our findings demonstrated that methylation and expression levels of *CDKN2A*, *BMP7*, *EDNRB*, *GSTP1* and *PTGS2* significantly correlated with sperm motility and semen pH. Specifically, *CDKN2A* methylation level in ESCs was negatively associated with total sperm motility and positively associated with motility d. In contrast, *CDKN2A* expression level was negatively associated with motility d. In ExU, *CDKN2A* expression level was positively associated with motility a. *BMP7* methylation in ESCs was significantly negatively correlated with motility a, motility c, and total motility. *EDNRB* methylation level in ESCs was negatively correlated with motility a and total motility. Interestingly, *BMP4* methylation in ExU and *BMP7* in EJ were significantly negatively correlated with semen pH. Additionally, the expression levels of *EDNRB* in EJ and *PTGS2* in ExU were significantly positively correlated with semen pH. Unexpectedly, semen pH negatively correlated with sperm motility b, contrasting with previous findings. Lastly, we found that the methylation levels of *CDKN2A* in leukocytes of EJ, leukocytes of ExU, and epithelial cells of ExU were significantly negatively correlated with sperm motility c.

In summary, the results above provide valuable insights into the epigenetic changes and gene expression alterations of TSGs associated with sperm motility and semen pH in CP/CPPS patients. Besides, they also provide significant implications for clinicians and researchers interested in understanding the correlations of etiology and pathogenesis of CP/CPPS, infertility, and PCa. The findings support previous studies suggesting that CP/CPPS is linked to reduced male fertility and also suggest a potential correlation between TSGs and infertility. Furthermore, individuals with CP/CPPS who exhibit lower-quality sperm are more vulnerable to infertility, as well as

an elevated risk of developing to PCa in later life, implying that sperm quality may also play a role in the prognosis and development of CP/CPPS. In addition, epigenetic changes and gene expression alterations in TSGs in CP/CPPS patients may contribute to reduced sperm quality and infertility. Therefore, TSG methylation and expression levels in liquid biopsies may be promising for evaluating infertility in CP/CPPS patients. These observations warrant further investigation into the underlying mechanisms that connect PCa and infertility and may aid in developing novel diagnostic and therapeutic strategies for these conditions.

4.5. Total exosome from ExU supernatant influences the polarization of THP-1 cells

THP-1 is a widely used monocyte cell line originally derived from an acute monocytic leukemia patient. These cells are characterized by their round, single-cell morphology and suspended growth pattern and are commonly employed as a model for studying monocyte/macrophage mechanisms, signaling pathways, and functions[176]. Differentiating these cells into M0, M1 and M2 macrophages allows for the investigation of their distinct roles in inflammation and disease. For example, differentiation of THP1 cells into M0 macrophages can be achieved through incubation with PMA, resulting in increased cell size and adhesivity. This process has been shown to involve the PI3K/Akt signaling pathway and BCL2 family genes, such as NF-κB, which contribute to the differentiation and survival of PMA-induced THP-1 cells[177,178].

Further differentiation of M0 macrophages into M1 and M2 macrophages can be accomplished by incubation with IFN-γ, LPS, IL-4, or IL-13, respectively. M1 macrophages are classically activated macrophages primarily responsible for pro-inflammatory responses, such as the secretion of pro-inflammatory cytokines, antigen presentation, immune surveillance, and involvement in positive immune responses. In addition, these cells can also kill pathogens by activating inducible nitric oxide synthase (INOS)[150]. In contrast, M2 macrophages are alternatively activated macrophages that mainly reduce inflammation and suppress immunoreactions by secreting anti-inflammatory cytokines such as IL-10 and TGF-β[179–183].

Macrophages play a critical role in the pathogenesis of PCa and CP/CPPS. The infiltration of M2 macrophages into PCa tissues has been associated with an unfavorable prognosis[184]. In addition, the number of macrophages is correlated with the levels of pro-inflammatory cytokines, such as IL-8 and IL-6, and polymorphonuclear elastase in the EJ of CP/CPPS patients[185].

Exosomes were for the first time introduced by Harding's group[186]. They are small membrane-bound extracellular vesicles measuring 30-150 nm in diameter, produced by most eukaryotic cells. These vesicles can be found in urine, blood, cerebrospinal fluid, and tissues and can also be isolated from the culture medium of *in vitro* cultured cells[187]. The contents of exosomes are diverse and depend on the cell of origin, including proteins, miRNAs, and mRNAs. The analysis of exosomes from various sources has the potential to provide valuable insights into the pathogenesis of various diseases[188]. Exosomes play a critical role in cell-to-cell communication, and it has been proposed that exosome-mediated transfer of cargo mRNA can influence target protein expression levels in recipient cells[189,190]. Moreover, the trafficking of exosomes is thought to impact the immune system and adaptive immune responses to tumors and pathogens[191]. For example, in CP/CPPS, an increased amount of exosomes containing miRNA-155 has been detected in prostatic fluid, which may enhance immune activities by being received by prostatic stromal cells[192].

Our study aimed to investigate the effect of exosomes isolated from the supernatant of EPS of CP/CPPS patients on the polarization of M0 macrophages. After a 24 h incubation, the CP/CPPS patient group showed significantly higher expression of *IL-1β* compared to the healthy controls, while *CCL18* exhibited an opposite trend. In the 48 h incubation group, both CP/CPPS patients and healthy controls showed higher expression levels of *TNF-α* and *CCL18* than the M0 controls. In addition, the CP/CPPS patient group showed a slightly higher expression level of *CCL22* than the healthy controls, while *CCL18* showed the same trend but was not statistically significant. Furthermore, the expression levels of *CDKN2A* were significantly lower in both CP/CPPS and healthy control groups after 24 h and 48 h treatment. In the 48 h group, the CP/CPPS group showed a slightly lower *CDKN2A* expression level than the healthy controls, but the difference was insignificant. Overall, the CP/CPPS patient

group exhibited the trend of increased expression levels of M1 markers and decreased M2 markers.

In conclusion, the present study provides evidence to suggest that exosomes derived from patients with CP/CPPS can modulate the polarization of M0 macrophages, promoting a shift toward the M1 phenotype. Moreover, the results indicate a potential association between CP/CPPS exosomes and decreased expression levels of *CDKN2A*, which may implicate the role of exosomes in modulating TSG expression. However, given the relatively small sample size of the study, it is necessary to include larger cohorts of ExU samples to obtain more representative information about the effects of exosomes on M0 macrophage polarization. Additionally, other prostate cancer-related TSGs should be evaluated to provide a more comprehensive understanding of the impact of exosomes on TSG expression. Future investigations should also focus on isolating and analyzing the specific contents of exosomes, such as prostate cancer-related mRNA and mature and precursor miRNA, to evaluate their influence on target protein production levels. Furthermore, comparative analyses between ExU and EJ supernatant-derived exosomes could be performed to gain insights into potential differences between exosomes from different sources. Such investigations will help elucidate further the role of exosomes in the pathogenesis of CP/CPPS, the correlation between PCa and CP/CPPS and identify novel therapeutic targets for managing CP/CPPS.

5. References

1. Nickel, J. C. *et al.* The Relationship between Prostate Inflammation and Lower Urinary Tract Symptoms: Examination of Baseline Data from the REDUCE Trial. *Eur. Urol.* **54**, 1379–1384 (2008).

2. Nickel, J. C. *et al.* Consensus development of a histopathological classification system for chronic prostatic inflammation. *BJU Int.* **87**, 797–805 (2001).

3. Krieger, J. N., Leroy Nyberg, J. & Nickel, J. C. NIH Consensus Definition and Classification of Prostatitis. *JAMA* **282**, 236–237 (1999).

4. Mahal, B. A. *et al.* The Role of Phenotyping in Chronic Prostatitis/Chronic Pelvic Pain Syndrome. *Curr. Urol. Rep.* **12**, 297–303 (2011).

5. Breser, M. L., Motrich, R. D., Sanchez, L. R., Mackern-Oberti, J. P. & Rivero, V. E. Expression of CXCR3 on Specific T Cells Is Essential for Homing to the Prostate Gland in an Experimental Model of Chronic Prostatitis/Chronic Pelvic Pain Syndrome. *J. Immunol.* **190**, 3121–3133 (2013).

6. Schaeffer, A. J., Wendel, E. F., Dunn, J. K. & Grayhack, J. T. Prevalence and Significance of Prostatic Inflammation. *J. Urol.* **125**, 215–219 (1981).

7. Wright, E. T., Chmiel, J. S., Grayhack, J. T. & Schaeffer, A. J. Prostatic Fluid Inflammation in Prostatitis. *J. Urol.* **152**, 2300–2303 (1994).

8. Ludwig, M., Schroeder-Printzen, I., Lüdecke, G. & Weidner, W. Comparison of expressed prostatic secretions with urine after prostatic massage—a means to diagnose chronic prostatitis/inflammatory chronic pelvic pain syndrome. *Urology* **55**, 175–177 (2000).

9. Luzzi, G. Chronic BlackwellScience,Ltd prostatitis and chronic pelvic pain in men: aetiology, diagnosis and management. (2002).

10. Clemens, J. Q., Meenan, R. T., O'Keeffe Rosetti, M. C., Gao, S. Y. & Calhoun, E. A. INCIDENCE AND CLINICAL CHARACTERISTICS OF NATIONAL INSTITUTES OF HEALTH TYPE III PROSTATITIS IN THE COMMUNITY. *J. Urol.* **174**, 2319–2322 (2005).

11. Shoskes, D. A. *et al.* IMPACT OF POST-EJACULATORY PAIN IN MEN WITH CATEGORY III CHRONIC PROSTATITIS/CHRONIC PELVIC PAIN SYNDROME. *J. Urol.* **172**, 542–547 (2004).

12. Nickel, J. C. *et al.* Leukocytes And Bacteria In Men With Chronic Prostatitis/Chronic Pelvic Pain Syndrome Compared To Asymptomatic Controls. *J. Urol.* **170**, 818–822 (2003).

13. Fan, D. *et al.* Study on the relationship between sex hormone changes and erectile dysfunction in patients with chronic prostatitis/chronic pelvic pain syndrome. *Ann. Palliat. Med.* **10**, 1739–1747 (2021).

14. John, H. *et al.* Immunological alterations in the ejaculate of chronic prostatitis patients: clues for autoimmunity. (2003).

15. Ponniah, S., Arah, I. & Alexander, R. B. PSA is a candidate self-antigen in autoimmune chronic prostatitis/chronic pelvic pain syndrome. *The Prostate* **44**, 49–54 (2000).

16. Chen, J. *et al.* The risk factors related to the severity of pain in patients with Chronic Prostatitis/Chronic Pelvic Pain Syndrome. *BMC Urol.* **20**, 154 (2020).

17. Moreira, D. M. *et al.* Smoking Is Associated with Acute and Chronic Prostatic Inflammation: Results from the REDUCE Study. *Cancer Prev. Res. (Phila. Pa.)* **8**, 312–317 (2015).

18. Shankar, E. *et al.* Inflammatory Signaling Involved in High-Fat Diet Induced Prostate Diseases. *J. Urol. Res.* **2**, (2015).

19. Wagenlehner, F. M. E. *et al.* National Institutes of Health Chronic Prostatitis Symptom Index (NIH-CPSI) Symptom Evaluation in Multinational Cohorts of Patients with Chronic Prostatitis/Chronic Pelvic Pain Syndrome. *Eur. Urol.* **63**, 953–959 (2013).

20. Polackwich, A. S. & Shoskes, D. A. Chronic prostatitis/chronic pelvic pain syndrome: a review of evaluation and therapy. *Prostate Cancer Prostatic Dis.* **19**, 132–138 (2016).

21. Murphy, S. F., Schaeffer, A. J. & Thumbikat, P. Immune mediators of chronic pelvic pain syndrome. *Nat. Rev. Urol.* **11**, 259–269 (2014).

22. Doiron, R. C., Shoskes, D. A. & Nickel, J. C. Male CP/CPPS: where do we stand? *World J. Urol.* **37**, 1015–1022 (2019).

23. Polackwich, A. S. & Shoskes, D. A. Chronic prostatitis/chronic pelvic pain syndrome: a review of evaluation and therapy. *Prostate Cancer Prostatic Dis.* **19**, 132–138 (2016).

24. de Lavor, É. M. *et al.* Essential Oils and Their Major Compounds in the Treatment of Chronic Inflammation: A Review of Antioxidant Potential in Preclinical Studies and Molecular Mechanisms. *Oxid. Med. Cell. Longev.* **2018**, e6468593 (2018).

25. Coussens, L. M. & Werb, Z. Inflammation and cancer. *Nature* **420**, 860–867 (2002).

26. Nathan, C. Points of control in inflammation. *Nature* **420**, 846–852 (2002).

27. Macarthur, M., Hold, G. L. & El-Omar, E. M. Inflammation and Cancer II. Role of chronic inflammation and cytokine gene polymorphisms in the pathogenesis of gastrointestinal malignancy. *Am. J. Physiol.-Gastrointest. Liver Physiol.* **286**, G515–G520 (2004).

28. Michels, N., van Aart, C., Morisse, J., Mullee, A. & Huybrechts, I. Chronic inflammation towards cancer incidence: A systematic review and meta-analysis of epidemiological studies. *Crit. Rev. Oncol. Hematol.* **157**, 103177 (2021).

29. Greten, F. R. & Grivennikov, S. I. Inflammation and Cancer: Triggers, Mechanisms, and Consequences. *Immunity* **51**, 27–41 (2019).

30. Hanahan, D. & Weinberg, R. A. The Hallmarks of Cancer. *Cell* **100**, 57–70 (2000).

31. Mantovani, A., Allavena, P., Sica, A. & Balkwill, F. Cancer-related inflammation. *Nature* **454**, 436–444 (2008).

32. Multhoff, G., Molls, M. & Radons, J. Chronic Inflammation in Cancer Development. *Front. Immunol.* **2**, (2012).

33. Cordon-Cardo, C. & Prives, C. At the Crossroads of Inflammation and Tumorigenesis. *J. Exp. Med.* **190**, 1367–1370 (1999).

34. Jiang, J. *et al.* The Role of Prostatitis in Prostate Cancer: Meta-Analysis. *PLoS ONE* **8**, (2013).

35. Miller, A. M. *et al.* CD4+CD25high T Cells Are Enriched in the Tumor and Peripheral Blood of Prostate Cancer Patients. *J. Immunol.* **177**, 7398–7405 (2006).

36. Lonkar, P. & Dedon, P. C. Reactive species and DNA damage in chronic inflammation: Reconciling chemical mechanisms and biological fates. *Int. J. Cancer J. Int. Cancer* **128**, 1999–2009 (2011).

37. Perletti, G. *et al.* The association between prostatitis and prostate cancer. Systematic review and meta-analysis. *Arch. Ital. Urol. E Androl.* **89**, 259–265 (2017).

38. Doat, S. *et al.* Prostatitis, other genitourinary infections and prostate cancer risk: Influence of non-steroidal anti-inflammatory drugs? Results from the EPICAP study. *Int. J. Cancer* **143**, 1644–1651 (2018).

39. Stikbakke, E. *et al.* Inflammatory serum markers and risk and severity of prostate cancer: The PROCA-life study. *Int. J. Cancer* **147**, 84–92 (2020).

40. Yli-Hemminki, T. H. *et al.* Histological inflammation and risk of subsequent prostate cancer among men with initially elevated serum prostate-specific antigen (PSA) concentration in the Finnish prostate cancer screening trial. *BJU Int.* **112**, 735–741 (2013).

41. Sutcliffe, S. *et al.* Gonorrhea, Syphilis, Clinical Prostatitis, and the Risk of Prostate Cancer. *Cancer Epidemiol. Prev. Biomark.* **15**, 2160–2166 (2006).

42. Karakiewicz, P. I. *et al.* Chronic inflammation is negatively associated with prostate cancer and high-grade prostatic intraepithelial neoplasia on needle biopsy. *Int. J. Clin. Pract.* **61**, 425–430 (2007).

43. Waddington, C. H. The Epigenotype. *Int. J. Epidemiol.* **41**, 10–13 (2012).

44. Wei, J.-W., Huang, K., Yang, C. & Kang, C.-S. Non-coding RNAs as regulators in epigenetics (Review). *Oncol. Rep.* **37**, 3–9 (2017).

45. Nishiyama, A. & Nakanishi, M. Navigating the DNA methylation landscape of cancer. *Trends Genet.* **37**, 1012–1027 (2021).

46. Irizarry, R. A. *et al.* The human colon cancer methylome shows similar hypo- and hypermethylation at conserved tissue-specific CpG island shores. *Nat. Genet.* **41**, 178–186 (2009).

47. Doi, A. *et al.* Differential methylation of tissue- and cancer-specific CpG island shores distinguishes human induced pluripotent stem cells, embryonic stem cells and fibroblasts. *Nat. Genet.* **41**, 1350–1353 (2009).

48. Baylin, S. B. & Jones, P. A. Epigenetic Determinants of Cancer. *Cold Spring Harb. Perspect. Biol.* **8**, a019505 (2016).

49. Moore, L. D., Le, T. & Fan, G. DNA Methylation and Its Basic Function. *Neuropsychopharmacology* **38**, 23–38 (2013).

50. Mishra, D. K. *et al.* Global Methylation Pattern of Genes in Androgen-Sensitive and Androgen-Independent Prostate Cancer Cells. *Mol. Cancer Ther.* **9**, 33–45 (2010).

51. Dor, Y. & Cedar, H. Principles of DNA methylation and their implications for biology and medicine. *The Lancet* **392**, 777–786 (2018).

52. Rouprêt, M. *et al.* Molecular Detection of Localized Prostate Cancer Using Quantitative Methylation-Specific PCR on Urinary Cells Obtained Following Prostate Massage. *Clin. Cancer Res.* **13**, 1720–1725 (2007).

53. Enokida, H. *et al.* Multigene Methylation Analysis for Detection and Staging of Prostate Cancer. *Clin. Cancer Res.* **11**, 6582–6588 (2005).

54. Jarrard, D. F. *et al.* Methylation of the Androgen Receptor Promoter CpG Island Is Associated with Loss of Androgen Receptor Expression in Prostate Cancer Cells. *Cancer Res.* **58**, 5310–5314 (1998).

55. Izbicka, E. *et al.* 5,6 Dihydro-5'-azacytidine (DHAC) restores androgen responsiveness in androgen-insensitive prostate cancer cells. *Anticancer Res.* **19**, 1285–1291 (1999).

56. Neste, L. V. *et al.* The Epigenetic promise for prostate cancer diagnosis. *The Prostate* **72**, 1248–1261 (2012).

57. Li, L.-C. *et al.* Frequent Methylation of Estrogen Receptor in Prostate Cancer: Correlation with Tumor Progression. *Cancer Res.* **60**, 702–706 (2000).

58. Shames, D., Minna, J. & Gazdar, A. DNA Methylation in Health, Disease, and Cancer. *Curr. Mol. Med.* **7**, 85–102 (2007).

59. Partin, A. W. *et al.* Clinical Validation of an Epigenetic Assay to Predict Negative Histopathological Results in Repeat Prostate Biopsies. *J. Urol.* **192**, 1081–1087 (2014).

60. Yegnasubramanian, S. *et al.* Hypermethylation of CpG Islands in Primary and Metastatic Human Prostate Cancer. *Cancer Res.* **64**, 1975–1986 (2004).

61. Bastian, P. J. *et al.* Diagnostic and Prognostic Information in Prostate Cancer with the Help of a Small Set of Hypermethylated Gene Loci. *Clin. Cancer Res.* **11**, 4097–4106 (2005).

62. Ellinger, J. *et al.* CpG Island Hypermethylation at Multiple Gene Sites in Diagnosis and Prognosis of Prostate Cancer. *Urology* **71**, 161–167 (2008).

63. Yoshida, B. A., Sokoloff, M. M. & Welch, D. R. Metastasis-Suppressor Genes: a Review and Perspective on an Emerging Field. *J. Natl. Cancer Inst.* **92**, 14 (2000).

64. Leiderman, Y. I., Kiss, S. & Mukai, S. Molecular Genetics of RB1——The Retinoblastoma Gene. *Semin. Ophthalmol.* **22**, 247–254 (2007).

65. Smith, A. L., Robin, T. P. & Ford, H. L. Molecular Pathways: Targeting the TGF-β Pathway for Cancer Therapy. *Clin. Cancer Res.* **18**, 4514–4521 (2012).

66. Nayak, S. K. & Kumar, P. S. P. and H. p53-Induced Apoptosis and Inhibitors of p53. *Current Medicinal Chemistry* http://www.eurekaselect.com/69540/article (2009).

67. Savage, K. I. & Harkin, D. P. BRCA1, a 'complex' protein involved in the maintenance of genomic stability. *FEBS J.* **282**, 630–646 (2015).

68. Rahman, N. & Scott, R. H. Cancer genes associated with phenotypes in monoallelic and biallelic mutation carriers: new lessons from old players. *Hum. Mol. Genet.* **16**, R60–R66 (2007).

69. Morris, L. G. T. & Chan, T. A. Therapeutic Targeting of Tumor Suppressor Genes. *Cancer* **121**, 1357–1368 (2015).

70. Wang, L.-H., Wu, C.-F., Rajasekaran, N. & Shin, Y. K. Loss of Tumor Suppressor Gene Function in Human Cancer: An Overview. *Cell. Physiol. Biochem.* **51**, 2647–2693 (2018).

71. Verdoodt, B. *et al.* Inverse association of p16 INK4a and p14 ARF methylation of the CDKN2a locus in different Gleason scores of prostate cancer. *Prostate Cancer Prostatic Dis.* **14**, 295–301 (2011).

72. Liu, F., Ventura, F., Doody, J. & Massagué, J. Human type II receptor for bone morphogenic proteins (BMPs): extension of the two-kinase receptor model to the BMPs. *Mol. Cell. Biol.* **15**, 3479–3486 (1995).

73. Wozney, J. M., Rosen, V. & Celeste, A. J. Novel Regulators of Bone Formation: **242**,.

74. Nohno, T. *et al.* Identification of a Human Type II Receptor for Bone Morphogenetic Protein-4 That Forms Differential Heteromeric Complexes with Bone Morphogenetic Protein Type I Receptors (∗). *J. Biol. Chem.* **270**, 22522–22526 (1995).

75. Chen, D., Zhao, M. & Mundy, G. R. Bone Morphogenetic Proteins. *Growth Factors* **22**, 233–241 (2004).

76. Kron, K. *et al.* Discovery of Novel Hypermethylated Genes in Prostate Cancer Using Genomic CpG Island Microarrays. *PLOS ONE* **4**, e4830 (2009).

77. Buijs, J. T. *et al.* BMP7, a putative regulator of epithelial homeostasis in the human prostate, is a potent inhibitor of prostate cancer bone metastasis in vivo. *Am. J. Pathol.* **171**, 1047–1057 (2007).

78. Harris, S. E. *et al.* Expression of bone morphogenetic protein messenger RNAs by normal rat and human prostate and prostate cancer cells. *The Prostate* **24**, 204–211 (1994).

79. Lamm, M. L. G. *et al.* Mesenchymal Factor Bone Morphogenetic Protein 4 Restricts Ductal Budding and Branching Morphogenesis in the Developing Prostate. *Dev. Biol.* **232**, 301–314 (2001).

80. Wahdan-Alaswad, R. S. *et al.* Insulin-Like Growth Factor I Suppresses Bone Morphogenetic Protein Signaling in Prostate Cancer Cells by Activating mTOR Signaling. *Cancer Res.* **70**, 9106–9117 (2010).

81. Brubaker, K. D., Corey, E., Brown, L. G. & Vessella, R. L. Bone morphogenetic protein signaling in prostate cancer cell lines. *J. Cell. Biochem.* **91**, 151–160 (2004).

82. Expression of BMP4 in prostate cancer - The Human Protein Atlas. https://www.proteinatlas.org/ENSG00000125378-BMP4/pathology/prostate+cancer.

83. Lee, C.-H. *et al.* Prognostic Value of Prostaglandin-endoperoxide Synthase 2 Polymorphisms in Prostate Cancer Recurrence after Radical Prostatectomy. *Int. J. Med. Sci.* **13**, 696–700 (2016).

84. Strand, S. H., Orntoft, T. F. & Sorensen, K. D. Prognostic DNA Methylation Markers for Prostate Cancer. *Int. J. Mol. Sci.* **15**, 16544–16576 (2014).

85. Murata, M. Inflammation and cancer. *Environ. Health Prev. Med.* **23**, 50 (2018).

86. Phé, V., Cussenot, O. & Rouprêt, M. Methylated genes as potential biomarkers in prostate cancer. *BJU Int.* **105**, 1364–1370 (2010).

87. Tan, D. S. W. *et al.* Intertumor heterogeneity of non-small-cell lung carcinomas revealed by multiplexed mutation profiling and integrative genomics. *Int. J. Cancer* **135**, 1092–1100 (2014).

88. Pantel, K. & Alix-Panabières, C. Circulating tumour cells in cancer patients: challenges and perspectives. *Trends Mol. Med.* **16**, 398–406 (2010).

89. Yee, N. S. Liquid Biopsy: A Biomarker-Driven Tool towards Precision Oncology. *J. Clin. Med.* **9**, 2556 (2020).

90. Kim, Y. *et al.* Targeted proteomics identifies liquid-biopsy signatures for extracapsular prostate cancer. *Nat. Commun.* **7**, (2016).

91. Okugawa, Y., Grady, W. M. & Goel, A. Epigenetic Alterations in Colorectal Cancer: Emerging Biomarkers. *Gastroenterology* **149**, 1204-1225.e12 (2015).

92. Lam, K., Pan, K., Linnekamp, J. F., Medema, J. P. & Kandimalla, R. DNA methylation based biomarkers in colorectal cancer: A systematic review. *Biochim. Biophys. Acta BBA - Rev. Cancer* **1866**, 106–120 (2016).

93. Sidransky, D. Emerging molecular markers of cancer. *Nat. Rev. Cancer* **2**, 210–219 (2002).

94. Mitomi, H. *et al.* Aberrant p16INK4a methylation is a frequent event in colorectal cancers: prognostic value and relation to mRNA expression and immunoreactivity. *J. Cancer Res. Clin. Oncol.* **136**, 323 (2009).

95. Lyberopoulou, A. *et al.* Identification of Methylation Profiles of Cancer-related Genes in Circulating Tumor Cells Population. *Anticancer Res.* **37**, 1105–1112 (2017).

96. Bakavicius, A. *et al.* Urinary DNA methylation biomarkers for prediction of prostate cancer upgrading and upstaging. *Clin. Epigenetics* **11**, (2019).

97. Silva, R. *et al.* Evaluating liquid biopsies for methylomic profiling of prostate cancer. *Epigenetics* **15**, 715–727.

98. Ge, G. *et al.* Urothelial Carcinoma Detection Based on Copy Number Profiles of Urinary Cell-Free DNA by Shallow Whole-Genome Sequencing. *Clin. Chem.* (2019) doi:10.1373/clinchem.2019.309633.

99. Hendriks, R. J. *et al.* Epigenetic markers in circulating cell-free DNA as prognostic markers for survival of castration-resistant prostate cancer patients. *The Prostate* **78**, 336–342 (2018).

100. Moryousef, J. *et al.* Overview of seminal fluid biomarkers for the evaluation of chronic prostatitis: a scoping review. *Prostate Cancer Prostatic Dis.* 1–14 (2021) doi:10.1038/s41391-021-00472-8.

101. Schagdarsurengin, U. *et al.* Chronic Prostatitis Affects Male Reproductive Health and Is Associated with Systemic and Local Epigenetic Inactivation of C-X-C Motif Chemokine 12 Receptor C-X-C Chemokine Receptor Type 4. *Urol. Int.* **98**, 89–101 (2017).

102. Yang, M. & Park, J. Y. DNA Methylation in Promoter Region as Biomarkers in Prostate Cancer. in *Cancer Epigenetics* (eds. Dumitrescu, R. G. & Verma, M.) vol. 863 67–109 (Humana Press, 2012).

103. Lee, Y.-C. *et al.* BMP4 Promotes Prostate Tumor Growth in Bone through Osteogenesis. *Cancer Res.* **71**, 5194–5203 (2011).

104. Markou, A. *et al.* Multiplex Gene Expression Profiling of In Vivo Isolated Circulating Tumor Cells in High-Risk Prostate Cancer Patients. *Clin. Chem.* **64**, 297–306 (2018).

105. Ma, Y. *et al.* Plastin 3 down-regulation augments the sensitivity of MDA-MB-231 cells to paclitaxel via the p38 MAPK signalling pathway. *Artif. Cells Nanomedicine Biotechnol.* **47**, 684–694 (2019).

106. Spanjol, J. *et al.* Role of bone morphogenetic proteins in human prostate cancer pathogenesis and development of bone metastases: immunohistochemical study. *Coll. Antropol.* **34 Suppl 2**, 119–125 (2010).

107. Cytokeratin expression patterns in normal and malignant urothelium: a review of the biological and diagnostic implications. *Histol. Histopathol.* 657–664 (1999) doi:10.14670/HH-14.657.

108. Windoffer, R., Beil, M., Magin, T. M. & Leube, R. E. Cytoskeleton in motion: the dynamics of keratin intermediate filaments in epithelia. *J. Cell Biol.* **194**, 669–678 (2011).

109. Herrmann, H., Bär, H., Kreplak, L., Strelkov, S. V. & Aebi, U. Intermediate filaments: from cell architecture to nanomechanics. *Nat. Rev. Mol. Cell Biol.* **8**, 562–573 (2007).

110. Altin, J. G. & Sloan, E. K. The role of CD45 and CD45-associated molecules in T cell activation. *Immunol. Cell Biol.* **75**, 430–445 (1997).

111. Trowbridge, I. S. & Thomas, M. L. CD45: An Emerging Role as a Protein Tyrosine Phosphatase Required for Lymphocyte Activation and Development. *Annu. Rev. Immunol.* **12**, 85–116 (1994).

112. Motrich, R. D. *et al.* Chronic Prostatitis/Chronic Pelvic Pain Syndrome patients show Th1 and Th17 self-reactive immune responses specific to prostate and seminal antigens and decreased semen quality. *BJU Int.* (2020) doi:10.1111/bju.15117.

113. Fu, W. *et al.* The Effect of Chronic Prostatitis/Chronic Pelvic Pain Syndrome (CP/CPPS) on Semen Parameters in Human Males: A Systematic Review and Meta-Analysis. *PLoS ONE* **9**, e94991 (2014).

114. Kalluri, R. & LeBleu, V. S. The biology, function, and biomedical applications of exosomes. *Science* **367**, eaau6977 (2020).

115. Bradley, J. TNF-mediated inflammatory disease. *J. Pathol.* **214**, 149–160 (2008).

116. Gaestel, M., Kotlyarov, A. & Kracht, M. Targeting innate immunity protein kinase signalling in inflammation. *Nat. Rev. Drug Discov.* **8**, 480–499 (2009).

117. Dinarello, C. A. Immunological and Inflammatory Functions of the Interleukin-1 Family. *Annu. Rev. Immunol.* **27**, 519–550 (2009).

118. Akhtari, M., Zargar, S. J., Vojdanian, M., Jamshidi, A. & Mahmoudi, M. Monocyte-derived and M1 macrophages from ankylosing spondylitis patients released higher TNF-α and expressed more IL1B in response to BzATP than macrophages from healthy subjects. *Sci. Rep.* **11**, 17842 (2021).

119. Azad, A. K., Rajaram, M. V. S. & Schlesinger, L. S. Exploitation of the Macrophage Mannose Receptor (CD206) in Infectious Disease Diagnostics and Therapeutics. *J. Cytol. Mol. Biol.* **1**, 1000003 (2014).

120. Kimura, S. *et al.* Relationship between CCL22 Expression by Vascular Smooth Muscle Cells and Macrophage Histamine Receptors in Atherosclerosis. *J. Atheroscler. Thromb.* **25**, 1240–1254 (2018).

121. Xu, Z.-J. *et al.* The M2 macrophage marker CD206: a novel prognostic indicator for acute myeloid leukemia. *Oncoimmunology* **9**, 1683347 (2019).

122. Schutyser, E., Richmond, A. & Van Damme, J. Involvement of CC chemokine ligand 18 (CCL18) in normal and pathological processes. *J. Leukoc. Biol.* **78**, 14–26 (2005).

123. Murray, P. J. & Wynn, T. A. Protective and pathogenic functions of macrophage subsets. *Nat. Rev. Immunol.* **11**, 723–737 (2011).

124. Greten, F. R. & Grivennikov, S. I. Inflammation and Cancer: Triggers, Mechanisms and Consequences. *Immunity* **51**, 27–41 (2019).

125. Forte, V. *et al.* Obesity, Diabetes, the Cardiorenal Syndrome, and Risk for Cancer. *Cardiorenal Med.* **2**, 143–162 (2012).

126. Terzić, J., Grivennikov, S., Karin, E. & Karin, M. Inflammation and Colon Cancer. *Gastroenterology* **138**, 2101-2114.e5 (2010).

127. Matysiak-Budnik, T. & Mégraud, F. Helicobacter pylori infection and gastric cancer. *Eur. J. Cancer* **42**, 708–716 (2006).

128. Dítě, P. *et al.* The Role of Chronic Inflammation: Chronic Pancreatitis as a Risk Factor of Pancreatic Cancer. *Dig. Dis.* **30**, 277–283 (2012).

129. Gurel, B. *et al.* Chronic Inflammation in Benign Prostate Tissue Is Associated with High-Grade Prostate Cancer in the Placebo Arm of the Prostate Cancer Prevention Trial. *Cancer Epidemiol. Biomarkers Prev.* **23**, 847–856 (2014).

130. Kwon, O.-J., Zhang, L., Ittmann, M. M. & Xin, L. Prostatic inflammation enhances basal-to-luminal differentiation and accelerates initiation of prostate cancer with a basal cell origin. *Proc. Natl. Acad. Sci.* **111**, (2014).

131. Sfanos, K. S. & De Marzo, A. M. Prostate cancer and inflammation: the evidence. *Histopathology* **60**, 199–215 (2012).

132. Gamell, C. *et al.* Reduced abundance of the E3 ubiquitin ligase E6AP contributes to decreased expression of the *INK4/ARF* locus in non–small cell lung cancer. *Sci. Signal.* **10**, eaaf8223 (2017).

133. Shima, K. *et al.* Prognostic Significance of CDKN2A (p16) Promoter Methylation and Loss of Expression in 902 Colorectal Cancers: Cohort Study and Literature Review. *Int. J. Cancer J. Int. Cancer* **128**, 1080–1094 (2011).

134. Ribas, C. *et al.* p16 gene methylation lacks correlation with angiogenesis and prognosis in multiple myeloma. *Cancer Lett.* **222**, 247–254 (2005).

135. Delgado-Cruzata, L. *et al.* DNA Methylation Changes Correlate with Gleason Score and Tumor Stage in Prostate Cancer. *DNA Cell Biol.* **31**, 187–192 (2012).

136. Bracken, A. P. *et al.* The Polycomb group proteins bind throughout the INK4A-ARF locus and are disassociated in senescent cells. *Genes Dev.* **21**, 525–530 (2007).

137. Jozwik, K. M. & Carroll, J. S. Pioneer factors in hormone-dependent cancers. *Nat. Rev. Cancer* **12**, 381–385 (2012).

138. Katoh, M., Igarashi, M., Fukuda, H., Nakagama, H. & Katoh, M. Cancer genetics and genomics of human FOX family genes. *Cancer Lett.* **328**, 198–206 (2013).

139. Li, Q. *et al.* FOXA1 mediates p16INK4a activation during cellular senescence. *EMBO J.* **32**, 858–873 (2013).

140. Pasini, D. & Di Croce, L. Emerging roles for Polycomb proteins in cancer. *Curr. Opin. Genet. Dev.* **36**, 50–58 (2016).

141. Versemann, L. *et al.* TP53-Status-Dependent Oncogenic EZH2 Activity in Pancreatic Cancer. *Cancers* **14**, 3451 (2022).

142. Burchfield, J. S., Li, Q., Wang, H. Y. & Wang, R.-F. JMJD3 as an epigenetic regulator in development and disease. *Int. J. Biochem. Cell Biol.* **67**, 148–157 (2015).

143. Pinton, G. *et al.* CDKN2A Determines Mesothelioma Cell Fate to EZH2 Inhibition. *Front. Oncol.* **11**, (2021).

144. Majid, S. *et al.* Genistein Induces the *p21WAF1/CIP1* and *p16INK4a* Tumor Suppressor Genes in Prostate Cancer Cells by Epigenetic Mechanisms Involving Active Chromatin Modification. *Cancer Res.* **68**, 2736–2744 (2008).

145. Yap, K. L. *et al.* Molecular Interplay of the Non-coding RNA ANRIL and Methylated Histone H3 Lysine 27 by Polycomb CBX7 in Transcriptional Silencing of INK4a. *Mol. Cell* **38**, 662–674 (2010).

146. Pacifico, A. & Leone, G. Role of p53 and CDKN2A Inactivation in Human Squamous Cell Carcinomas. *J. Biomed. Biotechnol.* **2007**, 43418 (2007).

147. Sakurai, N. *et al.* Influence of MIF polymorphisms on CpG island hyper-methylation of CDKN2A in the patients with ulcerative colitis. *BMC Med. Genet.* **21**, 201 (2020).

148. Mitchell, R. A. *et al.* Macrophage migration inhibitory factor (MIF) sustains macrophage proinflammatory function by inhibiting p53: Regulatory role in the innate immune response. *Proc. Natl. Acad. Sci.* **99**, 345–350 (2002).

149. Litvinov, S. V., Bakker, H. A. M., Gourevitch, M. M., Velders, M. P. & Warnaar, S. O. Evidence for a Role of the Epithelial Glycoprotein 40 (Ep-CAM) in Epithelial Cell-Cell Adhesion. *Cell Adhes. Commun.* **2**, 417–428 (1994).

150. Liu, Y. *et al.* Chronic prostatitis/chronic pelvic pain syndrome and prostate cancer: study of immune cells and cytokines. *Fundam. Clin. Pharmacol.* **34**, 160–172 (2020).

151. Brown, T. C., Sankpal, N. V. & Gillanders, W. E. Functional Implications of the Dynamic Regulation of EpCAM during Epithelial-to-Mesenchymal Transition. *Biomolecules* **11**, 956 (2021).

152. Went, P. T. H. *et al.* Frequent EpCam protein expression in human carcinomas. *Hum. Pathol.* **35**, 122–128 (2004).

153. Mahbub, S. B. *et al.* Non-invasive assessment of exfoliated kidney cells extracted from urine using multispectral autofluorescence features. *Sci. Rep.* **11**, 10655 (2021).

154. Zafarullah, M., Jasoliya, M. & Tassone, F. Urine-Derived Epithelial Cell Lines: A New Tool to Model Fragile X Syndrome (FXS). *Cells* **9**, 2240 (2020).

155. Lazzeri, E. *et al.* Human Urine-Derived Renal Progenitors for Personalized Modeling of Genetic Kidney Disorders. *J Am Soc Nephrol* 20 (2015).

156. Shi, Y. *et al.* Differentiation Capacity of Human Urine-Derived Stem Cells to Retain Telomerase Activity. *Front. Cell Dev. Biol.* **10**, (2022).

157. Rao, D. A. *et al.* A protocol for single-cell transcriptomics from cryopreserved renal tissue and urine for the Accelerating Medicine Partnership (AMP) RA/SLE network. 275859 Preprint at https://doi.org/10.1101/275859 (2018).

158. Boonen, K. J. M., Koldewijn, E. L., Arents, N. L. A., Raaymakers, P. A. M. & Scharnhorst, V. Urine flow cytometry as a primary screening method to exclude urinary tract infections. *World J. Urol.* **31**, 547–551 (2013).

159. Miltenyi, S., Müller, W., Weichel, W. & Radbruch, A. High gradient magnetic cell separation with MACS. *Cytometry* **11**, 231–238 (1990).

160. Elsasser-Beile, U., Buhler, P. & Wolf, P. Targeted Therapies for Prostate Cancer Against the Prostate Specific Membrane Antigen. *Curr. Drug Targets* **10**, 118–125 (2009).

161. Shu, C., Zhang, X., Aouizerat, B. E. & Xu, K. Comparison of methylation capture sequencing and Infinium MethylationEPIC array in peripheral blood mononuclear cells. *Epigenetics Chromatin* **13**, 51 (2020).

162. Sadikovic, B. *et al.* Clinical epigenomics: genome-wide DNA methylation analysis for the diagnosis of Mendelian disorders. *Genet. Med.* **23**, 1065–1074 (2021).

163. Koelsche, C. *et al.* Sarcoma classification by DNA methylation profiling. *Nat. Commun.* **12**, 1–10 (2021).

164. Ferreyra Vega, S. *et al.* DNA methylation profiling for molecular classification of adult diffuse lower-grade gliomas. *Clin. Epigenetics* **13**, 102 (2021).

165. Dirks, R. A. M., Stunnenberg, H. G. & Marks, H. Genome-wide epigenomic profiling for biomarker discovery. *Clin. Epigenetics* **8**, 122 (2016).

166. Suárez-Álvarez, B., Baragaño Raneros, A., Ortega, F. & López-Larrea, C. Epigenetic modulation of the immune function. *Epigenetics* **8**, 694–702 (2013).

167. Krakhotkin, D. V., Chernylovskyi, V. A., Bakurov, E. E. & Sperl, J. Evaluation of influence of the UPOINT-guided multimodal therapy in men with chronic prostatitis/chronic pelvic pain syndrome on dynamic values NIH-CPSI: a prospective, controlled, comparative study. *Ther. Adv. Urol.* **11**, 1756287219857271 (2019).

168. Clemens, J. Q. *et al.* Rescoring the NIH Chronic Prostatitis Symptom Index (NIH-CPSI): Nothing New. *Prostate Cancer Prostatic Dis.* **12**, 285–287 (2009).

169. Litwin, M. S. *et al.* THE NATIONAL INSTITUTES OF HEALTH CHRONIC PROSTATITIS SYMPTOM INDEX: DEVELOPMENT AND VALIDATION OF A NEW OUTCOME MEASURE. *J. Urol.* **162**, 369–375 (1999).

170. Shoskes, D. A. The Challenge of Erectile Dysfunction in the Man with Chronic Prostatitis/Chronic Pelvic Pain Syndrome. *Curr. Urol. Rep.* **13**, 263–267 (2012).

171. Chung, S.-D., Keller, J. J. & Lin, H.-C. A case-control study on the association between chronic prostatitis/chronic pelvic pain syndrome and erectile dysfunction: CHRONIC PROSTATITIS AND ERECTILE DYSFUNCTION. *BJU Int.* **110**, 726–730 (2012).

172. Berg, E. *et al.* Chronic Prostatitis/Chronic Pelvic Pain Syndrome Leads to Impaired Semen Parameters, Increased Sperm DNA Fragmentation and Unfavorable Changes of Sperm Protamine mRNA Ratio. *Int. J. Mol. Sci.* **22**, 7854 (2021).

173. Marconi, M., Pilatz, A., Wagenlehner, F., Diemer, T. & Weidner, W. Impact of infection on the secretory capacity of the male accessory glands. *Int. Braz. J. Urol.* **35**, 299–309 (2009).

174. Dhumal, S. S., Naik, P., Dakshinamurthy, S. & Sullia, K. Semen pH and its correlation with motility and count - A study in subfertile men. *JBRA Assist. Reprod.* **25**, 172–175 (2021).

175. Zhou, J. *et al.* The Semen pH Affects Sperm Motility and Capacitation. *PLoS ONE* **10**, e0132974 (2015).

176. Chanput, W., Mes, J. J. & Wichers, H. J. THP-1 cell line: An in vitro cell model for immune modulation approach. *Int. Immunopharmacol.* **23**, 37–45 (2014).

177. Zeng, C. *et al.* Pathways related to PMA-differentiated THP1 human monocytic leukemia cells revealed by RNA-Seq. *Sci. China Life Sci.* **58**, 1282–1287 (2015).

178. Busca, A., Saxena, M., Iqbal, S., Angel, J. & Kumar, A. PI3K/Akt regulates survival during differentiation of human macrophages by maintaining NF-κB-dependent expression of antiapoptotic Bcl-xL. *J. Leukoc. Biol.* **96**, 1011–1022 (2014).

179. Germano, G. *et al.* Role of Macrophage Targeting in the Antitumor Activity of Trabectedin. *Cancer Cell* **23**, 249–262 (2013).

180. Mosser, D. M. & Edwards, J. P. Exploring the full spectrum of macrophage activation. *Nat. Rev. Immunol.* **8**, 958–969 (2008).

181. Biswas, S. K. & Mantovani, A. Macrophage plasticity and interaction with lymphocyte subsets: cancer as a paradigm. *Nat. Immunol.* **11**, 889–896 (2010).

182. Grohmann, U. *et al.* Positive Regulatory Role of IL-12 in Macrophages and Modulation by IFN-γ. *J. Immunol.* **167**, 221–227 (2001).

183. Van Ginderachter, J. A. *et al.* Classical and alternative activation of mononuclear phagocytes: Picking the best of both worlds for tumor promotion. *Immunobiology* **211**, 487–501 (2006).

184. Lundholm, M. *et al.* Secreted Factors from Colorectal and Prostate Cancer Cells Skew the Immune Response in Opposite Directions. *Sci. Rep.* **5**, 15651 (2015).

185. Aghazarian, A., Plas, E., Stancik, I., Pflüger, H. & Lackner, J. New Method for Differentiating Chronic Prostatitis/Chronic Pelvic Pain Syndrome IIIA From IIIB Involving Seminal Macrophages and Monocytes. *Urology* **78**, 918–923 (2011).

186. Harding, C. & Stahl, P. Transferrin recycling in reticulocytes: pH and iron are important determinants of ligand binding and processing. *Biochem. Biophys. Res. Commun.* **113**, 650–658 (1983).

187. Spaull, R. *et al.* Exosomes populate the cerebrospinal fluid of preterm infants with post-haemorrhagic hydrocephalus. *Int. J. Dev. Neurosci.* **73**, 59–65 (2019).

188. Nuzhat, Z. *et al.* Tumour-derived exosomes as a signature of pancreatic cancer - liquid biopsies as indicators of tumour progression. *Oncotarget* **8**, 17279–17291 (2016).

189. Balaj, L. *et al.* Tumour microvesicles contain retrotransposon elements and amplified oncogene sequences. *Nat. Commun.* **2**, 180 (2011).

190. Oushy, S. *et al.* Glioblastoma multiforme-derived extracellular vesicles drive normal astrocytes towards a tumour-enhancing phenotype. *Philos. Trans. R. Soc. B Biol. Sci.* **373**, 20160477 (2018).

191. Li, X.-B., Zhang, Z.-R., Schluesener, H. J. & Xu, S.-Q. Role of exosomes in immune regulation. *J. Cell. Mol. Med.* **10**, 364–375 (2006).

192. Zhao, B. *et al.* Prostatic fluid exosome-mediated microRNA-155 promotes the pathogenesis of type IIIA chronic prostatitis. *Transl. Androl. Urol.* **10**, 1976–1987 (2021).

6. Supplement

Table 4: Characteristics and measured parameters of patients and healthy controls

Characteristics	Patients (n=45), mean±SD	Healthy controls (n=30), mean±SD	P value
Age (years)	42.9±11.685	28.07±4.82	p<0.0001
IPSS	12.97±7.329	3.42±2.80	p<0.0001
CPSI I	11.78±3.95	1.13±2.51	p<0.0001
CPSI II	4.35±2.91	1.42±1.38	p<0.0001
CPSI III	9.00±2.42	1.21±1.79	p<0.0001
CPSI total	24.95±7.69	3.75±4.68	p<0.0001
Prostate volume (mL)	18.94±13.37	N/A	N/A
CRP (mg/l)	0.92±1.00	N/A	N/A
PSA (ng/mL)	1.07±0.48	N/A	N/A
Zinc	10.51±10.61	4.22±2.97	p=0.0234
Sperm motility a	18.78±14.36	38.18±14.55	p<0.0001
Sperm motility b	23.81±9.55	21.68±7.58	p=0.0967
Sperm motility c	9.00±5.77	12.79±6.27	p=0.0082
Sperm motility total	51.59±20.78	72.64±9.62	p<0.0001

Table 5: Mean of TSGs methylation and expression levels of patients and healthy controls

Exprimental results	Patients (n=41), Mean±SD	Healthy controls (n=30), Mean±SD	P value
Pyro *CDKN2A* EJ (%)	13.29±10.31 (n=31)	4.41±5.16 (n=25)	p<0.0001
Pyro *CDKN2A* ExU (%)	20.01±15.74 (n=37)	7.36±8.56 (n=23)	p=0.0027
Pyro *EDNRB* EJ (%)	4.58±3.48 (n=40)	1.82±2.43 (n=27)	p<0.0001
Pyro *EDNRB* ExU (%)	8.37±11.84 (n=36)	4.50±10.61 (n=24)	p=0.026
Pyro *PTGS2* EJ (%)	5.45±3.15 (n=41)	3.56±1.20 (n=26)	p=0.0469
Pyro *PTGS2* ExU (%)	19.80±23.18 (n=33)	7.57±6.44 (n=24)	ns
Pyro *PITX2* EJ (%)	3.40±6.83 (n=39)	1.99±2.11 (n=28)	ns
Pyro *PITX2* ExU (%)	4.01±9.72 (n=29)	3.72±7.14 (n=20)	ns
Pyro *BMP4* EJ (%)	3.74±2.38 (n=37)	2.40±1.88 (n=28)	p=0.0132
Pyro *BMP4* ExU (%)	2.49±1.69 (n=38)	2.32±1.56 (n=27)	ns
Pyro *BMP7* EJ (%)	4.31±4.88 (n=38)	1.50±1.05 (n=29)	p<0.0001
Pyro *BMP7* ExU (%)	3.98±4.25 (n=36)	3.83±3.16 (n=26)	ns
Pyro *GSTP1* EJ (%)	1.87±3.32 (n=38)	1.90±2.25 (n=27)	ns
Pyro *GSTP1* ExU (%)	9.36±18.03 (n=34)	4.43±7.89 (n=24)	ns
qPCR *CDKN2A* EJ (-ΔCt)	-5.39±2.09 (n=35)	-3.91±2.01(n=29)	p=0.0044
qPCR *CDKN2A* ExU (-ΔCt)	-4.81±1.75 (n=32)	-3.32±1.79 (n=26)	p<0.0001
qPCR *EDNRB* EJ (-ΔCt)	-6.97±6.04 (n=29)	-4.58±2.45 (n=21)	ns
qPCR *EDNRB* ExU (-ΔCt)	-4.84±1.91 (n=32)	-5.05±1.91 (n=27)	ns
qPCR *PTGS2* EJ (-ΔCt)	-2.50±3.31 (n=37)	-0.19±2.67 (n=28)	p=0.0318
qPCR *PTGS2* ExU (-ΔCt)	-3.58±2.55 (n=33)	-1.79±3.14 (n=25)	p=0.0016
qPCR *PITX2* EJ (-ΔCt)	-0.67±1.65 (n=31)	-1.16±0.92 (n=28)	ns

qPCR *PITX2* ExU (-ΔCt)	-1.99±2.08 (n=25)	-1.74±1.25 (n=21)	ns
qPCR *BMP4* EJ (-ΔCt)	-3.32±2.62 (n=33)	-2.81±2.20 (n=24)	ns
qPCR *BMP4* ExU (-ΔCt)	-4.52±2.77 (n=34)	-4.77±2.51 (n=24)	ns
qPCR *BMP7* EJ (-ΔCt)	-5.24±1.19 (n=33)	-5.06±0.74 (n=27)	ns
qPCR *BMP7* ExU (-ΔCt)	-4.67±1.67 (n=32)	-4.22±2.26 (n=26)	ns
qPCR *GSTP1* EJ (-ΔCt)	-3.37±1.47 (n=34)	-4.89±1.24 (n=28)	p=0.001
qPCR *GSTP1* ExU (-ΔCt)	-5.85±2.93 (n=28)	-6.46±3.62 (n=26)	ns

Table 10: Overview of correlation analysis of promoter methylation among selected TSGs (Part 1)

		Pyro_CDKN2A_EJ	Pyro_CDKN2A_ExU	Pyro_EDNRB_EJ	Pyro_EDNRB_ExU	Pyro_PTGS2_EJ	Pyro_PTGS2_ExU	Pyro_PITX2_EJ
Pyro_CDKN2A_EJ	Correlation Coefficient	1						
	Sig. (2-tailed)							
	N	54						
Pyro_CDKN2A_ExU	Correlation Coefficient	0.27	1					
	Sig. (2-tailed)	0.092						
	N	40	53					
Pyro_EDNRB_EJ	Correlation Coefficient	.346*	.400**	1				
	Sig. (2-tailed)	0.016	0.005					
	N	48	48	61				
Pyro_EDNRB_ExU	Correlation Coefficient	0.252	0.157	.417**	1			
	Sig. (2-tailed)	0.112	0.303	0.003				
	N	41	45	50	54			
Pyro_PTGS2_EJ	Correlation Coefficient	0.227	0.044	.287*	0.058	1		
	Sig. (2-tailed)	0.121	0.767	0.032	0.694			
	N	48	47	56	48	60		
Pyro_PTGS2_ExU	Correlation Coefficient	0.036	0.101	0.091	0.11	0.173	1	
	Sig. (2-tailed)	0.828	0.505	0.538	0.461	0.245		
	N	39	46	48	47	47	53	
Pyro_PITX2_EJ	Correlation Coefficient	-0.187	0.118	-0.177	-0.143	-0.056	0.084	1
	Sig. (2-tailed)	0.197	0.426	0.197	0.339	0.681	0.57	
	N	49	48	55	47	56	48	60
Pyro_PITX2_ExU	Correlation Coefficient	-0.025	-0.187	0.029	0.021	-0.225	.373*	0.129
	Sig. (2-tailed)	0.891	0.247	0.856	0.894	0.157	0.014	0.435
	N	33	40	42	41	41	43	39
Pyro_BMP4_EJ	Correlation Coefficient	0.041	0.187	0.131	0.139	0.268	-0.178	-0.044
	Sig. (2-tailed)	0.789	0.203	0.343	0.356	0.053	0.242	0.752
	N	45	48	54	46	53	45	53
Pyro_BMP4_ExU	Correlation Coefficient	0.005	0.151	0.132	.290*	0.024	.435**	-0.06
	Sig. (2-tailed)	0.975	0.294	0.341	0.037	0.865	0.001	0.669
	N	44	50	54	52	53	53	53
Pyro_BMP7_EJ	Correlation Coefficient	0.226	.285*	.380**	0.126	0.253	0.181	-0.165
	Sig. (2-tailed)	0.122	0.047	0.004	0.393	0.06	0.224	0.221
	N	48	49	56	48	56	47	57
Pyro_BMP7_ExU	Correlation Coefficient	0.025	-.335*	0.123	-0.029	0.061	0.124	0.132
	Sig. (2-tailed)	0.876	0.02	0.387	0.841	0.673	0.387	0.356
	N	43	48	52	50	51	51	51
Pyro_GSTP1_EJ	Correlation Coefficient	-0.147	-0.068	0.071	0.03	-0.101	-0.196	.395**
	Sig. (2-tailed)	0.331	0.646	0.607	0.84	0.471	0.192	0.004
	N	46	48	55	49	53	46	52
Pyro_GSTP1_ExU	Correlation Coefficient	0.172	-0.155	0.043	0.237	-0.116	0.065	-0.098
	Sig. (2-tailed)	0.295	0.308	0.767	0.109	0.437	0.667	0.518
	N	39	45	49	47	47	46	46

Table 11: Overview of correlation analysis of promoter methylation among selected TSGs (Part 2)

		Pyro_PITX2_ExU	Pyro_BMP4_EJ	Pyro_BMP4_ExU	Pyro_BMP7_EJ	Pyro_BMP7_ExU	Pyro_GSTP1_EJ	Pyro_GSTP1_ExU
Pyro_PITX2_EJ	Correlation Coefficient							
	Sig. (2-tailed)							
	N							
Pyro_PITX2_ExU	Correlation Coefficient	1						
	Sig. (2-tailed)							
	N	45						
Pyro_BMP4_EJ	Correlation Coefficient	0.034	1					
	Sig. (2-tailed)	0.836						
	N	40	59					
Pyro_BMP4_ExU	Correlation Coefficient	0.046	-0.042	1				
	Sig. (2-tailed)	0.766	0.768					
	N	44	51	59				
Pyro_BMP7_EJ	Correlation Coefficient	-0.062	.294*	0.16	1			
	Sig. (2-tailed)	0.703	0.03	0.253				
	N	40	55	53	61			
Pyro_BMP7_ExU	Correlation Coefficient	.476**	-0.145	0.117	-0.073	1		
	Sig. (2-tailed)	0.001	0.326	0.396	0.615			
	N	43	48	55	50	56		
Pyro_GSTP1_EJ	Correlation Coefficient	0.159	-0.055	-.334*	-0.154	0.224	1	
	Sig. (2-tailed)	0.328	0.697	0.015	0.27	0.118		
	N	40	52	52	53	50	59	
Pyro_GSTP1_ExU	Correlation Coefficient	-0.05	0.176	0.206	0.052	-0.213	-0.261	1
	Sig. (2-tailed)	0.763	0.246	0.147	0.73	0.133	0.076	
	N	39	45	51	46	51	47	52

Table 12: Overview of correlation analysis of mRNA expression levels among selected TSGs (Part 1)

		qPCR_CDKN2A_EJ	qPCR_CDKN2A_ExU	qPCR_EDNRB_EJ	qPCR_EDNRB_ExU	qPCR_PTGS2_EJ	qPCR_PTGS2_ExU	qPCR_PITX2_EJ
qPCR_CDKN2A_EJ	Correlation Coefficient	1						
	Sig. (2-tailed)							
	N	64						
qPCR_CDKN2A_ExU	Correlation Coefficient	.297*	1					
	Sig. (2-tailed)	0.021						
	N	60	63					
qPCR_EDNRB_EJ	Correlation Coefficient	0.106	0.195	1				
	Sig. (2-tailed)	0.474	0.194					
	N	48	46	50				
qPCR_EDNRB_ExU	Correlation Coefficient	-.287*	-0.164	-0.202	1			
	Sig. (2-tailed)	0.030	0.218	0.194				
	N	57	58	43	59			
qPCR_PTGS2_EJ	Correlation Coefficient	.352**	0.104	0.203	-0.120	1		
	Sig. (2-tailed)	0.005	0.424	0.161	0.373			
	N	63	61	49	57	65		
qPCR_PTGS2_ExU	Correlation Coefficient	0.162	.389**	0.191	0.169	0.134	1	
	Sig. (2-tailed)	0.237	0.003	0.221	0.214	0.325		
	N	55	56	43	56	56	58	
qPCR_PITX2_EJ	Correlation Coefficient	0.194	-0.060	0.087	-0.056	0.018	-0.025	1
	Sig. (2-tailed)	0.152	0.661	0.566	0.691	0.897	0.864	
	N	56	55	46	52	57	51	59
qPCR_PITX2_ExU	Correlation Coefficient	0.159	.492**	-0.091	-0.287	0.142	0.058	-0.094
	Sig. (2-tailed)	0.307	0.001	0.615	0.056	0.357	0.706	0.555
	N	43	45	33	45	44	45	42
qPCR_BMP4_EJ	Correlation Coefficient	0.203	-0.038	.436**	-0.198	.316*	-0.013	-0.031
	Sig. (2-tailed)	0.133	0.787	0.002	0.164	0.017	0.929	0.830
	N	56	53	47	51	57	49	51
qPCR_BMP4_ExU	Correlation Coefficient	-0.065	-0.174	-0.159	.506**	-0.062	0.102	-0.133
	Sig. (2-tailed)	0.637	0.191	0.308	0.000	0.648	0.474	0.356
	N	55	58	43	54	56	52	50
qPCR_BMP7_EJ	Correlation Coefficient	0.173	-.356**	-0.012	0.047	0.195	0.118	-0.061
	Sig. (2-tailed)	0.189	0.007	0.936	0.738	0.142	0.406	0.665
	N	59	56	44	54	58	52	53
qPCR_BMP7_ExU	Correlation Coefficient	-0.004	.368**	0.045	-0.137	0.127	.426**	-0.094
	Sig. (2-tailed)	0.980	0.005	0.775	0.314	0.350	0.001	0.518
	N	55	57	43	56	56	55	50
qPCR_GSTP1_EJ	Correlation Coefficient	-.305*	-0.065	-0.114	0.141	-.262*	-.325*	.375**
	Sig. (2-tailed)	0.018	0.626	0.442	0.304	0.043	0.018	0.005
	N	60	58	48	55	60	53	55
qPCR_GSTP1_ExU	Correlation Coefficient	0.048	0.076	-0.168	-0.260	-0.066	0.166	0.082
	Sig. (2-tailed)	0.740	0.590	0.314	0.062	0.641	0.246	0.575
	N	51	53	38	52	52	51	49

Table 13: Overview of correlation analysis of mRNA expression levels among selected TSGs (Part 2)

		qPCR_PITX2_ExU	qPCR_BMP4_EJ	qPCR_BMP4_ExU	qPCR_BMP7_EJ	qPCR_BMP7_ExU	qPCR_GSTP1_EJ	qPCR_GSTP1_ExU
qPCR_PITX2_ExU	Correlation Coefficient	1.000						
	Sig. (2-tailed)							
	N	46						
qPCR_BMP4_EJ	Correlation Coefficient	-0.120	1.000					
	Sig. (2-tailed)	0.473						
	N	38	57					
qPCR_BMP4_ExU	Correlation Coefficient	-0.177	0.034	1.000				
	Sig. (2-tailed)	0.267	0.818					
	N	41	48	58				
qPCR_BMP7_EJ	Correlation Coefficient	-0.067	-0.010	-0.006	1.000			
	Sig. (2-tailed)	0.682	0.945	0.965				
	N	40	51	52	60			
qPCR_BMP7_ExU	Correlation Coefficient	.433**	0.031	-0.108	0.029	1.000		
	Sig. (2-tailed)	0.004	0.833	0.442	0.837			
	N	43	49	53	52	58		
qPCR_GSTP1_EJ	Correlation Coefficient	0.157	-0.203	-0.061	0.078	-0.084	1.000	
	Sig. (2-tailed)	0.326	0.137	0.666	0.565	0.548		
	N	41	55	53	57	53	62	
qPCR_GSTP1_ExU	Correlation Coefficient	0.192	0.055	-0.238	0.195	.527**	0.205	1.000
	Sig. (2-tailed)	0.218	0.725	0.100	0.183	0.000	0.157	
	N	43	44	49	48	52	49	54

Table 14: Overview of mRNA expression and methylation correlations among selected TSGs (Part 1)

		qPCR_CDKN2A_EJ	qPCR_CDKN2A_ExU	qPCR_EDNRB_EJ	qPCR_EDNRB_ExU	qPCR_PTGS2_EJ	qPCR_PTGS2_ExU	qPCR_PITX2_EJ
Pyro_CDKN2A_EJ	Correlation Coefficient	-0.148	-0.201	-0.134	0.180	-0.235	-0.033	0.109
	Sig. (2-tailed)	0.315	0.171	0.417	0.242	0.104	0.832	0.470
	N	48	48	39	44	49	44	46
Pyro_CDKN2A_ExU	Correlation Coefficient	-0.167	-0.247	-.415*	0.241	-0.239	-0.126	0.104
	Sig. (2-tailed)	0.240	0.077	0.011	0.088	0.091	0.392	0.490
	N	51	52	37	51	51	48	46
Pyro_EDNRB_EJ	Correlation Coefficient	-0.226	-.336**	-0.064	0.094	-.318*	-0.246	0.066
	Sig. (2-tailed)	0.087	0.010	0.671	0.499	0.014	0.076	0.641
	N	58	58	47	54	59	53	53
Pyro_EDNRB_ExU	Correlation Coefficient	-0.079	-.348*	0.025	0.118	-0.109	-0.119	-0.178
	Sig. (2-tailed)	0.576	0.011	0.881	0.403	0.443	0.412	0.230
	N	52	52	40	52	52	50	47
Pyro_PTGS2_EJ	Correlation Coefficient	-0.158	-0.119	-0.092	0.035	0.169	-0.104	0.148
	Sig. (2-tailed)	0.240	0.378	0.542	0.804	0.205	0.465	0.291
	N	57	57	46	53	58	52	53
Pyro_PTGS2_ExU	Correlation Coefficient	0.098	0.061	-0.292	-0.095	-0.022	-0.223	-0.018
	Sig. (2-tailed)	0.500	0.669	0.080	0.504	0.881	0.120	0.902
	N	50	52	37	52	51	50	48
Pyro_PITX2_EJ	Correlation Coefficient	.354**	0.173	-0.106	-.306*	.273*	-0.104	-0.030
	Sig. (2-tailed)	0.007	0.199	0.500	0.026	0.038	0.462	0.828
	N	57	57	43	53	58	52	54
Pyro_PITX2_ExU	Correlation Coefficient	0.267	.494**	0.073	-0.278	-0.148	0.230	0.157
	Sig. (2-tailed)	0.087	0.001	0.688	0.068	0.345	0.138	0.339
	N	42	44	33	44	43	43	39
Pyro_BMP4_EJ	Correlation Coefficient	-0.146	-0.211	-0.017	0.169	0.017	-0.126	0.067
	Sig. (2-tailed)	0.282	0.122	0.911	0.236	0.903	0.382	0.639
	N	56	55	45	51	57	50	51
Pyro_BMP4_ExU	Correlation Coefficient	0.042	-0.031	-0.124	0.070	0.019	-0.162	0.054
	Sig. (2-tailed)	0.761	0.819	0.430	0.600	0.891	0.234	0.702
	N	56	58	43	58	57	56	52
Pyro_BMP7_EJ	Correlation Coefficient	-0.191	-0.181	-0.278	0.178	-0.162	-0.248	-0.010
	Sig. (2-tailed)	0.150	0.177	0.067	0.203	0.221	0.077	0.941
	N	58	57	44	53	59	52	54
Pyro_BMP7_ExU	Correlation Coefficient	.322*	0.207	0.087	-.284*	0.216	0.197	0.271
	Sig. (2-tailed)	0.019	0.129	0.590	0.035	0.117	0.158	0.057
	N	53	55	41	55	54	53	50
Pyro_GSTP1_EJ	Correlation Coefficient	0.062	0.013	0.153	-0.095	0.161	0.209	-0.203
	Sig. (2-tailed)	0.645	0.924	0.317	0.498	0.231	0.144	0.153
	N	57	56	45	53	57	50	51
Pyro_GSTP1_ExU	Correlation Coefficient	-0.062	-0.099	0.006	0.058	-0.179	-0.241	-0.086
	Sig. (2-tailed)	0.673	0.491	0.974	0.685	0.212	0.095	0.576
	N	49	51	37	51	50	49	45

Table 15: Overview of mRNA expression and methylation correlations among selected TSGs (Part 2)

		qPCR_PITX2_ExU	qPCR_BMP4_EJ	qPCR_BMP4_ExU	qPCR_BMP7_EJ	qPCR_BMP7_ExU	qPCR_GSTP1_EJ	qPCR_GSTP1_ExU
Pyro_CDKN2A_EJ	Correlation Coefficient	-0.079	-0.117	-0.063	0.041	-0.027	0.258	0.086
	Sig. (2-tailed)	0.656	0.461	0.683	0.787	0.860	0.083	0.599
	N	34	42	44	46	44	46	40
Pyro_CDKN2A_ExU	Correlation Coefficient	-0.064	-0.239	0.075	0.152	-0.103	0.236	0.050
	Sig. (2-tailed)	0.701	0.114	0.612	0.302	0.485	0.103	0.748
	N	38	45	48	48	48	49	44
Pyro_EDNRB_EJ	Correlation Coefficient	-0.024	0.128	0.088	0.041	-0.174	0.249	0.082
	Sig. (2-tailed)	0.880	0.366	0.530	0.766	0.205	0.064	0.577
	N	42	52	53	54	55	56	49
Pyro_EDNRB_ExU	Correlation Coefficient	0.083	0.002	0.246	0.250	-0.144	0.264	0.047
	Sig. (2-tailed)	0.603	0.990	0.092	0.083	0.319	0.067	0.756
	N	42	47	48	49	50	49	46
Pyro_PTGS2_EJ	Correlation Coefficient	0.145	0.085	0.026	-0.087	-0.029	.268*	0.007
	Sig. (2-tailed)	0.353	0.554	0.853	0.533	0.840	0.048	0.963
	N	43	51	53	53	52	55	48
Pyro_PTGS2_ExU	Correlation Coefficient	0.255	0.220	0.165	-0.038	-0.022	-0.059	0.139
	Sig. (2-tailed)	0.107	0.152	0.258	0.799	0.879	0.692	0.337
	N	41	44	49	47	51	48	50
Pyro_PITX2_EJ	Correlation Coefficient	0.222	0.204	-0.162	-0.020	0.127	-.333*	0.021
	Sig. (2-tailed)	0.162	0.156	0.246	0.884	0.370	0.013	0.885
	N	41	50	53	54	52	55	49
Pyro_PITX2_ExU	Correlation Coefficient	.345*	0.161	-0.246	-0.145	0.285	-0.204	0.238
	Sig. (2-tailed)	0.039	0.334	0.121	0.379	0.061	0.202	0.129
	N	36	38	41	39	44	41	42
Pyro_BMP4_EJ	Correlation Coefficient	-0.156	0.118	-0.044	0.026	-0.075	0.185	0.091
	Sig. (2-tailed)	0.344	0.410	0.759	0.851	0.600	0.180	0.546
	N	39	51	50	53	51	54	46
Pyro_BMP4_ExU	Correlation Coefficient	0.062	0.142	.278*	0.146	0.249	0.134	0.232
	Sig. (2-tailed)	0.684	0.326	0.042	0.296	0.064	0.336	0.094
	N	45	50	54	53	56	54	53
Pyro_BMP7_EJ	Correlation Coefficient	-0.089	0.092	0.129	0.111	-0.153	.336*	0.011
	Sig. (2-tailed)	0.579	0.522	0.364	0.418	0.280	0.011	0.941
	N	41	51	52	55	52	56	48
Pyro_BMP7_ExU	Correlation Coefficient	.402**	.324*	-0.061	-0.132	.386**	-0.165	0.240
	Sig. (2-tailed)	0.006	0.026	0.669	0.360	0.004	0.248	0.093
	N	45	47	51	50	53	51	50
Pyro_GSTP1_EJ	Correlation Coefficient	0.150	0.272	-0.084	0.042	0.137	-0.197	-0.065
	Sig. (2-tailed)	0.356	0.051	0.556	0.766	0.339	0.146	0.665
	N	40	52	51	53	51	56	47
Pyro_GSTP1_ExU	Correlation Coefficient	-0.196	-0.069	0.063	-0.036	-0.163	-0.006	0.170
	Sig. (2-tailed)	0.207	0.658	0.675	0.813	0.263	0.966	0.264
	N	43	43	47	46	49	47	45

Table 16: Baseline characteristics of the participants, where sorted epithelial cells and leukocytes have been investigated

Characteristics	Patients (n=34), mean±SD	Healthy controls (n=26), mean±SD	p value
Age (years)	39.46±12.04	26.89±3.82	p<0.0001
IPSS	11.24±7.38	4.50±4.02	p<0.0001
CPSI I	11.18±4017	0.19±0.63	p<0.0001
CPSI II	3.84±2.95	1.65±1.96	p=0.0005
CPSI III	8.79±2.37	0.38±0.57	p<0.0001
CPSI total	23.18±8.34	2.23±2.70	p<0.0001
CRP (mg/l)	1.61±3.42	N/A	N/A
PSA (ng/mL)	0.96±0.88	N/A	N/A
Sperm motility a	18.12±8.64	20.80±12.55	ns
Sperm motility b	31.68±10.70	30.24±4.46	ns
Sperm motility c	8.92±4.10	15.20±8.01	ns
Sperm motility total	61.17±8.48	66.24±9.24	ns

Table 17: Overview of *CDKN2A* methylation and mRNA expression levels in sorted epithelial cells and leukocytes

Experimental results	Patients (n=34), mean±SD	Healthy controls (n=26), mean±SD	p value
Pyro_*CDKN2A*_EJ_EPI (%)	3.98±3.84 (n=30)	2.23±1.01 (n=24)	ns
Pyro_*CDKN2A*_EJ_LEU (%)	4.73±6.57 (n=26)	1.98±0.82 (n=22)	ns
Pyro_*CDKN2A*_ExU_EPI (%)	6.36±8.67 (n=29)	2.24±1.11 (n=26)	p=0.0019
Pyro_*CDKN2A*_ExU_LEU (%)	4.54±4.42 (n=28)	2.22±1.07 (n=25)	p=0.0346
qPCR_*CDKN2A*_EJ_EPI (-ΔCt)	-6.01±2.25 (n=25)	-4.66±1.30 (n=22)	p=0.01
qPCR_*CDKN2A*_EJ_LEU (-ΔCt)	-5.78±2.03 (n=25)	-4.29±1.22 (n=23)	p=0.0009
qPCR_*CDKN2A*_ExU_EPI (-ΔCt)	-4.96±1.61 (n=29)	-4.69±1.68 (n=26)	ns
qPCR_*CDKN2A*_ExU_LEU (-ΔCt)	-5.73±2.14 (n=28)	-6.11±1.64 (n=26)	ns

Table 18: Correlations of IPSS and CPSI scores to TSGs methylation levels

		IPSS	CPSI I	CPSI II	CPSI III	CPSI Total
Pyro_CDKN2A_EJ	Correlation Coefficient	.312*	.313*	0.241	.343*	.328*
	Sig. (2-tailed)	0.033	0.034	0.106	0.020	0.026
	N	47	46	46	46	46
Pyro_CDKN2A_ExU	Correlation Coefficient	.447**	.406**	.368*	.338*	.393**
	Sig. (2-tailed)	0.002	0.006	0.014	0.025	0.008
	N	45	44	44	44	44
Pyro_EDNRB_EJ	Correlation Coefficient	.559**	.493**	.469**	.451**	.496**
	Sig. (2-tailed)	0.000	0.000	0.000	0.001	0.000
	N	54	53	53	53	53
Pyro_EDNRB_ExU	Correlation Coefficient	0.221	0.226	0.173	0.185	0.209
	Sig. (2-tailed)	0.136	0.130	0.249	0.218	0.163
	N	47	46	46	46	46
Pyro_PTGS2_EJ	Correlation Coefficient	.291*	.340*	0.168	.394**	.329*
	Sig. (2-tailed)	0.039	0.015	0.237	0.004	0.019
	N	51	51	51	51	51
Pyro_PTGS2_ExU	Correlation Coefficient	0.069	0.183	0.064	0.180	0.180
	Sig. (2-tailed)	0.648	0.230	0.676	0.237	0.237
	N	46	45	45	45	45
Pyro_PITX2_EJ	Correlation Coefficient	-0.048	-0.095	0.101	-0.003	-0.039
	Sig. (2-tailed)	0.733	0.502	0.474	0.983	0.782
	N	53	52	52	52	52
Pyro_PITX2_ExU	Correlation Coefficient	-0.066	0.006	-0.040	-0.163	-0.014
	Sig. (2-tailed)	0.697	0.974	0.817	0.343	0.934
	N	37	36	36	36	36
Pyro_BMP4_EJ	Correlation Coefficient	.406**	.294*	.346*	.290*	.327*
	Sig. (2-tailed)	0.003	0.038	0.014	0.041	0.021
	N	51	50	50	50	50
Pyro_BMP4_ExU	Correlation Coefficient	-0.062	-0.006	-0.085	-0.017	-0.037
	Sig. (2-tailed)	0.667	0.966	0.551	0.907	0.799
	N	51	51	51	51	51
Pyro_BMP7_EJ	Correlation Coefficient	.466**	.556**	.289*	.558**	.531**
	Sig. (2-tailed)	0.001	0.000	0.037	0.000	0.000
	N	52	52	52	52	52
Pyro_BMP7_ExU	Correlation Coefficient	-0.072	-0.072	-0.040	-0.062	-0.055
	Sig. (2-tailed)	0.623	0.632	0.789	0.678	0.713
	N	49	47	47	47	47
Pyro_GSTP1_EJ	Correlation Coefficient	0.050	-0.010	0.132	0.025	0.035
	Sig. (2-tailed)	0.729	0.943	0.361	0.866	0.807
	N	51	50	50	50	50
Pyro_GSTP1_ExU	Correlation Coefficient	0.176	-0.002	0.208	0.028	0.058
	Sig. (2-tailed)	0.253	0.991	0.180	0.857	0.710
	N	44	43	43	43	43

Table 19: Correlations of IPSS and CPSI scores to TSGs expression levels

		IPSS	CPSI I	CPSI II	CPSI III	CPSI Total
qPCR_CDKN2A_EJ	Correlation Coefficient	-.327*	-.378**	-.270*	-.416**	-.396**
	Sig. (2-tailed)	0.014	0.004	0.047	0.002	0.003
	N	56	55	55	55	55
qPCR_CDKN2A_ExU	Correlation Coefficient	-0.156	-.394**	-0.105	-.371**	-.345*
	Sig. (2-tailed)	0.254	0.003	0.448	0.006	0.011
	N	55	54	54	54	54
qPCR_EDNRB_EJ	Correlation Coefficient	-0.116	-.372*	-0.019	-.368*	-.334*
	Sig. (2-tailed)	0.453	0.014	0.902	0.015	0.029
	N	44	43	43	43	43
qPCR_EDNRB_ExU	Correlation Coefficient	0.107	0.167	0.161	0.109	0.160
	Sig. (2-tailed)	0.454	0.247	0.264	0.453	0.268
	N	51	50	50	50	50
qPCR_PTGS2_EJ	Correlation Coefficient	-0.195	-0.252	-0.104	-0.226	-0.234
	Sig. (2-tailed)	0.151	0.064	0.451	0.098	0.085
	N	56	55	55	55	55
qPCR_PTGS2_ExU	Correlation Coefficient	-0.267	-.362**	-0.192	-.413**	-.366**
	Sig. (2-tailed)	0.058	0.010	0.182	0.003	0.009
	N	51	50	50	50	50
qPCR_PITX2_EJ	Correlation Coefficient	0.007	0.087	0.046	0.098	0.082
	Sig. (2-tailed)	0.961	0.546	0.753	0.500	0.571
	N	51	50	50	50	50
qPCR_PITX2_ExU	Correlation Coefficient	0.100	0.054	0.151	0.069	0.087
	Sig. (2-tailed)	0.539	0.747	0.367	0.679	0.603
	N	40	38	38	38	38
qPCR_BMP4_EJ	Correlation Coefficient	-0.125	-0.241	-0.077	-0.157	-0.204
	Sig. (2-tailed)	0.399	0.102	0.607	0.291	0.168
	N	48	47	47	47	47
qPCR_BMP4_ExU	Correlation Coefficient	0.095	0.136	0.110	0.046	0.085
	Sig. (2-tailed)	0.506	0.347	0.448	0.751	0.558
	N	51	50	50	50	50

qPCR_BMP7_EJ	Correlation Coefficient	-0.146	0.061	-0.123	-0.085	-0.031
	Sig. (2-tailed)	0.297	0.667	0.384	0.549	0.830
	N	53	52	52	52	52
qPCR_BMP7_ExU	Correlation Coefficient	-0.178	-0.257	-0.068	-0.194	-0.189
	Sig. (2-tailed)	0.211	0.072	0.637	0.178	0.188
	N	51	50	50	50	50
qPCR_GSTP1_EJ	Correlation Coefficient	0.260	.350*	0.138	.413**	.335*
	Sig. (2-tailed)	0.060	0.011	0.327	0.002	0.015
	N	53	52	52	52	52
qPCR_GSTP1_ExU	Correlation Coefficient	-0.077	-0.081	-0.023	-0.060	-0.085
	Sig. (2-tailed)	0.606	0.593	0.881	0.690	0.577
	N	47	46	46	46	46

Table 20: Correlations of sperm motilities and PH values to TSGs methylation levels

		Sperm PH value	Sperm motility a	Sperm motility b	Sperm motility c	Sperm motility d	Sperm motility total
Pyro_CDKN2A_EJ	Correlation Coefficient	0.068	-0.142	-0.057	-0.138	.338*	-.319*
	Sig. (2-tailed)	0.644	0.329	0.698	0.345	0.017	0.025
	N	49	49	49	49	49	49
Pyro_CDKN2A_ExU	Correlation Coefficient	-0.272	-0.149	0.124	-0.264	0.234	-0.250
	Sig. (2-tailed)	0.051	0.293	0.382	0.059	0.099	0.073
	N	52	52	52	52	51	52
Pyro_EDNRB_EJ	Correlation Coefficient	-0.124	-.315*	0.028	-0.233	.379**	-.414**
	Sig. (2-tailed)	0.344	0.014	0.830	0.073	0.003	0.001
	N	60	60	60	60	59	60
Pyro_EDNRB_ExU	Correlation Coefficient	-0.220	-0.035	-0.003	-0.145	0.068	-0.105
	Sig. (2-tailed)	0.114	0.803	0.984	0.300	0.629	0.455
	N	53	53	53	53	52	53
Pyro_PTGS2_EJ	Correlation Coefficient	-0.010	-0.245	0.130	-0.062	0.199	-0.201
	Sig. (2-tailed)	0.938	0.063	0.331	0.643	0.134	0.131
	N	58	58	58	58	58	58
Pyro_PTGS2_ExU	Correlation Coefficient	-0.254	0.131	-0.012	-0.164	-0.056	0.081
	Sig. (2-tailed)	0.069	0.353	0.932	0.245	0.697	0.570
	N	52	52	52	52	51	52
Pyro_PITX2_EJ	Correlation Coefficient	-0.192	0.036	-0.199	0.045	-0.165	0.084
	Sig. (2-tailed)	0.148	0.789	0.135	0.736	0.219	0.529
	N	58	58	58	58	57	58
Pyro_PITX2_ExU	Correlation Coefficient	0.142	.335*	-0.037	-0.165	-0.178	0.189
	Sig. (2-tailed)	0.358	0.026	0.809	0.285	0.252	0.219
	N	44	44	44	44	43	44
Pyro_BMP4_EJ	Correlation Coefficient	-0.035	-0.239	0.246	-0.043	0.100	-0.149
	Sig. (2-tailed)	0.794	0.073	0.066	0.750	0.462	0.270
	N	57	57	57	57	56	57
Pyro_BMP4_ExU	Correlation Coefficient	-.377**	-0.002	-0.105	-0.138	0.036	-0.056
	Sig. (2-tailed)	0.004	0.988	0.435	0.302	0.790	0.677
	N	58	58	58	58	57	58
Pyro_BMP7_EJ	Correlation Coefficient	-.283*	-.302*	.405**	-.413**	0.242	-.337**
	Sig. (2-tailed)	0.030	0.020	0.001	0.001	0.067	0.009
	N	59	59	59	59	58	59
Pyro_BMP7_ExU	Correlation Coefficient	0.225	0.006	-.347**	-0.074	0.021	-0.060
	Sig. (2-tailed)	0.098	0.964	0.010	0.594	0.882	0.666
	N	55	55	55	55	54	55
Pyro_GSTP1_EJ	Correlation Coefficient	0.187	-0.061	-.266*	-0.175	0.096	-0.151
	Sig. (2-tailed)	0.159	0.649	0.044	0.189	0.476	0.258
	N	58	58	58	58	57	58
Pyro_GSTP1_ExU	Correlation Coefficient	-0.126	0.108	0.160	0.273	-0.145	0.207
	Sig. (2-tailed)	0.376	0.453	0.261	0.053	0.317	0.145
	N	51	51	51	51	50	51

Table 21: Correlations of sperm motilities and PH values to TSGs expression levels

		Sperm PH value	Sperm motility a	Sperm motility b	Sperm motility c	Sperm motility d	Sperm motility total
qPCR_CDKN2A_EJ	Correlation Coefficient	-0.027	0.108	-0.005	0.107	-.268*	0.218
	Sig. (2-tailed)	0.836	0.401	0.969	0.406	0.037	0.088
	N	62	62	62	62	61	62
qPCR_CDKN2A_ExU	Correlation Coefficient	0.124	.298*	-0.211	-0.020	-0.234	0.207
	Sig. (2-tailed)	0.337	0.019	0.101	0.876	0.069	0.107
	N	62	62	62	62	61	62
qPCR_EDNRB_EJ	Correlation Coefficient	.356*	-0.064	-0.257	0.054	-0.001	-0.018
	Sig. (2-tailed)	0.013	0.664	0.078	0.716	0.996	0.905
	N	48	48	48	48	48	48
qPCR_EDNRB_ExU	Correlation Coefficient	0.009	0.108	-0.002	-0.056	-0.048	0.050
	Sig. (2-tailed)	0.945	0.420	0.990	0.677	0.725	0.709
	N	58	58	58	58	57	58
qPCR_PTGS2_EJ	Correlation Coefficient	0.058	0.123	-0.117	0.077	-.278*	.257*
	Sig. (2-tailed)	0.654	0.337	0.361	0.547	0.029	0.042
	N	63	63	63	63	62	63
qPCR_PTGS2_ExU	Correlation Coefficient	.403**	.393**	-.305*	-0.105	-0.248	0.220
	Sig. (2-tailed)	0.002	0.002	0.021	0.436	0.066	0.100
	N	57	57	57	57	56	57
qPCR_PITX2_EJ	Correlation Coefficient	-0.106	-0.104	0.086	-0.042	0.103	-0.093
	Sig. (2-tailed)	0.432	0.441	0.526	0.754	0.450	0.491
	N	57	57	57	57	56	57
qPCR_PITX2_ExU	Correlation Coefficient	-0.226	-0.128	-0.137	-0.007	0.151	-0.185
	Sig. (2-tailed)	0.132	0.398	0.363	0.965	0.322	0.219
	N	46	46	46	46	45	46
qPCR_BMP4_EJ	Correlation Coefficient	0.174	-0.134	-0.178	-0.167	0.034	-0.093
	Sig. (2-tailed)	0.205	0.330	0.194	0.224	0.805	0.501
	N	55	55	55	55	54	55
qPCR_BMP4_ExU	Correlation Coefficient	-0.041	-0.146	0.009	0.006	0.097	-0.099
	Sig. (2-tailed)	0.763	0.278	0.948	0.967	0.474	0.463
	N	57	57	57	57	57	57
qPCR_BMP7_EJ	Correlation Coefficient	-0.218	0.033	0.133	-0.100	-0.058	0.060
	Sig. (2-tailed)	0.100	0.807	0.321	0.454	0.669	0.654
	N	58	58	58	58	57	58
qPCR_BMP7_ExU	Correlation Coefficient	-0.004	0.110	-0.183	-0.035	-0.009	-0.028
	Sig. (2-tailed)	0.975	0.414	0.172	0.794	0.949	0.836
	N	57	57	57	57	56	57
qPCR_GSTP1_EJ	Correlation Coefficient	-.281*	-0.245	0.207	-0.103	.262*	-0.247
	Sig. (2-tailed)	0.029	0.060	0.112	0.435	0.045	0.057
	N	60	60	60	60	59	60
qPCR_GSTP1_ExU	Correlation Coefficient	0.032	0.026	-0.063	-0.153	0.102	-0.096
	Sig. (2-tailed)	0.819	0.854	0.655	0.273	0.473	0.493
	N	53	53	53	53	52	53

7. Acknowledgement

I would like to seize this opportunity to express my sincerest gratitude to Prof. Dr. rer. nat. Undraga Schagdarsurengin and Prof. Dr. med. Florian Wagenlehner, my esteemed supervisors, for granting me the remarkable opportunity to embark on my doctoral thesis under their guidance. I am genuinely grateful for their unwavering support, mentorship, and invaluable advice throughout the process. Their belief in my abilities has been instrumental in my personal and professional growth. I sincerely appreciate their valuable contributions.

I would also like to extend my heartfelt thanks to the doctors in UKGM and my fellow lab mates, Dr. Temuujin Dansranjavin, Prof. Dr. Adrian Pilatz, Prof. Dr. Hans-Christian Schuppe, Dr. rer. nat. Andreas Fröbius,, Dr. rer. nat. Nihan Ozturk and Dr. med. Florian Dittmar, their support and assistance have been invaluable throughout the project. In addition, Nils Nessheim and Alexander Kruse have all played a significant role in supporting me throughout my research.

Furthermore, I would like to express my deep appreciation for the exceptional working environment fostered by the team. Special thanks go to Mrs. Barbara Fröhlich, Mrs. Tania Bloch, and Mrs. Kerstin Wilhelm for their excellent technical assistance, support in collecting clinical samples, and for creating a warm and welcoming atmosphere in the lab.

I am sincerely grateful to the students, Deborah Dengler, Marc Manthey, Laura Schneider, and Marie Dippel, who have provided valuable support during the project. Their contributions have been precious and greatly appreciated.

Moreover, I would like to express my heartfelt appreciation to Hicham Houhou and Mudassar Mughal, who have not only been colleagues but have become dear friends. Thank you for your assistance and support during our time in the lab and for the beautiful coffee breaks and lunchtime conversations that made the journey all the more enjoyable.

I would like to extend my profound appreciation to the esteemed funding body, the Deutsche Forschungsgemeinschaft (DFG), which enabled the fruition of my doctoral research and graciously supported my endeavors over three years. Furthermore, I am deeply honored to have been affiliated with the IRTG at Giessen University, where I received invaluable assistance throughout my doctoral journey. I am particularly grateful to Prof. Dr. Andreas Meinhardt, the spokesperson for the IRTG, and the diligent IRTG administrative coordinator, Pia Jürgens. Their unwavering commitment and involvement significantly contributed to realizing my research objectives.

Additionally, I would like to extend my gratitude to the Giessen Graduate School for Life Sciences and the Ph.D. programs of the JLU for their commitment to providing enriching seminars, workshops, and conferences. These opportunities have played a pivotal role in my academic and professional development.

Finally, I want to express my most profound appreciation to my family and my wife, Maria, for their unwavering support and encouragement throughout my thesis journey. To my dearest Mama and Papa, I am profoundly thankful for your constant presence and unwavering support throughout my academic journey, particularly as a doctoral candidate.

8. Contributions

Publications:

Schneider, L., Dansranjav, T., Neumann, E., **Yan, H.**, Pilatz, A., Schuppe, H.-C., Wagenlehner, F. & Schagdarsurengin, U. Post-prostatic-massage urine exosomes of men with chronic prostatitis/chronic pelvic pain syndrome carry prostate-cancer-typical microRNAs and activate proto-oncogenes. *Molecular Oncology* **17,** 445–468 (2023).

Yan, H., Dittmar, F., Schagdarsurengin, U. & Wagenlehner, F. The Clinical Application and Potential Roles of Circulating Tumor Cells in Bladder Cancer and Prostate Cancer. Urology 145, 30–37 (2020).

Conferences and presentations

Yan H., Dengler D., Manthey M., Pilatz A., Schuppe H-C., Wagenlehner F., Schagdarsurengin U. Epigenetic Dysregulation of Tumor Suppressor Genes in CP/CPPS: Studies on liquid biopsies for biomarker development. *13. AuF-Symposium*, Erlangen, Germany, 2022

Yan, H., Dengler, D., Manthey, M., Pilatz, A., Schuppe, H.-C., Wagenlehner, F. & Schagdarsurengin, U. A0121 - Epigenetic dysregulation of tumor suppressor genes in CP/CPPS: Studies on liquid biopsies for biomarker development. *37th Annual EAU Congress*, Amsterdam Netherland, 2022

Manthey, M., **Yan, H.**, Dengler, D., Pilatz, A., Schuppe, H.-C., Wagenlehner, F. & Schagdarsurengin, U. A0030 - Role of epigenetics in the neurogenic inflammation in patients suffering CP/CPPS and relevance for the precision medicine. *37th Annual EAU Congress*, Amsterdam, Netherland, 2022

Yan H., Dengler D., Pilatz A., Schuppe H-C., Wagenlehner F. and Schagdarsurengin U. Epigenetic Dysregulation of Tumor Suppressor Genes in CP/CPPS: studies on liquid biopsies for biomarker development. *12. AuF-Symposium*, Berlin, Germany, 2021. (Poster)

Dengler, D., **Yan H.**, Schuppe, H.-C., Nesheim, N., Pilatz, A., Dansranjavin, T., Wagenlehner, F. & Schagdarsurengin, U. 1131 - Studies on liquid biopsies of CP/CPPS patients reveal epigenetic dysregulation of tumor suppressor genes and suggest a risk for prostate cancer. *35th Annual EAU Virtual Congress,* 2020 (Poster)

Yan H, Dengler D, Pilatz A, Schuppe H-C, Wagenlehner F and Schagdarsurengin U. Methylation of Tumor Suppressor Genes in CP/CPPS: studies on liquid biopsies for biomarker development. *12TH MEETING OF THE NETWORK FOR YOUNG RESEARCHERS IN ANDROLOGY (NYRA).* Giessen, Germany, 2019